Master's thesis

NTNU
Norwegian University of Science and Technology
Faculty of Engineering
Department of Geoscience and Petroleum

Niklas Kjenstadbakk Brede

Soft ground tunneling in glacial deposits

Implementation of the Steel Pipe Umbrella method for the Drammen tunnel

Master's thesis in Geotechnology
Supervisor: Ola Fredin
June 2023

NTNU
Norwegian University of
Science and Technology

Niklas Kjenstadbakk Brede

Soft ground tunneling in glacial deposits

Implementation of the Steel Pipe Umbrella method for the Drammen tunnel

Master's thesis in Geotechnology
Supervisor: Ola Fredin
June 2023

Norwegian University of Science and Technology
Faculty of Engineering
Department of Geoscience and Petroleum

NTNU
Norwegian University of
Science and Technology

Abstract

The ongoing construction of the Drammen tunnel, as part of the new double-track railway project from Drammen to Kobbervikdalen, includes a $290m$ section built as a soft ground tunnel within glacial till. Soft ground tunnels are challenging projects that require both proper design and execution. As urban areas expand, often situated on soil, there is a growing demand for efficient utilization of underground spaces. Veidekke, the project contractor, has chosen to extensively reinforce the ground using a jet grouting method for tunnel construction. However, it is believed that the construction process could be optimized in terms of cost, and emissions, while still being safe by employing the steel pipe umbrella method.

To assess the feasibility of utilizing the steel pipe umbrella method for tunnel construction, an extensive investigation was conducted to examine the ground conditions at the construction site. Preliminary investigations for the project were studied thoroughly. A sample was collected from the construction site, and laboratory tests including grain size distribution and XRD analysis were performed at NTNU. The obtained parameter values were then used for stability calculations. The analysis began with simpler analytical and empirical calculations, progressing to more complex numerical modeling. The analytical and empirical solutions highlighted the immediate support requirements and the magnitude of support needed. Additionally, the results demonstrated that a larger overburden contributes to increased stability of the tunnel.

The stability analysis of the Joberget soil tunnel design utilized a two-dimensional finite element method with the RS2 software. The calculations focused on evaluating the maximum total displacement. Two cross-sections and one longitudinal section were modeled to gain insights into the tunnel's stability. The pipe umbrella support method was simulated using an improved material layer over the crown of the tunnel. The results disclosed that by subdividing the face correctly, installing heavy support immediately, and keeping the excavation lengths short, stability of the tunnel can be ensured.

The limiting factor of this analysis was the uncertainties in the modeling parameters. With more reliable parameter values, the models would align more closely with reality, potentially reducing the need for excessive caution. Increased focus on preliminary investigations is on this basis recommended to prevent tunneling projects from being over-dimensioned and account for more emissions.

Sammendrag

Som en del av det nye dobbeltsporede jernbaneprosjektet fra Drammen til Kobbervikdalen har Drammenstunnelen blitt drevet. Den inkluderer en løsmassetunnel på $290m$ som går igjennom morenematerial. Løsmassetunneler er utfordrende prosjekter som krever både nøyaktig prosjektering og utførelse. Byer er ofte lokalisert på løsmasser, og med utvidelsen av byene kommer et økende behov for å utnytte undergrunnen effektivt. Entreprenøren Veidekke som er ansvarlig for driving av Drammenstunnelen har valgt å forsterke grunnen med jet grout før tunneldrivingen. Det antas immdlertidig at byggeprosessen kan optimaliseres med tanke på kostnader og utslipp, og samtidigt være trygg ved å bruk av stålrørsparaplymetoden.

For å vurdere gjennomførbarheten av å benytte stålrørsparaplymetoden som drivemetode, ble det gjennomført omfattende undersøkelse av grunnforholdene. Forundersøkelser for prosjektet ble studert grundig. Også prøvematerialet ble samlet inn fra byggeplassen, og labratorietestene kornfordeling og XRD-analyse ble utført ved laboratoriet på Petroleums Teknisk Senter, NTNU. De oppnådde parameterverdiene ble deretter brukt til stabilitetsberegninger. Analysen begynte med enklere analytiske og empiriske beregninger, og gikk videre til mer kompleke beregnigsmetoder i form av numerisk modellering. De analytiske og empiriske løsningene fremhevet at sikring av tunnelne må skje umiddelbart og størrelsen av sikringen nødvendig ble funnet. I tillegg viste resultatene at en større overdekning bidrar til økt stabilitet i tunnelen.

Stabilitetsanalysen av Joberget jordtunneldesign benyttet en todimensjonal endelig elementmetode ved programvaren RS2. Beregningene fokuserte på å evaluere den totale deformasjonen målt i modellene. To tverrsnitt og ett lengdesnitt ble modellert for å få innsikt i tunnelens stabilitet. Sålrørsparaplymetoden ble simulert ved å danne et lag av forsterket materiale over tunnelens krone. Resultatene avslørte at ved å dele opp stuffen riktig, installere tung støtte umiddelbart og holde utgravningslengdene korte, kan tunnelens stabilitet forsikres.

Den største usikkerheten i analysen var de benyttede parameterene. Med mer pålitelige parameterverdier vil modellene være mer på linje med virkeligheten, og potensielt redusere behovet for overdreven forsiktighet når tunnelprosjekter skal planlegges. På bakgrunn av dette anbefales et økt fokus på gode forundersøkelser for å hindre at tunnelprosjekter blir unødvendig overdimensjonert og står for mer utslipp.

Acknowledgements

This thesis concludes the Master's degree in Geotechnology – Engineering Geology and Rock Mechanics. It was submitted to the Department of Geosciences and Petroleum at the Norwegian University of Science and Technology (NTNU). The work on this thesis has been carried out during the spring semester of 2023.

Firstly, I want to thank my supervisor Ola Fredin for all the help and conversations during this year. I also want to thank Einar Helgasson of Veidekke for all the information provided, and the tour of the construction site. Thanks to Bent Aagaard who with his expertise has been of great help to me. The presentation Bent gave about the Joberget tunnel during my third year of this degree got me interested in soft ground tunneling and made me want to write my master's thesis on the subject. For help in the laboratory, I want to thank Jon Runar Drotninghaug and Laurentius Tijhuis.

Lastly, I want to thank my classmates. It has been five years of a lot of work but even more fun!

Trondheim, 8th June 2023

Niklas Kjenstadbakk Brede

Contents

List of Figures

List of Tables

1 Introduction

1.1 Background

Norway is a country characterized by its many mountains, which have led to many rock tunnels and a high international level of skill in rock tunneling. Soft ground tunnels, on the other hand, are not as common in Norway. But surrounding some of the biggest cities, especially in the Oslo area and Trondheim, there are large amounts of sedimentary deposits. As the cities grow, the need to utilize the underground also increases. The benefit of being able to build tunnels in soft ground conditions will become even more useful in the future. Experience from operating in soft ground is also important for projects where zones of weak ground are met unexpectedly.

As part of InterCity's investment in Eastern Norway, a new double-track railway is being built from Drammen to Kobbervikdalen. As part of this project, the Drammenstunnel is being built. Work on the Drammen tunnel is still ongoing (spring 2023), and is expected to be completed in the summer of 2025 (Backer 2022). The entire project consists of a $12km$ new double-track railway and the rebuilding of Drammen Station. The tunnel has been driven and is $7km$ long. $830m$ of this tunnel is driven through soil, $540m$ of the tunnel was constructed using the cut-and-cover method and the remaining $290m$ is a true soft ground tunnel. The method used to construct this part of the tunnel is through reinforcing the ground with jet grout.

There is no standard for driving soft ground tunnels in Norway as of today. This is because, in general, not many soft ground tunnels have been constructed in this country. Any project that involves tunnel construction through soil is perceived as advanced and is generally avoided. The projects usually have a foreign party with more experience involved. As a result of little experience and excessively strict requirements, projects can be over-dimensioned. This is not desirable for either time consumption, cost, or environmental emissions. Another reason why projects are over-dimensioned is that it tends to be forgotten that the projects are still a matter of tunnel driving and not just a question of how much load from overlying masses is present. Of course, a tunnels load bearing arch still applies and all the overlying mass can't be considered as "dead weight".

1.2 Objective and questions

The objective of this thesis is to evaluate the steel pipe umbrella-method as an alternative for the construction of the Drammen tunnel. The evaluation will include a feasibility analysis, where the stability and need for support are analyzed for the steel pipe umbrella method. The stability will then be investigated through empirical and analytical calculations before also numerical modeling will be utilized. Another

objective is to compare the cost of the two methods. Important for these analyses is that the input data is as accurate as possible. A sample of the till at the site is collected and a grain size distribution and an XRD analysis will be performed in the laboratory. Since the work on the tunnel already has started the geotechnical parameters of the ground has already been investigated, and the results of these investigations have been used to complete the analyzes in this thesis.
To succeed in fulfilling these objectives research questions have been formulated:

- Could the tunnel have been constructed successfully using the steel pipe umbrella method?
- What measures must be applied for the tunnel to obtain its stability using the steel pipe umbrella method?
- To analyze the stability, analytical, empirical, and numerical methods are used, how well do these methods concur with each other?
- Could the use of the steel pipe umbrella method have made the project more cost-effective?

2 Soft ground tunneling

Soft ground tunnels require more support and specialized techniques to handle the ground conditions. Including the ground conditions of clay, silt, sand, gravel, and till, as well as very weak and or fractured rock. Tunnels like this are most common in urban areas at shallow depths. This is because cities often are located, at least partly, on sedimentary deposits. Soft ground tunnels can also be useful as a landslide measure by constructing the tunnel under talus fields. In the case of driving a rock tunnel unintentionally into a zone of weak ground, the knowledge of constructing soft ground tunnels is valuable.

This chapter is based on the literature study 'Drivemetoder og grunnforhold for løsmassetunneler i Norge' written by the author in the fall of 2022 for the course 'TGB4570 - Engineering Geology, Project Assignment' (Brede 2022).

2.1 Methods of soft ground tunneling

There are a number of methods used for driving soft ground tunnels. In this chapter, the most common will be presented. Equal for all these methods is that they all stabilize the ground around the tunnel profile, and they all have some form of system for controlling the pore pressure gradient. Control of the groundwater is arguably the most important and hardest challenge of building a soft ground tunnel. Lowering the groundwater is the easiest way to solve this problem. This however is not always acceptable because the lowering of groundwater can cause settlement problems at the surface. In special situations, but not uncommon in Norway, quick clay may be close to the construction site. In this case, the consequences of lowering the groundwater could cause a quick clay collapse and disaster.

2.1.1 Jet grouting

Jet grouting is a method used for improving the strength of soil. This is done by spraying a cement-based mixture, together with water, into the ground at high pressure, while drilling into the ground. Thereafter the drill is pulled up, and a grouted pillar is left in the ground.

The pillars can be compared to concrete, of which the soil makes up the aggregates. The strength of - grouted pillars varies depending on the kind of soil they are constructed in, but they are rarely as strong as actual concrete. However, the pillars are much stronger than untreated soil. More specifically, the strength of the pillars is dependent on the pressure, the pull-up speed, the rotation speed, and the properties of the soil. The size of the jet pillars depends on which method of jet grouting is used. There are four methods of jet grouting; J1, J2, J3, and EC1. The difference between the J-methods is the number of nozzles used for spraying mixture, air, and water. The EC1 method removes the soil completely before the hole left in

the ground is filled with actual structural concrete.

Since the soil has a large impact on the resulting strength, a jet grouted pillar can have internal variations. Besides, increasing the strength of the ground, jet grout is relatively impermeable. For that reason, jet grouting can be used for water sealing. This is used in projects where a specific degree of impermeability is required.

The use of jet grouting in connection with soft ground tunnels is usually related to reinforcing an enclosure around the tunnel profile. A jet grout construction like this can be built either from the ground surface or ahead of the tunnel face. Jet grouted pillars can also be established as a measure of groundwater control to keep groundwater away from the tunnel (Jetgrunn 2022).

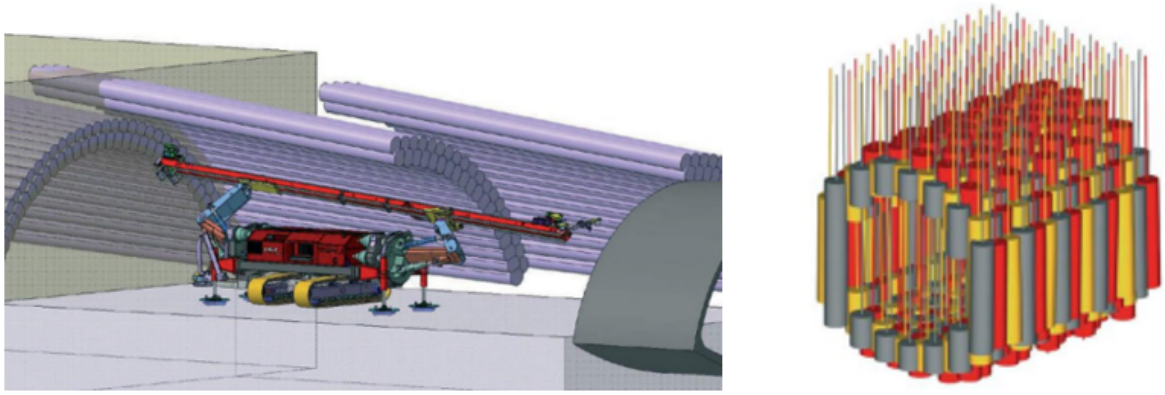

Figure 2.1: On the left, horizontal cone-shaped jet pillars are constructed from the face of the tunnel. On the right, a ring of jet pillars has been constructed by vertical drilling (Hæstad and Backer 2020).

2.1.2 Steel pipe umbrella

The steel pipe umbrella method is a construction method that is used in both soil and weak rock. The method consists of boring steel pipes almost horizontally in front of the tunnel face over the crown of the tunnel. The steel pipe umbrella increases the stability of the soil over the crown of the tunnel by transferring the loads to the longitudinal direction. The steel pipes are self-drilling with a diameter between $100 - 180mm$ and a length of $10 - 30m$ (AG 2015). Together they create a fan-like formation. The fans must overlap to maintain rigidity. In particularly weak ground conditions, a double overlap of the fans can also be established or two steel pipes can be drilled in instead of one. Grouting is then done at low pressure through the steel pipes, this is done to seal the masses in between the pipes as well as improve the stiffness of the steel pipes (Dywidag-Systems 2010).

The advantages of this method are that it is relatively simple and also cost-effective. The steel pipes

can be operated with a normal drilling rig, which means that no special additional equipment is needed. Assessments can be made at the face of the tunnel while driving is ongoing which makes it very adaptable. This method is also one of the quicker ones. However, driving a tunnel with a steel pipe umbrella requires extensive knowledge of the ground conditions, not all ground conditions are suitable. The soil must be stable enough for it to be possible to establish temporary protection before collapses can potentially occur. Using the steel pipe umbrella method when constructing below the groundwater table is a challenge. This is possible but places great demands on water control. Grouting and drainage wells are measures used to control inflow when driving below the groundwater table (Aagaard 2020).

2.1.3 Ground freezing

Ground freezing is a method that can be used in all cases of unstable ground. By freezing the water present in the ground the strength of the ground increases and it becomes impermeable. In the case of constructing a soft ground tunnel, the ground is held stable until the establishment of support is finished. When this is done the system is turned off and the ground begins to thaw. Ground freezing is also used for other forms of construction, including construction pits, shafts, ditches, and as groundwater barriers against, for example, the spread of pollution (GEOFROST 2022).

The ground freezing system consists of freezer pipes that are drilled all around the tunnel profile. An antifreeze liquid circulates through the freezer pipes. The liquid used is often either liquid nitrogen or brine. Nitrogen freezing freezes the ground faster but in return costs more and is somewhat more difficult to set up (Eidesen 2013). After a long enough time, this system has made a zone of the desired sub-freezing temperature around the applicable area. The temperature is an important parameter for calculating the strength of the freezing zone. After the free pore water in the soil has frozen, the bound porewater will eventually also freeze with decreasing temperature. This is the reason why a lower temperature will give a freezing zone greater strength (GEOFROST 2022).

The factors that must be known for the dimension of the frozen zone are (Eidesen 2013):

- **External loads:** Sediment and water pressure from the surrounding ground.
- **Material properties for the frozen soil:** The ability of the soil to conduct heat has a great influence on the freezing rate. The strength of the frozen soil also determines how low a temperature is needed.
- **Size of permanent support:** Requirements for the strength and dimensions of the permanent protection are determined by the external loads and the additional load from firing salvos.
- **Operation plan through frozen zone:** Determining the operating cycle and, in particular, the

section lengths helps to calculate the time consumption for the project. Time consumption is an important factor for calculating costs. The section length also helps to determine how long the frozen ground is exposed before permanent support is established.

It takes time before a frost zone is established and the construction itself must be performed with caution, therefore the method is time-consuming. The cost of freezing is high compared to other ground improvement methods. Ground freezing is therefore often used where other alternatives are not sufficient. An advantage of ground freezing is that the method is well suited to soils of all grain sizes. Although cost largely precludes ground freezing if there are other possible alternatives, the method has several favorable advantages. A low CO_2 footprint is one of them. Resources, energy, and the area of influence are also smaller than when using most other methods (Eidesen 2013).

2.1.4 Cut-and-cover

The objective of this method consists of digging a construction pit before casting a concrete culvert down the pit. After the culvert is finished, it is dug over again. The method is also known as the "open cut"-method. This is the oldest form of constructing a tunnels in soil. But since the method relies on digging from the ground surface it is not a 'true' soft ground tunnel. It is often financially beneficial, but it also has its disadvantages. Excavating an open construction pit disturbs the environment and requires a lot of space. All infrastructure on the tunnel route must be removed. The excavated masses must also be stored somewhere before they are placed back over the culvert. In order to minimize additional costs, it is beneficial for the masses to be stored close to the facility. Although the method requires space, it is commonly used in urban areas. In addition to disturbing the external environment, this form of tunnel construction cannot be done too deep. In order for it to be feasible and at the same time economical, these construction pits are rarely dug deeper than 30 meters. The cut-and-cover method is best suited for shallow tunnels in flat terrain (WSP 2022).

There are two different ways to build an open construction pit, “bottom-up” or “top-down”. Both methods are illustrated in figure 2.2. Bottom-up is the traditional excavation method. Here, retaining walls are first established, before the pit is excavated in sections followed by retaining buoys. When the desired depth is reached, the culvert is cast and the pit is refilled. The "top-down" method also uses retaining walls for excavation, but secant walls or slurry walls are used. These walls function directly as the finished tunnel walls. When the excavation reaches the depth where the tunnel's roof should be, the roof is cast, with an opening so that further excavation can continue deeper. The culvert is now being cast in stages together with the excavation from the roof down to the sole. With this method, approximately half of the pit can also be covered so that traffic can continue as usual on ground level (Railsystem 2022).

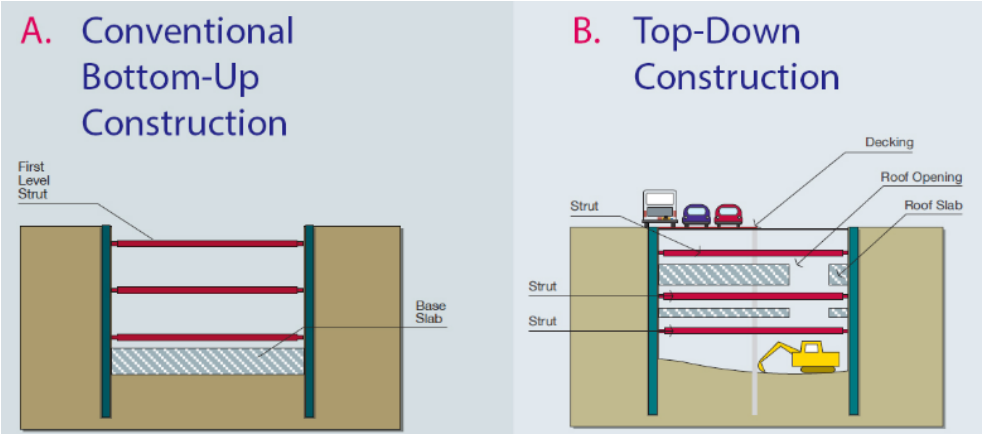

Figure 2.2: A. illustrates the "bottom up" method and B. shows the "top-down" method (Railsystem 2022).

2.2 Soil tunneling in Norway

2.2.1 Quartanary deposits in Norway

Norway's present-day landscape has been shaped over the course of the last 2.6 million years, which corresponds to the geological period of the Quaternary. Preceding the Quaternary were the Neogene era, which commenced 23 million years ago, and the Paleogene era, which started 66 million years ago. At the outset of the Paleogene era, Norway was worn down to a flat terrain, known as the Paleogene surface. Subsequently, the land began to rise, and throughout the Paleogene and into the Neogene era, river valleys, and undulating topography characterized the topography. The Quaternary period witnessed the arrival of glaciers during multiple glacials (ice ages), which further carved the river valleys into the landscape we recognize today. It is believed that there were approximately 40 ice ages throughout the Quaternary period, separated by warmer and ice-free periods. However, only remnants of the last two glacials can be discerned in modern-day terrain, due to the fact that the ice sheet $20,000$ years ago blanketed the entire country and removed almost all of the previous deposits. The most recent ice age is called Weichsel, and the penultimate one is known as Saahlian. Remnants of the Sahle stadial can be found in very few locations in Norway, including Fjøsanger, Karmøy, and Frøya (Ramberg, Bryhni, and Nøttvedt 2007).

In Norway, the most prevalent type of soil is till, which is soil that has been directly deposited by glaciers. The second most common soil type is glacifluvial deposits, which can take the form of either glacial river deposits or glacial lake deposits. Lacustrine deposits follow in third place, and marine deposits are the fourth most common soil type. The abundance of till is what distinguishes the soil of Norway and Scandinavia from that of countries farther south on the continent. Due to the immense weight of the ice sheet, the till can be overconsolidated and possess robust properties. The boundary between soil and solid rock is distinctly demarcated in Norway, with often unweathered basement rocks underlying the glacial

sediments. However, outside of the former glaciations, in southern parts of Europe the transition between sediment and bedrock is often more gradual due to pervasive chemical weathering of the bedrock, which there is the dominant form for soil (Ramberg, Bryhni, and Nøttvedt 2007).

2.2.2 Norway compared to Europe

Soft ground tunnels are more common in Europe than they are in Norway. A simple reason for this is the fact that there is much more soil further south in Europe. Norway consists of approximately 50% exposed bedrock (Palmstrom n.d.), and all of the soil is of Quaternary origin. In Europe, there are more variations of soil, some of which are well-suited for constructing tunnels. Because of this, the professional competence and experience for building soft ground tunnels are higher in Europe outside of Scandinavia.

The Quarternary deposits of Norway and the rest of Scandinavia is young, they have all been deposited during and after the last ice age. The last ice age, Weichsel, came to an end approximately $11,000$ years ago (Ramberg, Bryhni, and Nøttvedt 2007). Quaternary glaciations did not affect the landscape further south in Europe, which means the soils are of different origins and compositions. There are some exceptions, for example in the Alps and the Pyrenees, which were glaciated and Quarternary deposits can be found. Much of the unconsolidated deposits southwest in Europe stem from weathered rock. This soil is much older and has the potential of being accumulated thus having great strength. Quarternary deposits such as overconsolidated till also have great strength but deposits like this are rarely thicker than $5m$ (Halvdorsen 1977). The deposits of Eastern Europe are dominated by loess. Loess is wind-deposited soil with grain size, silt, and fine sand that has accumulated. The loess in Europe mainly comes from the till and glacial outwash plains that used to lay before the ice sheets. With the prevailing wind, the fine grains that had been eroded down by the glacier were transported south of the ice and further east in Europe with the main direction of the wind. Loess deposits can be several hundreds of meters ("Loess in Europe—its spatial distribution based on a European Loess Map, scale 1:2,500,000" 2007).

The most used method for building soft ground tunnels in the world is by Tunnel Boring Machines (TBM). There are two different TBM machines used for soft ground tunneling, Earth Pressure Balance Machines (EPBMs) and Slurry Shield TBMs. The difference between a TBM used in soil opposed to a TBM used in rock is their ability to create overpressure at the tunnel face to keep the soil and the groundwater situation under control (Jakobsen 2014). The reason why TBMs are not used in Norway is that it is not cost-effective for short tunnel lengths. This is mainly because the amount of soil in Norway does not allow for it. Tunnel jacking is another method used for constructing tunnels in soil on the continent. By utilizing large hydraulic jacks, pre-casted tunnel elements are pushed through the ground one by one (*Box jacking* 2022).

2.2.3 Examples of soil tunnels in Norway

The Tyholt tunnel

The Tyholt tunnel is the first modern tunnel in Norway constructed in soft ground. The tunnel's route is below the city of Trondheim. Out of the $2785m$ of the total tunnel, $268m$ goes through soil. The work on the tunnel was first started during the second world war in 1942 by the Germans who occupied Norway at the time. The existing railway was viewed as too vulnerable to air strikes by the occupying forces. Because the ground conditions were so demanding, including sensitive and even quick clay, the work on the tunnel went slow and had many setbacks. The contractors of the tunnel were switched back and forth between German and Norwegian companies. It was not until 1946 any major progress was made when it was decided that the shield method was going to be attempted (Hansen 2016).

The shield method is one of the first methods of constructing soft ground tunnels. It consists of pushing a framework through the soil, before digging the soil out of the individual frames. Behind the framework, there is a tube that holds the masses from the already dug-out tunnel. Behind the tube, a permanent lining is built. The method was invented by Marc Brunel, a French-born engineer that used the method to make the first successful tunnel beneath the Thames. An illustration of Brunel's machine can be seen in figure 2.3. Today this method of constructing a tunnel is outdated, but the principles of shield tunneling are still in principle applicable for TBM tunneling (Dash 2012).

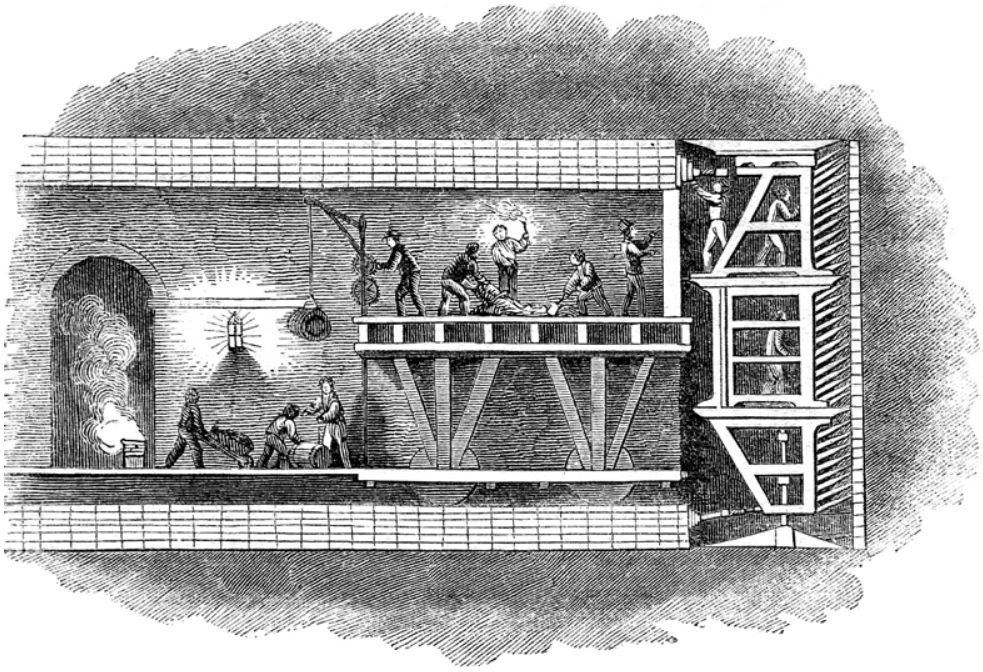

Figure 2.3: The figure shows a drawing of the machine used by Brunel to make the first tunnel underneath the Thames (Dash 2012).

The shield used for the Tyholt tunnel was a cylinder with a radius of $8m$. This cylinder was pushed into the clay by 30 hydraulic pumps that altogether had the capacity to move $2000ton$. The shield was pushed $75cm$ before the clay was dug out by hand. This process can be seen in figure 2.4. Behind the cylinder, a lining of bricks was built. When the mortar between the bricks was dry the shield could be pushed another $75cm$. This way the tunnel had a progress rate of $4.5m$ a week (Hansen 2016).

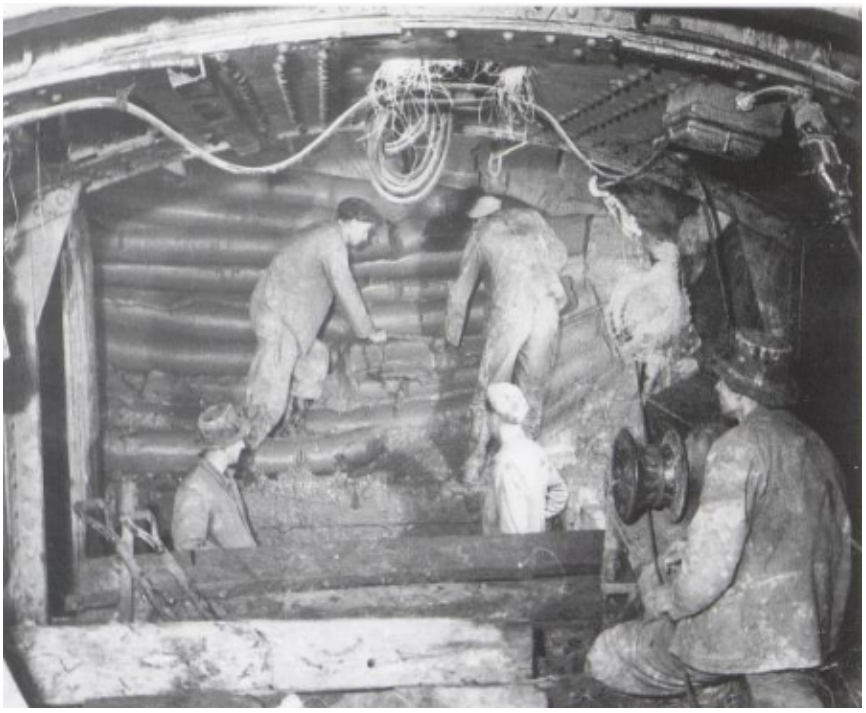

Figure 2.4: The picture was taken of workers digging out the clay at the face of the shield. The upper part of the shield can be seen in the upper part of the picture (Hansen 2016).

Even though there was extensive drainage of the clay before the shield tunneling was started about half of the Tyholt tunnel length had to be done under affixed air pressure. By installing air pressure locks, the face of the tunnel could be under the pressure of as much as $2atm$ which was enough to hold the water and soil masses out of the tunnel. Despite this, there were many instances of unfortunate events during the construction. There were several clay slides, one case of fire at the tunnel face, and several cases of diver sickness (decompression sickness) as a result of the workers moving in and out of increased pressure. The tunnel was finalized in 1950, but because of poor finance the rails were not laid and the tunnel was not open for traffic until 1957. The tunnel is today only used for some freight trains as well as for turning trains around (Hansen 2016).

The Oslofjord tunnel

In 1997, the work on a tunnel beneath the Oslo fjord was started. The tunnel is a subsea tunnel and is $7.2km$ long. The geology the tunnel goes through is mainly pre-Cambrian gneisses. The preliminary

investigations done in the tunnel planning phase were refraction seismic, core samples, and seismic tomography. The result showed that the rock had been deformed and altered, and there were several weak zones and one fault zone. A stretch of the geology and the weakness zones can be seen in figure 2.5. The most critical weakness zone was the zone with the least rock coverage just outside of Hurum. After further investigations, it was concluded that the zone could be run through with the standard procedure. When construction came close to the zone, tests from the tunnel face revealed that the zone consisted of soil. The construction was stopped $15m$ from the zone (Andreassen 1999).

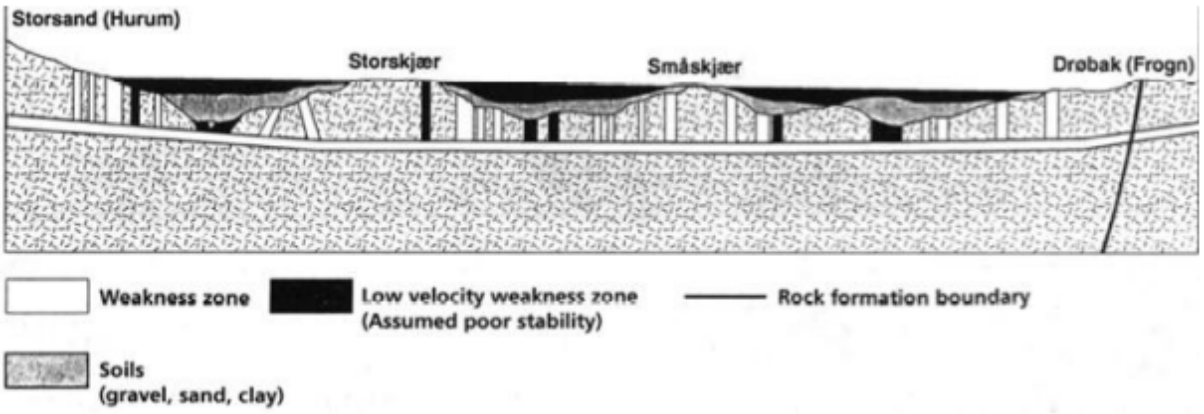

Figure 2.5: Longitunal section of the Oslofjordtunnels route with the results of the preliminary investigations (Andreassen 1999).

Since it was not possible to avoid the problematic zone, a bypass tunnel was made under the zone. Access was now available from both sides of the tunnel. The contractor together with a group of consultants decided that the best and safest way to get through the zone would be by ground freezing. It was estimated that the freezing zone had to be able to hold full water pressure of $1.2MPa$, as well as $0.2MPa$ of earth pressure. This meant that the freezing zone had to reach a temperature of -28°C. To make this happen two rows of freezing pipes were installed, altogether 115 pipes. It took 18 months from the zone being detected until it was ready to be excavated. The zone was excavated using normal drill and blast procedures, although a special kind of explosives made for cold temperatures was used. Full concrete lining was installed as the permanent lining. The soil zone extended the project for two years. The tunnel opened for traffic in the year 2000 (*FREEZING 120 MBSL IN THE OSLOFJORD SUBSEA TUNNEL* 2022).

The Strindheim tunnel

The Strindheim tunnel is a $2.5km$ long tunnel located in central Trondheim. From the western entrance, the tunnel is built by a cut-and-cover construction of $330m$ before it goes into rock. The area of the construction pit consisted of sensitive clay, lots of traffic, and infrastructure, as well as some protected

buildings of high historic value. The consequences of failure were therefore high, as was the difficulty of the project. The project is regarded as one of the most complex construction projects completed in Norway, and in 2014 it won the prize "Construction Project of the Year" (Harald Inge Johnsen 2011).

There were set high demands for minimal water leakage into the pit, this was done to ensure the stability of the sensitive clay. The chosen retaining walls used were pipe walls with a new lock in-between system. This new lock was optimized to be as impermeable as possible. To ensure that the border between the pipes and the rock was waterproof it was grouted cement through the bottom of the pipes. The pipes themselves were also filled with cement where it was needed. In the areas where sensitive clay was in contact with the pipes, the clay was jet grouted to increase the friction between the two materials. To make the sensitive clay in the construction pit manageable, it was mixed with a lime and cement mixture. This made the process of digging the clay out of the pit easier by doubling the shear strength of the clay. As the digging went on, bracing beams were installed to replace the tensions removed. When all the masses of the construction pit were removed a square cement culvert was cast. Thereafter the pit was filled with fill mass and infrastructure and traffic could return. The cut-and-cover construction of the Strindheim tunnel is a complex form of bottom-up construction (Gylland 2012).

The Joberget tunnel

With the exception of the Tyholt tunnel, the Joberget tunnel was the first planned true soft ground tunnel in Norway. The steel pipe umbrella method was used in this project. The tunnel is located in Voss and is built in connection with the avalanche safety measure project on E39. The first $100m$ of the tunnel goes through glacial till. This construction approach was chosen because of the risk of rock avalanches in the area above the entrance.

After the preliminary investigations, the use of the steel pipe umbrella method was chosen. Despite being below the groundwater table, this method was evaluated as possible because of the compact till of high strength. As a measure for water control, there were multiple drainage wells installed. It was also found that the sole of the tunnel would be in rock throughout the whole length, which stabilizes the tunnel further. The rock mass in the tunnel sole was good-quality phyllite.

Seven fans of steel pipes were installed in the tunnel roof, all fans overlapping with $3m$. After the installation of a fan, cement was grouted through the steel pipes. In posterity, it was discovered that this did not improve neither the stability nor impermeability of the surrounding till. The excavations were done in sections of $1m$ in the heading. After three sections of excavations in the heading, the bench succeeded in sections of $4m$. After each section, shotcrete was applied with a reinforcing mesh or reinforced shotcrete. The tunnel was finished and opened for traffic in 2016 (Langåker 2014).

The Kronstad tunnel

The Kornstad tunnel is a pedestrian tunnel in Bergen. The entire tunnel is $465m$ long and around $45m$ of the tunnel goes through soil. A unique detail of this tunnel is that its path goes straight under a cemetery. Both ground freezing and steel pipe umbrella methods were considered for the construction. By considering flexibility and minimizing disturbance of the surrounding area the steel pipe umbrella method was chosen.

The steel pipes installed were $12m$ long and were only installed over the crown of the tunnel. $1m$ sections were excavated at a time before it was secured immediately with shotcrete. Displacements was a major concern, therefore instruments were installed to measure displacement every fourth meter in the tunnel and every fifth meter on the surface. Alarm values for settlement both in the tunnel and on the surface were established. When these values were violated improvement of the lining was carried out. Despite caution regarding displacements, a collapse occurred in the tunnel during construction. $15m^3$ of sediments and debris from the cemetery fell into the tunnel, the slide also incorporated a grave (Kristine Hausberg Kjeilen 2022). A picture of the collapse can be seen in figure 2.6.

Figure 2.6: Picture of the avalanche in the Kronstad tunnel (Marita RamsvikKyrre Kjellevold 2022).

3 Method

To answer the research questions, a comprehensive methodology was employed. Firstly the area of interest was investigated. The geology, geotechnical parameters, and groundwater situation were studied through desk studies. Much of this information was obtained from previous reports of the area, but also from aerial photos from norgeibilder and specific geological maps provided by NGU (NGU 2023a; norgeibilder 2023). The construction site was visited on 28.03.2022, and a tour of the site, as well as useful experience-based information, was given by Einar Helgasson from Veidekke AS. A sample of the excavated till was brought back to the laboratory in Trondheim. A grain size distribution and an XRD analysis were performed on the sample.

With an understanding of the ground conditions of the area, the design of the steel pipe umbrella and plan for the construction of the tunnel was carried out. When designing the steel pipe umbrella the ground conditions are of the utmost importance. Also, empirical experiences from Norway and the rest of the world have been of great use. Especially the experiences from the Joberget tunnel which shares many similarities to the Drammen tunnel were useful. The planning consisted of dimensioning the steel pipe umbrella, planning excavation sections, subdividing the tunnel face, support of the tunnel, and how the groundwater could be dealt with. The plans made at this stage are qualified guesses and assumptions that will be modified and confirmed when further calculations are carried out.

After an initial plan for how the project was to be carried out, more detailed planning was to be started. Starting with simple analytical solutions and moving on to more complex solutions through numerical modeling. The analytical solutions are done to get a first-order impression of how the ground will react to the excavation of a tunnel. Keep in mind that these analytical solutions are for an initial impression and simplifications are made. For example, ground improvement of the steel pipe umbrella is not considered.

With a first-order understanding of the ground response and support pressures needed, detailed calculations and testing is done through numerical modeling. The numerical modeling is executed in the software RS2 provided by Rocscience. Combining the parameters obtained and the design made, stability of the tunnel is examined at two locations as cross-sections and one longitudinal section. A comprehensive study of variables is done where the influence of groundwater, different parameters, and the different field stresses are studied. To estimate the need for support an analysis where the thickness of support liners was also carried out.

A summarized discussion of the proposed method is then presented. Results of both the analytical and numerical calculations are compared to each other and assumptions for the project made earlier in the

thesis. Following this, the cost of the proposed execution of the project is then estimated. The cost of the current execution of the project is also estimated so that the two can be compared. To conclude, final results obtained and further recommendations for similar projects are given.

In figure 3.1, a flowchart of the methodology of the study done for this thesis is found.

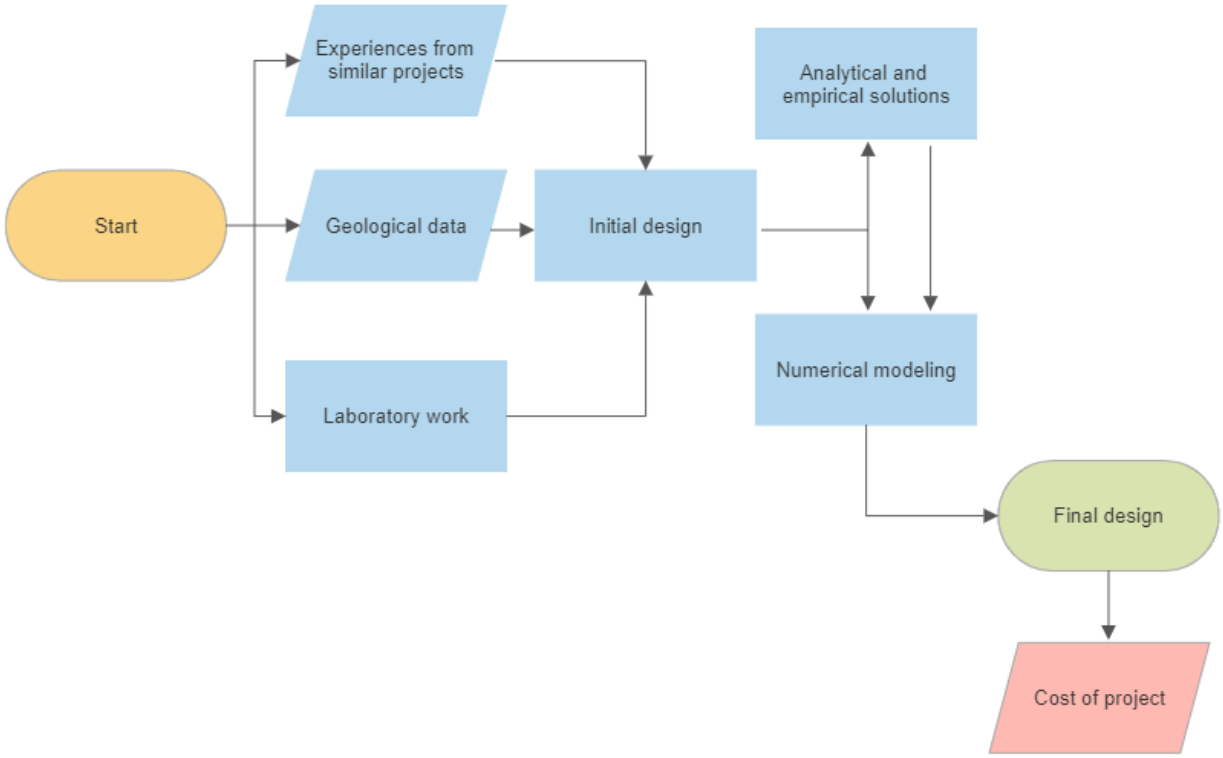

Figure 3.1: Flowchart of the methodology of the thesis.

4 The Drammen tunnel

4.1 Introduction

The Drammen tunnel is part of the project Drammen-Kobbervikdalen which consists of $12km$ of double-track railway between Drammen and Kobbervikdalen. A map of Drammen is viewed in figure 4.1, and the project can be seen in figure 4.2, UDK02 is marked as a black rectangle. This development will transform the railway track between Oslo and Tønsberg, Hamar, and Fredrikstad into a continuous double-track with a speed standard of $250km/h$. The project is estimated to cost 13 billion NOK and will be opened for traffic in 2025. The Drammen tunnel stretches over the approximately $7km$ distance between Drammen Sation and Gulskogen Station. The construction of this distance is sub-divided into three contracts (Backer 2021):

- UDK01 - $6km$ of rock tunnel
- UDK02 - $540m$ of cut-and-cover tunnel and $290m$ soft ground tunnel
- UDK03 - Development of Drammen Station

Figure 4.1: A map of Scandinavia highlighting Drammen (Google 2023).

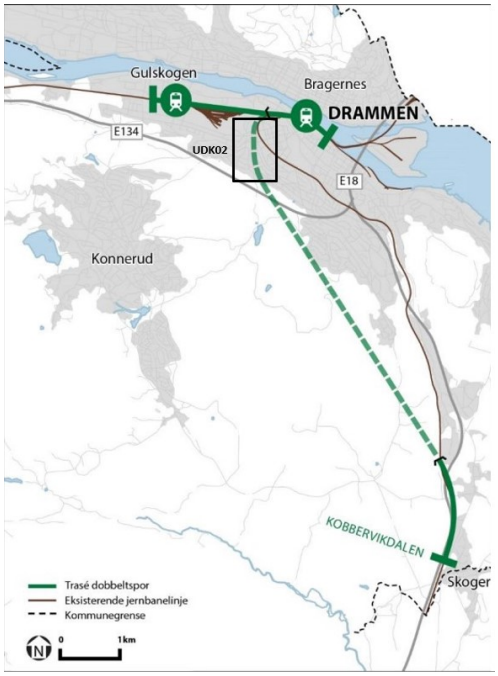

Figure 4.2: Map viewing the project of UDK02 (Hæstad and Backer 2020).

BaneNor granted UDK02 through a competitive tender. It started with a dialogue phase where parties that were present met and discussed technical solutions, timelines, economy, and organization of work. The dialogue phase then lead to a tender procedure where the contract was awarded competitively. Veidekke

entrepenør AS was given UDK02 on the premise of their solution of using jet grouting around the tunnel to keep the cavity free from water and stabilize the ground during excavation. As with other projects involving soft ground tunnels in Norway, there was a criterion of cooperation with a foreign constructor with experience in the field. Therefore, the international consulting firm ILF Consulting Engineers partook in the design and planning of the tunnel.

4.2 Geology of the area

The area of interest is situated bordering soil and igneous rock, this can be seen in figure 4.3 which shows an excerpt from NGU's bedrock database, the route of the tunnel is shown as the black line going straight through the red rectangle (NGU 2023a). The depth to bedrock at the separation of the railways is $100m$ and decreases to $15 - 25m$ at the transition from soil-to-rock tunnel. The igneous rock in this case is rhomb porphyry. In figure 4.3 rhomb porphyry is viewed as purple. The bedrock is estimated to follow the slope of the ground surface. The soil of the area is till. Above the layer of till there is a thinner layer of topsoil, the thickness of this layer is approximately $1 - 2m$. There is a thin layer of marine clay between the bedrock and the topsoil in the lower region of the route. This layer of marine clay continues north and is barely in the tunnel route. The properties and characteristics of both the rhomb porphyry and the till are described in detail in chapter 5 and later in this chapter.

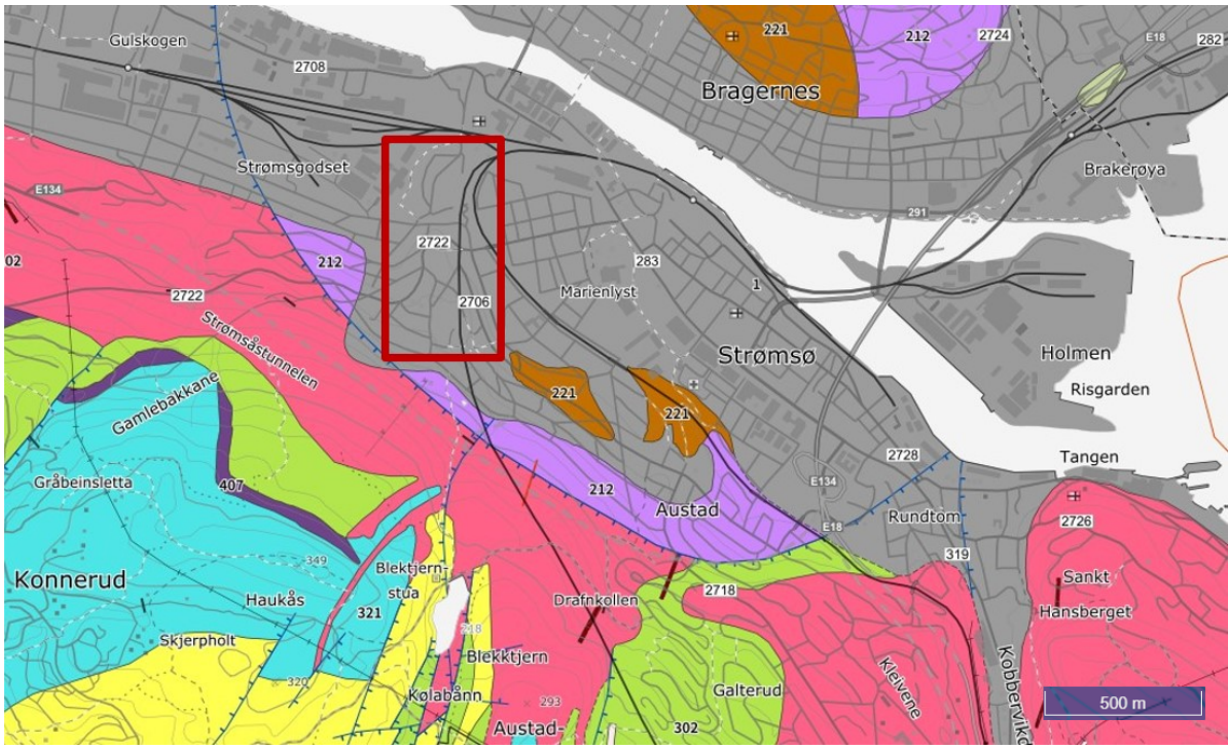

Figure 4.3: Bedrock geology of Drammen. The area of UDK02 is highlighted as a red rectangle (NGU 2023a).

From where the rail tracks separate and southwards the terrain rises and forms a ridge. At the separation, the layer of marine clay is $15m$. The thickness of the marine clay decreases further south and is only present at the very start of the tunnel route. The till is assumed to be last deglaciation ice-contact deposits. During the deglaciation, the ice would be in direct contact with the sea, below the marine limit, and glaciofluvial material was transported under the ice and deposited at the ice front. Material of finer grain sizes was transported further and deposited as marine sediments in the fjord. The ice-contact deposits make up a ridge in the north-south direction and pinches out under marine clay in both the eastern and western directions. The ice-contact has its distal side in the east and its proximal side in the west, making the slope in the western direction steeper. This can be seen in figure 4.4 where the thickness of the marine clay deposits in the area is shown (Norconsult 2018b).

The groundwater level was estimated to be approximately $5m$ above sea level, increasing a bit upwards in the terrain together with the bedrock surface. This correlates to $0.5 - 3m$ above the bedrock surface. The reason for the inconsistency is due to the groundwater level changing with the weather. Because of concern for settlements in the marine clay, but also for unstabilizing potentially sensitive clay, lowering the groundwater table was not allowed in this project.

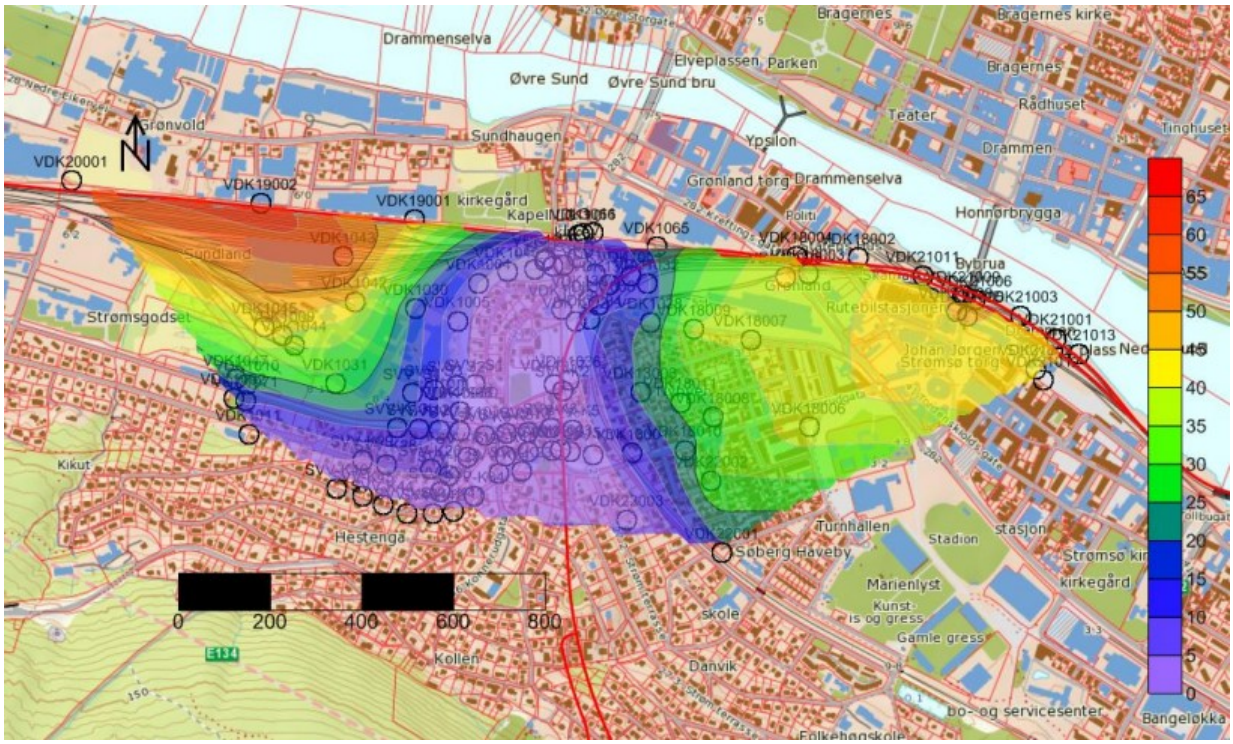

Figure 4.4: Thickness of the clay deposits in meters in the UDK02 area.(Norconsult 2018b)

4.2.1 Rhomb porphyry

Rhomb porphyry is a type of igneous rock that is only found in only five places around the world (NGU 2023b). It is characterized by its distinctive texture consisting of large rhomb-shaped crystals, known as phenocrysts. The phenocrysts exist because the melt did not have time to fully crystallize before emerged at the ground surface. A close relative of the rhomb porphyry is the Larvikite which is made from the same melt but the crystallization process finished underneath the ground. The phenocrysts are typically mainly composed of feldspars and are typically white or light-colored and stand out against the darker matrix. The matrix of rock rhomb porphyry is often made up of fine-grained dark red feldspar and quartz minerals. This type of rock is commonly used in construction as a decorative stone (NGU 2023b).

In figure 4.5 a picture of one of the core samples from borehole "Rock_4" is presented. An overview of the different boring holes can be found in the appendix B.1. The rhomb porphyry at the site in Drammen is composed of a finely-grained silicate matrix that is dark red in color, punctuated by sporadic phenocrystals of alkali-feldspar. The joints in the rock are typically rough and undulating, although some of them are more planar. In certain areas, the rock material appears discolored, and small cavities measuring $2 - 15mm$ are present. The joints and some of the cavities are filled with hard minerals.

Figure 4.5: Core sample from "Rock_4", box 2, $32.5 - 35.25m$, the rock core is dry at the top of the picture and wet at the bottom (NGI 2022).

4.2.2 Glacial till

Till is a soil type that is formed as a result of glacial activities. It is essentially a mixture of rock debris, sand, silt, and clay that has been deposited by glaciers. Till has a varying degree of coarseness and grain size distribution. It is often associated with mountainous regions and can be found in areas that have experienced significant glacial activity in the past, such as Scandinavia, the Alps, and northern North America. In figure 4.6 a core sample of till from borehole "Rock_5" is presented. The till of the site can be described as deposits of terminal moraine. It contains little fine-grained sediments, with a percentage of less than 10%. The finer-grained sediments were transported further away from the ice contact. The till generally consists of much sand with an average of 58% (Norconsult 2018a). More details regarding the properties of the till will be provided in the subsequent chapter.

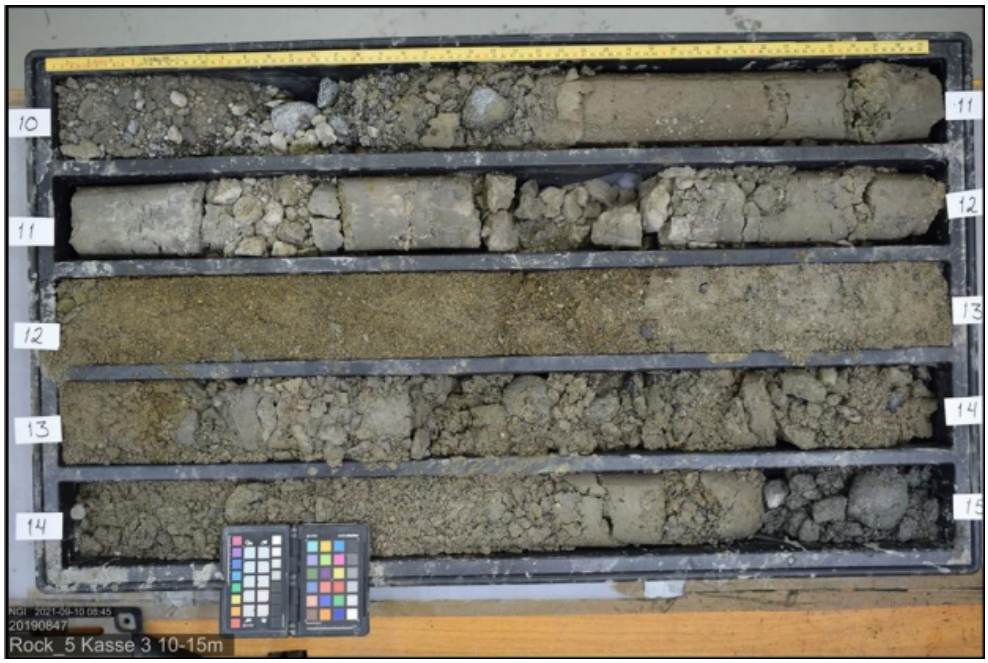

Figure 4.6: Core sample from "Rock_45", box 3, $10 - 15m$ (NGI 2022).

4.3 Geotechnical parameters

Extensive investigations of the site have been carried out. The investigations include total soundings, core samplings, grain-size distributions, and geophysical tests carried out with georadar, ERT, MASW, and refraction seismic. An overview of the locations of the profiles and wells can be found in appendix B.2. The surveys done to find the grain size distribution, unit weight, and seismic velocities were executed by Ruden AS Geo Solutions in 2017.

4.3.1 Grain size distrubion

Based on the report NGI (2022) Ruden conducted a total of 165 grain size distribution measurements and plotted them as grain size distribution diagrams. The grain size distribution of well #25 is presented in figure 4.7, together with its USCS classification. The rest of the grain size distribution curves for the wells bored by Ruden is found in appendix B.

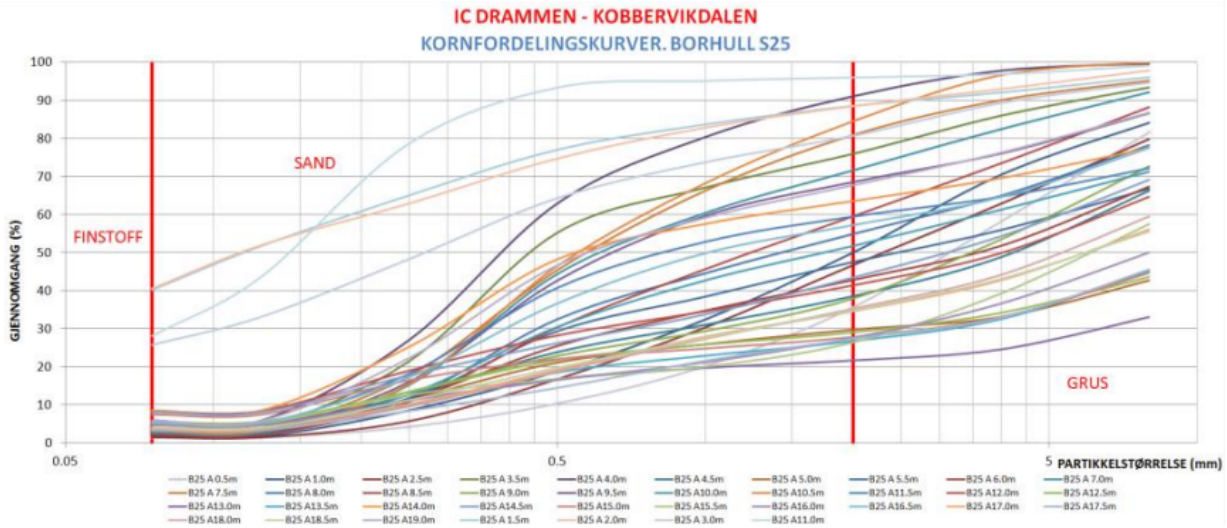

Figure 4.7: Grain size distribution of wells bored by Ruden AS Geo solutions (NGI 2022).

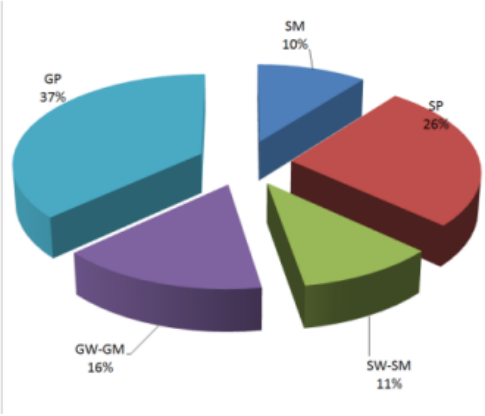

Figure 4.8: USCS-distribution of well #25 (NGI 2022).

Table 4.1: The Unified Soil Classification System (USCS)

Symbol	Description
GP	Poorly graded gravel
GW-GM	Well-to-medium graded gravel
SM	Silty sand
SP	Single graded sand
SW-SM	Well-to-medium graded sand

Taking all grain size distribution curves into consideration 84% of the samples show a fine-graded content under 10%. On average the sand contents are leading with 57%. There are however uncertainties regarding the disturbance of the samples.

4.3.2 Unit weight

The unit weight is measured at 0.5 meter depth intervals in wells #15, #17, #22, #23, #24, and #25, see B.2. The unit weight is found through the matrix's density and porosity. These parameters are found through textural analysis of the samples collected from each borehole. The survey employs the method of Chapuis (2012) to estimate the minimum and maximum void ratio (e) of the formation using the uniformity coefficient (CU) and the roundness factor (RF). The roundness factor of a sample can be determined by analyzing representative subsample of individual grains. Each grain is categorized into one of six roundness categories, with an associated roundness factor between 0 and 1. This evaluation is typically performed by observation and comparison to a reference chart. A roundness factor chart can be found in the appendix, B.3. The uniformity coefficient is found through grain size distribution of the samples. The diameter corresponding to 10% and 60% finer, found in the grain size distribution curve is used to calculate the uniformity coefficient (NGI 2022):

$$C_u = \frac{D_{60}}{D_{10}} \tag{4.1}$$

The void ratio for each sample is then given by (Chapuis 2012):

$$\begin{aligned}\frac{1}{e_{max}} = \; & [-0.1457RF^3 \text{ - } 1.3857RF^2 + 1.9933RF \text{ - } 0.0931]ln(C_u) \\ & + [4.3209RF^3 \text{ - } 8.6685RF^2 + 5.9588RF \text{ - } 0.1552]\end{aligned} \tag{4.2}$$

and

$$\begin{aligned}\frac{1}{e_{min}} = \; & [7.9767RF^3 \text{ - } 14.623RF^2 + 8.8518RF \text{ - } 0.721]ln(C_u) \\ & + [21.319RF^3 \text{ - } 32.949RF^2 + 17.206RF \text{ - } 1.0033]\end{aligned} \tag{4.3}$$

The maximum and minimum porosity can now be determined (NGI 2022):

$$n = \frac{e}{1+e} \tag{4.4}$$

Through XRD analysis, the mineralogy of the samples can be evaluated. The samples are divided into large, $d > 0.5mm$, and fine, $d > 0.5mm$, grains. The procedures of an XRD analysis are further presented in chapter 5. When the rock is known, the known density of this rock is then multiplied by the percentage of rock (NGI 2022). In figure 4.9 the density of the samples is presented together with the

E-modulus.

4.3.3 Young's modulus

Young's modulus (E-modulus) curves have been found for the same wells used to find the density of the soil. The dynamic E-modulus is obtained by combining the unit weight found down each well and the values of V_p from seismic surveys done close to the specific well, and the Poisson's ratio (Subsurfwiki 2023). The dynamic Poisson's ratio then also has been used, and it is estimated to be $\nu = 0.45$, following Norconsult (2018a).

Dynamic Young's modulus is measured under a dynamic loading condition, where the load is applied rapidly to the material. The dynamic Young's modulus represents the ratio of stress to strain in the dynamic response of the material. The static E-modulus is what applies to the design of the Drammen tunnel, as the till material should be considered to respond elastically to the applied load (Gheibi and Hedayat n.d.).

The static Young's modulus, on the other hand, is measured under a static loading condition, where the load is applied gradually and held constant for a period of time, allowing the material to deform elastically. The static Young's modulus represents the slope of the stress-strain curve in the linear elastic region of the material (Gheibi and Hedayat n.d.).

V_p, ν, and ρ are used to evaluate Young's dynamic modulus at $0.5m$ intervals down each well using the following approach (Subsurfwiki 2023):

$$E = 3K(1 - 2\nu) \tag{4.5}$$

Where K is the bulk modulus and ν is the Poisson's ratio. The bulk modulus is found using the P-wave velocity, V_p, and the unit weight, ρ (Subsurfwiki 2023):

$$K = \frac{M(1 + \nu)}{3(1 - \nu)} \tag{4.6}$$

Where M is the P-wave modulus found by multiplying the unit weight and the P-wave velocity squared (Subsurfwiki 2023):

$$M = \rho \cdot V_p^2 \tag{4.7}$$

Ruden calculated the E-modulus by the use of the S-wave velocity. A problem with using the value for the velocity of shear waves is that the soil is unsaturated, meaning the waves will go through some voids with water. Shear waves do not go through water, leaving elevated values for V_s. This is not the case for

P-waves, which do go through liquids. To account for this Ruden calculated a new V_s directly from the V_p value. In this thesis, the E-modulus was calculated avoiding the use of V_s (Gheibi and Hedayat n.d.).

After using equation 4.5 to calculate the dynamic E-modulus, Alpan (1970) approach is used to find the static E-modulus. This approach divides the dynamic E-modulus by 4 to find the static E-modulus:

$$E_{sta} = \frac{E_{dyn}}{4} \tag{4.8}$$

The calculations done for well #25 are presented below in figure 4.9. This well is one of the wells that initially should obtain the most accurate results as the seismic profile L10 runs very close to the well.

Well 25 & L10

Depth	Vp (m/s)	ν	M(Pa)	K(Pa)	Unit weight(kg/m^3)	E-dyn (MPa)	E-sta (MPa)
0.5	359.8	0.45	253410198.3	253410198.3	1957.5	76	19
1	359.8	0.45	256219394.4	256219394.4	1979.2	77	19
15	603.5	0.45	766666786.3	766666786.3	2105	230	58
2	603.5	0.45	782218649.3	782218649.3	2147.7	235	59
2.5	603.5	0.45	743648572.1	743648572.1	2041.8	223	56
3	603.5	0.45	793108595.6	793108595.6	2177.6	238	59
3.5	603.5	0.45	709995360.2	709995360.2	1949.4	213	53
40	603.5	0.45	696847297.9	696847297.9	1913.3	209	52
45	740.1	0.45	1196062555	1196062555	2183.6	359	90
5	740.1	0.45	1225805272	1225805272	2237.9	368	92
5.5	740.1	0.45	1185874442	1185874442	2165	356	89
6	740.1	0.45	1183519125	1183519125	2160.7	355	89
6.5	740.1	0.45	1083938537	1083938537	1978.9	325	81
7	740.1	0.45	1090894937	1090894937	1991.6	327	82
7.5	740.1	0.45	1083828987	1083828987	1978.7	325	81
8	740.1	0.45	1143916944	1143916944	2088.4	343	86
8.5	740.1	0.45	1135865048	1135865048	2073.7	341	85
9	740.1	0.45	1169825425	1169825425	2135.7	351	88
9.5	740.1	0.45	1115379273	1115379273	2036.3	335	84
10	740.1	0.45	1174536058	1174536058	2144.3	352	88
10.5	740.1	0.45	1079392229	1079392229	1970.6	324	81
11	740.1	0.45	1107656026	1107656026	2022.2	332	83
11.5	740.1	0.45	1133947930	1133947930	2070.2	340	85
12	740.1	0.45	1172016417	1172016417	2139.7	352	88
12.5	740.1	0.45	1196938951	1196938951	2185.2	359	90
13	740.1	0.45	1201594810	1201594810	2193.7	360	90
13.5	740.1	0.45	1188229758	1188229758	2169.3	356	89
14	740.1	0.45	1134824327	1134824327	2071.8	340	85
14.5	740.1	0.45	1192118769	1192118769	2176.4	358	89
15	740.1	0.45	1205976794	1205976794	2201.7	362	90
15.5	740.1	0.45	1194912284	1194912284	2181.5	358	90
16	740.1	0.45	1190858949	1190858949	2174.1	357	89
16.5	740.1	0.45	1133235858	1133235858	2068.9	340	85
17	740.1	0.45	1164676594	1164676594	2126.3	349	87
17.5	2561.8	0.45	14158626228	14158626228	2157.4	4248	1062
18	2561.8	0.45	14184221223	14184221223	2161.3	4255	1064
18.5	2561.8	0.45	14159282510	14159282510	2157.5	4248	1062
19	2561.8	0.45	13401276888	13401276888	2042	4020	1005
					2098	310	77

Figure 4.9: Young's modulus and unit weight calculation of well #25.

The average unit weight down the well is:

$$\gamma = 2098kg/m^3 \tag{4.9}$$

The average static E-modulus down the well is:

$$E_{sta} = 77MPa \tag{4.10}$$

The calculations for wells #17 and #24 can be found in the appendix B. The average of these three wells' geotechnical parameters is: The average unit weight:

$$\gamma = 2009kg/m^3 \tag{4.11}$$

The average static E-modulus:

$$E_{sta} = 77.5MPa \tag{4.12}$$

The availability and accuracy of the P-waves is the primary factor of uncertainty for the calculation of the E-modulus. Another uncertainty source is the calculation of the unit weight, as there is used an average of the minimum and maximum void ratio. The quality of data collected for wells #22, #23, and #15 was of poor quality and was therefore not included in the study of the E-modulus.

4.4 Groundwater situation

Having information on the groundwater situation is crucial when constructing a tunnel in soil because groundwater can have a significant impact on the construction process and the tunnel's long-term stability. Pore water pressure on the tunnel face can cause serious instability problems during construction. High water pressures can also cause uplift forces, leading to upward displacement of the tunnel. The groundwater can also cause damage to the tunnel lining if not properly managed. This damage can lead to leaks, which can reduce the structural integrity of the tunnel over time. Therefore, it is essential to have accurate data and control over the groundwater situation (Jones 2022).

4.4.1 Groundwater table

There have been bored 20 wells in soil and three rock wells in the area around UDK02 for mapping and monitoring of groundwater levels. The location of wells is shown in figure B.10 in appendix B.

The measurements from the tensiometers were done to investigate the groundwater level of the area as

well as for mapping the seasonal changes in the groundwater. The measurements were carried out at 7 wells located in the area most relevant to the UDK02. The time frame of the measurements was from February 2017 to April 2018. A graph illustrating the groundwater level at the different wells towards the height above sea level can be seen in figure 4.10. The columns in the graph show the monthly precipitation (Norconsult 2018b).

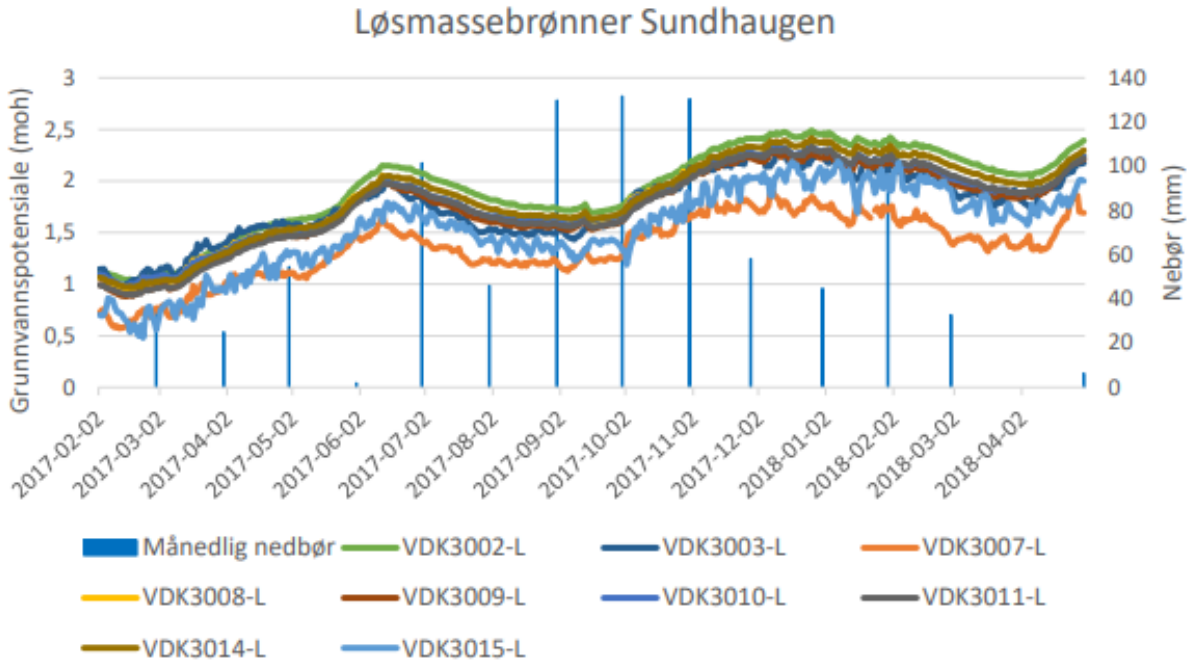

Figure 4.10: Graph of the groundwater table in the area of the soil tunnel.

A strong correlation can be observed among most of the wells, where groundwater levels vary from an approximate elevation of $+0.9$ during February 2017 to an elevation of $+2.5$ by December 2017. Generally, the groundwater tends to increase following periods of rainfall and snowmelt and decrease during dry spells. It can be observed that the water table follows the slope of the bedrock.

4.4.2 Hydraulic conductivity

Using the grain size distribution the hydraulic conductivity can be calculated with the Gustafsons method (Svensson 2014):

$$K = E(C_u) \cdot (\frac{d_{10}}{1000})^2 \tag{4.13}$$

Where:

$$C_u = \frac{d_{60}}{d_{10}} \tag{4.14}$$

The hydraulic conductivity values calculated for the samples range between $8.8 \cdot 10^{-9} m/s$ and $8.6 \cdot 10^{-3} m/s$. About half of the samples have a hydraulic conductivity that falls between $1 \cdot 10^{-}4 m/s$ and

$4 \cdot 10^{-}4m/s$, with a median value of approximately $2 \cdot 10^{-}4m/s$. The porosity values calculated for the samples vary between $7 - 23\%$, with a median value of 14%(Norconsult 2018b).

There is also a bored one pumping well for the purpose of conducting a pumping test. The location of the pumping well is in the till close to the transition from soil to rock on the tunnel route. When a pumping test is performed, water is pumped in a steady state for an hour to a day. Observational wells nearby are then studied to see how the water levels changes by the pumping. Through the Theim equation parameters such as hydraulic conductivity can be found (Svensson 2014).

$$K = \frac{Qlog(\frac{r_2}{r_1})}{1.366(h_2^2 - h_1^2)} \tag{4.15}$$

Where r_1 is the distance to the nearest observation well, and r_2 is the distance to the furthest. h_x is the saturated thickness at the given observation well, and Q is the pumping rate. The three pumping tests done at Drammen gave the values $1.19 \cdot 10^{-4}m/s$, $1.57 \cdot 10^{-4}m/s$, and $2.34 \cdot 10^{-4}m/s$ for hydraulic conductivity.

Permeability testing done in the laboratory has been conducted by Norconsult. At the wells, VDK15001 and VDK15021 soil samples of 3-depth intervals have been tested. The results of the testing can be seen in tables 4.2 and 4.3 (Norconsult 2018b).

Table 4.2: Results of permeability testing for well VDK15001.

Depth (m)	K (m/s)
$5 - 16$	$2.76 \cdot 10^{-5}$
$28 - 32$	$9.25 \cdot 10^{-5}$
$38 - 42$	$4.78 \cdot 10^{-6}$

Table 4.3: Results of permeability testing for well VDK15021.

Depth (m)	K (m/s)
$1 - 4.5$	$2.93 \cdot 10^{-5}$
$15 - 21$	$5.86 \cdot 10^{-7}$

4.5 Execution of the project

Veidekke's solution to the project was by utilizing jet grout to make a ring around the tunnel to stabilize the masses and keep the groundwater out of the tunnel. Because interference with the groundwater was not allowed, this was seen as the safest option. The first $540m$ of the Drammen tunnel however is constructed as a cut-and-cover construction (Backer 2021).

The cut-and-cover portion of the tunnel was constructed using sheet pile walls to form the construction pit. The material in the pit included both clay and till. Although some of the clay was quick, it did not pose any problems during construction. However, in the final $70m$ of the pit, sheet piles could not be used due to the presence of larger-scale rocks in the till. Instead, cast-in-place reinforced concrete walls, known as secant pile walls, were used. To prevent water leakage at the connections between the secant piles, jet grouting was performed. Jet grouting was also carried out in the bottom of the pit to keep water from entering the pit. To make excavation of the clay masses easier, they were stabilized with lime-cementing. Steel beams were then installed as the pit was excavated to account for the pressure of the excavated masses. Two rows of steel beams were needed in the pit. Once the excavation was complete, a culvert was cast and the pit was filled over. The construction followed a bottom-up cut-and-cover approach and can be considered a classic example of this technique. Figure 4.11 shows a photo taken by the author on November 28, 2022, looking into the construction pit where the secant pile walls transition to the soil tunnel (Backer 2021). More pictures taken by the author can be found in the appendix D.

Figure 4.11: Picture of the entrance of the soft ground tunnel taken from inside the construction pit.

The ground was improved in connection with the soil tunnel using vertical jet grouted piles from the surface. A cylinder of jet grouted piles was created to stabilize the soil and form a waterproof construction to keep the tunnel dry. To maintain the stability of the tunnel face during excavation, three jet grouted piles were also constructed in the middle of the tunnel's cross-section. The construction was divided into 11 chambers, separated by a continuous wall of jet grouted piles, as shown in figure A.1, and A.2 in the appendix that illustrates a longitudinal section of the jet grouted pile structure and the chambers. The purpose of this was to drain the chambers before excavation began, ensuring that they did not encounter any water. When attempting to drain the first chambers, almost no water was pumped up. Digging through the material confirmed that it was almost completely dry, despite preliminary investigations indicating that the groundwater table should have been approximately in the middle of the profile (Backer 2021).

Based on the preliminary investigations, the entire soil tunnel is situated in till. This till turned out to be well-suited for making jet grouted piles. The minimum requirement for the strength of the piles was $2MPa$. Samples of the piles were taken for testing in the laboratory. The laboratory tests were carried out by SINTEF. The achieved USC strength of the piles had an average of $9.37MPa$ and a maximum value of $20.81MPa$. Although the stability of the soil was not a problem, it made the excavation process tougher (BaneNor 2021).

When the rock was encountered in the sole of the tunnel during driving, there was discovered a compact layer of clay of approximately $1m$. This clay layer was not mapped during the preliminary investigations. The discovery of this layer was concerning because clays tend to hold water. A layer of water holding clay could in the worst-case scenario cause a collapse in the tunnel. The clay layer was investigated and turned out not to hold significant amounts of water, the driving could therefore be continued without measures (Backer 2022).

The tunnel cross-section was divided into three sections for excavation: heading, bench, and sole. The first $10m$ from the tunnel was a massive block jet piled block. Since the jet piles achieved such a high level of strength, it was time-consuming to spike through the block. To begin with, the excavation length was $1.3m$before temporary protection in the form of steel arches and shotcrete with mesh reinforcement was established. Shotcrete, armor, and bolts were also used to secure the tunnel face in addition to the three jet piles. Throughout the excavation process, the tunnel was systematically measured and monitored using displacement gauges, with additional monitoring carried out on the surface. No measurements exceeded $5mm$. When $50m$ of excavation was completed, the stability was better than anticipated, so the section length was extended to $2.1m$ (Backer 2022).

The entire heading was excavated before work commenced on the bench. After all sections had been

excavated, the tunnel was more or less circular in shape. Temporary lining was immediately installed to secure the tunnel, and permanent lining was put in place after the entire tunnel had been excavated. To make the tunnel stable and waterproof, fiber cloth and a PVC membrane were first installed, followed by $30cm$ of reinforced concrete around the profile. This permanent lining was designed to withstand full earth and water pressure from the surrounding masses (Backer 2022).

Since the permanent lining was designed to withstand full earth and water pressure the jet grout structure was not considered to be part of the support when designing the final lining. Neither the jet piles nor the temporary lining was counted as a support measure. Including the jet grouted piles and the temporary lining as part of the permanent lining was not permitted by the client. An argument for this is that the jet piles do not have a sufficient lifespan for them to be considered permanent support.

5 Laboratory work

The laboratory work consisted of a grain size distribution and an XRD test. The work was carried out at the rock mechanic laboratory at Petroleum Teknisk Senter, NTNU.

5.1 The sample

The sample on which the tests were performed comes from the excavated mass from the soil tunnel collected at the construction site. As described in chapter 4.5 there are jet grouted vertical piles in the profile to ensure the stability of the tunnel face. This means that when the tunnel is excavated they dig through both till and jet grouted piles. There is for that reason a significant probability that some of this jet grout is included in the sample. Because of this, an XRD analysis was performed. In addition to showing the mineral composition of the excavated soil, the XRD would give an estimate of how much grout the sample held.

5.2 Grain size distrubution

The sample taken from the construction site in Drammen had a dry weight of $5255.2g$. With the largest grain diameter of well over $45mm$, according to the ISO standard 17892-4:2016 a sample of $20kg$ shold then be used (*ISO 17892-4:2016 Geotechnical investigation and testing – Laboratory testing of soil – Part 4: Determination of particle size distribution* 2016). In order to make the measurement as accurate as possible without the sufficient amount of sample material, the material below $4mm$ was split down to a smaller amount. After the sieving of the split sample was completed, the proportions in each fraction were multiplied by the ratio between the weight of the split sample and the weight of the original sample for the material below $4mm$. This ratio was found to be 7.345.

Some of the material with a larger grain diameter clearly had cement surrounding it. This material was removed from the sample. The material accounted for $409g$, this material can be seen in figure 5.1.

Figure 5.1: Material covered by grout removed from the sample.

5.2.1 Method

Wet-sieving After the material that was visibly covered by jet grout had been removed from the sample, it was wet-sieved. Wet-sieving was carried out to try to wash the smaller particles from the larger ones, as it was observed that smaller particles had formed a coating around the larger ones. Standard sieve sets with square meshes and distilled water were used. The material was flushed through the sieves, starting with the largest sieve. The material that went through the sieve was then flushed through the next sieve. After the sieving using the smallest sieve was done the material was put in the drying cabinet in their respective fractions.

Dry-sieving

After the samples had dried completely, the sieves were assembled in a shaking machine. The shaking machine was activated for a duration of 10 minutes. Once the shaking process concluded, the sieves were sieved by hand to ensure proper separation. After the completion of the dry sieving procedure, the respective fractions were transferred to labeled sample bags and weighed. The fraction with particle sizes smaller than $0.063mm$ was put into the container containing the rest of the fraction $< 0.063mm$ obtained from the wet sieving process.

5.2.2 Results

The results were obtained by graphing the cumulative percentage of the material of the respective grain sizes, against their grain size. In figure 5.2 the grain size distribution graph is presented. The points along the curve refer to the values of material at each sieve. In figure C.1 the appendix the spreadsheet used to calculate the grain size distribution.

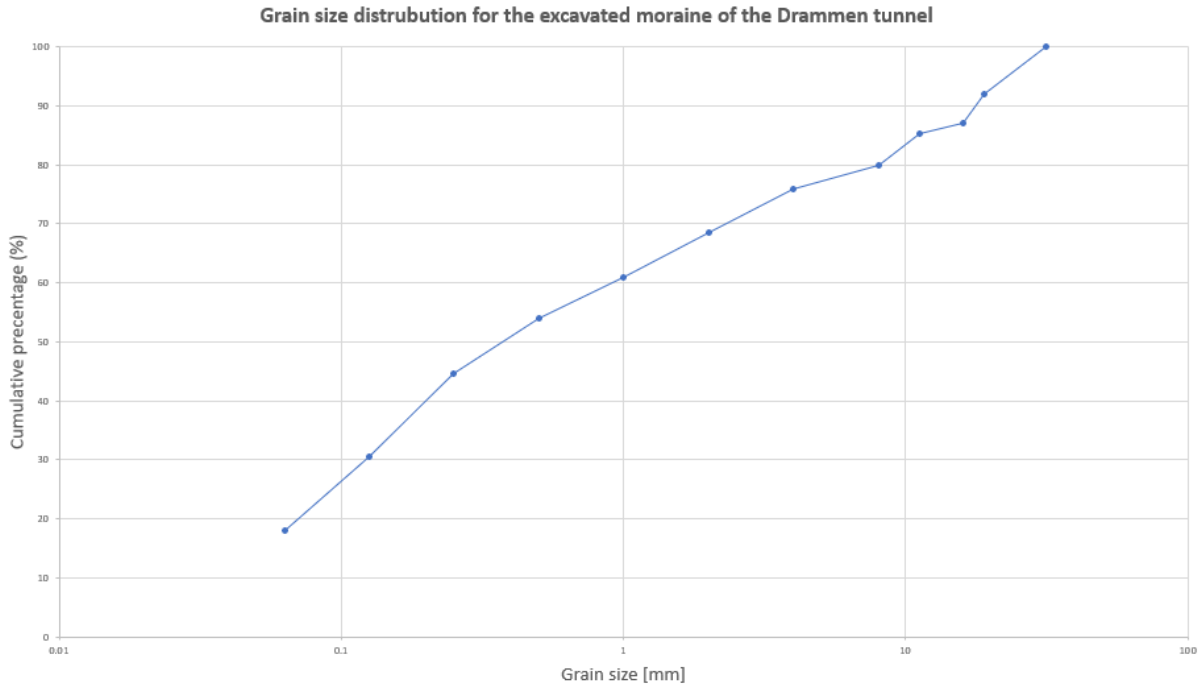

Figure 5.2: Grain size distribution of the excavated material of the Drammen tunnel.

5.2.3 Discussion

The resulting grain size distribution clearly proves that the soil is of till material. The grain sizes range from under $0.063mm$ to blocks bigger than $25cm$. The larger blocks were excluded when the sample was obtained so they did not get an unproportionate part of the distribution graph.

The obtained graph measures up well with the previous test performed by Ruden, found in figure 4.7. The majority of the material is in the sand fraction, which makes up 43% of the sample. 32% of the material is larger than the sand fraction, and 18% is finer. The fraction of fines is larger than most of the previous tests. The extra amount of fines are believed to be grout from the jet grouted piles. Even though the sample was thoroughly washed before the sieving to try to separate the grout from the grains some of it did not wash off, as seen in figure5.1. Since the grout is of such fine grain sizes it adds to the amount of fines in the sample.

Another plausible reason for the increased amount of fines is that the sample comes from already excavated masses. The excavation of the tunnel is done by heavy machinery through pricking and excavators. The process of excavation could break down the grains into smaller pieces. The fact that the sample is undoubtedly heavily disturbed compared to the closer-to-in-situ samples taken by Ruden can be the reason for the increased amount of the fraction sizes smaller than $0.063mm$

5.3 XRD

The XRD analysis is conducted on the fraction less than $0.063mm$*.*

5.3.1 Theory

XRD analysis is a quantitative test used to identify the minerals present in a sample. It works by detecting the interference that occurs when X-rays are reflected from the crystal lattice of the mineral. It is governed by Bragg's law, which states (Ali, Chiang, and Santos 2022):

$$n\lambda = 2d \cdot \sin\theta \tag{5.1}$$

Where n is an integer, λ is the wavelength, and d is the lattice spacing characteristic of the individual minerals. The instrument sends X-rays into the sample at varying angles of incidence. Then registers reflexes at the corresponding angle of incidence measuring θ. By measuring θ knowing the values of n and λ, it becomes possible to calculate the lattice spacing and compare it to standard curves. This comparison allows the determination of the specific minerals present in the sample. The mineral phases are identified using the software "Diffrac.eva." For mineral quantification, the program "Topas" is utilized, implementing Rietveld's method. Rietveld's method utilizes the least-squares approach to refine a theoretical line profile, adjusting it to nearly match the measured profile. The refinement process continues until the theoretical line aligns with the measured line using the least-squares criterion (Ali, Chiang, and Santos 2022).

5.3.2 Method

Prior to the testing, the sample of fines underwent crushing and was grounded using a disc mill. This is done to ensure the suitability of the machine. The sample must be crushed and ground to a particle size below $10\mu m$. The quantification method employed is based on Rietveld analysis and carried out utilizing the Bruker-provided D8 Advance machine. The machine ran for approximately 1 hour before finishing.

5.3.3 Results

In table 5.1 the results of the XRD analysis are presented. The diffractogram can be seen in figure 5.3.

Table 5.1: Precentage of minerals in the <0.063mm-fraction of the sample.

Mineral	Precentage [%]
Quartz	39
Alkali feldspar	13
Plagioclase	11
Amphibole	7
Calcite	6
Mica	6
Pyroxen	3
Chlorite	2

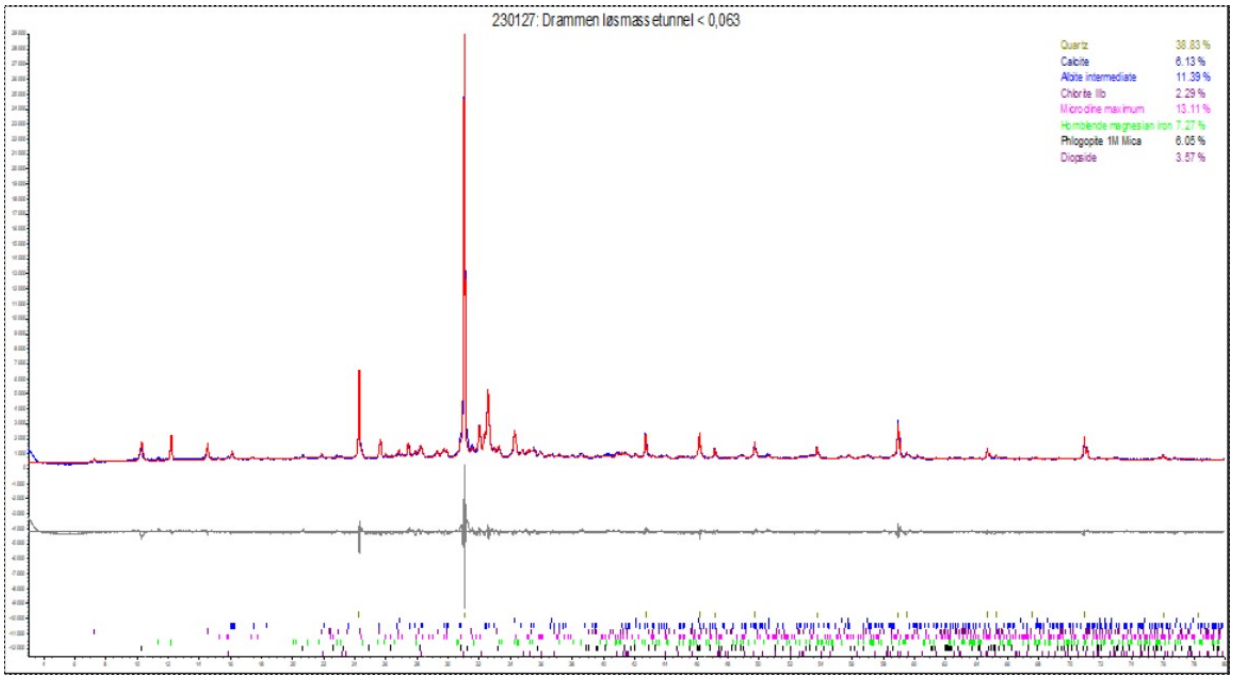

Figure 5.3: Result of the XRD-analysis.

5.3.4 Discussion

The results of the XRD analysis do not reveal a large amount of minerals associated with grout. Indicating that the washing of the sample was more successful than first expected. And also that the larger amounts of fines are due to the mechanical forces the sample has been exposed to. An amount of 39% quartz is found through the XRD analysis. Quartz is a hard and durable mineral. For the sake of stability for the tunnel, this is positive. But for the actual excavation of the tunnel quartz is hard on the equipment and the excavation will be more time-consuming.

6 Application of the steel pipe umbrella method

6.1 The method

The steel pipe umbrella arch method is the most flexible, feasible, and efficient pre-reinforcement technique available. It is easy to execute and suitable for various types of ground conditions. The method is an alteration of the more traditional spiling method. The pipe umbrella method and spiling share certain similarities as their main principle of spiling ahead of the tunnel face. However, when it comes to challenging ground conditions, the pipe umbrella method offers several advantages. For instance, steel pipes can be installed simultaneously with the case-drilling method to prevent borehole collapse. Additionally, the stiffer and larger diameter steel pipes used in the pipe umbrella method can take on heavier loads compared to the pipes used for spiling. The pipe umbrella method also allows for more accurate drilling because of the more robust pipes, bored lengths can reach $15 - 20m$ without deviation. The most significant advantage of the pipe umbrella method is the ability to inject grout through the steel pipes and surrounding material. The New Austrian Tunneling Method (NATM) is usually the construction method used in combination with the steel pipe umbrella method (Tan 2005).

Essentially, the pipe umbrella acts as a reinforced arch that transfers the ground load above the tunnel to the installed support. Steel pipes are installed to form an arch in the shape of an umbrella around the tunnel crown. After the steel pipes are installed they are grouted with concrete to further improve their stiffness. Thus, stabilizing the tunnel face area in both transverse and longitudinal directions. This pre-reinforcement technique improves ground conditions and contributes to the final stabilization of the permanent lining by limiting displacements (Tan 2005). The installation of the pipes with their grouting also lowers the permeability of the surrounding ground. This is crucial when water inflow is arguably the biggest concern when using the method. It is essential to note that it is the liner that carries the tunnel. The steel pipes simply distribute the weight more efficiently and increase the stability of the tunnel in a longer time perspective significantly. A typical choice for the liner is a combination of wire mesh, lattice girders, and shotcrete.

The construction of the arch is done by drilling almost horizontally in front of the tunnel face. The steel pipes are usually self-drilling with diameters normally ranging between 100-180 millimeters and a length of $10 - 30$ meters (AG 2015). The length and thickness of the steel pipes vary depending on the ground conditions. The most common length used is $12 - 15m$. This is usually sufficient for weak rock and courser-grained soil. In cases of fine-grained soil such as clay longer pipes can be applied. An important aspect of a pipe roof structure is that the umbrellas must overlap to maintain their rigidness. In cases of particularly weak ground conditions, a double overlap of the umbrellas can also be established or two steel

pipes can be drilled where there normally only is one (Dywidag-Systems 2010). A picture illustrating how the steel pipe umbrella arch could look can be seen in figure 6.1.

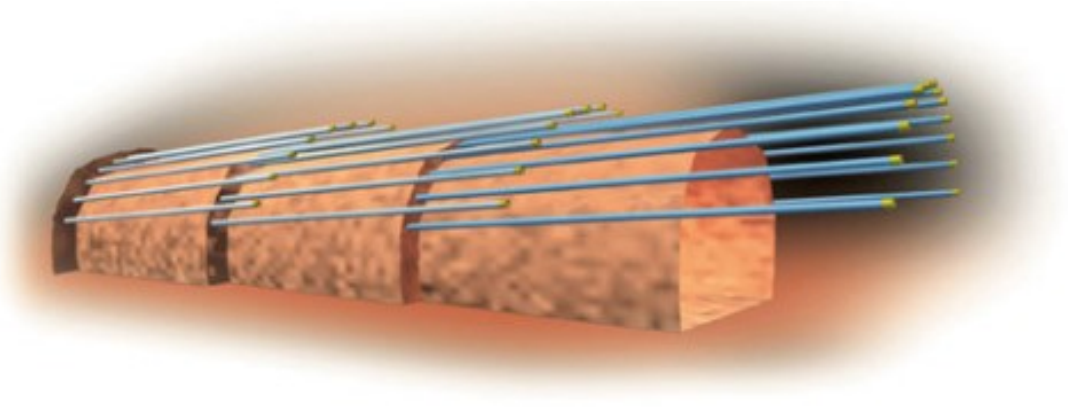

Figure 6.1: A 3D-view of a steel pipe umbrella construction (Tan 2005).

6.2 Application for the Drammen tunnel

The dimensioning of steel pipe umbrella support systems lacks widely accepted and standardized design rules at present. Rather, there have been developed some standard guidelines through common practice (Volkmann and Schubert 2011). When proposing the implementation of the steel pipe umbrella method for the construction of the Drammen tunnel there are several factors to consider. First and foremost the ground conditions must be suitable for the method. On account of the site investigations and testing associated with the construction of the tunnel, this is believed to be the case. The ground conditions are to a certain degree similar to the conditions of the Joberg tunnel. Both tunnels are located in tightly packed till under the water table. The experiences of Joberget could therefore be utilized. The ground conditions of the two projects are similar, a table comparing the parameters of the till in the two projects can be seen in table 6.1. Since the Joberget tunnel was a very successful project some of the designs are imitated. Keep in mind that the method is highly flexible and adaptations are easily implemented. To keep control over the stability of the tunnel while constructing monitoring must be utilized. Both inside the tunnel and on the ground surface.

Table 6.1: Comprason of the geotechnical parameters of the till at Drammen and Joberget.

Parameter	**Drammen**	**Joberget**
Unit weight [kN/m^3]	20	23
Young's modulus [MPa]	77	50
Poisson's ratio	0.3	0.35
Friction angle [°]	40	39
Coheison [kPa]	5	0.17

6.3 Sectioning

To minimize the displacements of the tunnel while excavating the excavation process is divided into sections. There are numerous ways of sectioning out a tunnel face. One of the most common forms of sectioning is to divide the tunnel face into a heading and a bench. This approach is considered sufficient in Drammen because of the relatively sturdy till. If the ground conditions were weaker the tunnel face could be considered divided into even more sections. In figure 6.2, a cross-section illustrating the face of the tunnel being constructed with the steel pipe umbrella method.

The excavation length of each section is a typical dynamic decision. A standard approach is to begin carefully with short section lengths. For thereafter assess if the ground conditions could allow for an increase of the section length. Therefore, the section length at Drammen would initially be $1m$ for the heading. After four sections of the heading are excavated, the excavation of the beach follows. Meaning the excavation length of the bench would be $4m$.

6.4 Dimentions of the steel pipe umbrella

Extent of umbrella

The first umbrella of steel pipes would be installed into the till as the first action of construction. The area which the umbrella would cover, at least the crown of the tunnel must be covered. The question however if the umbrella should follow down the walls of the tunnel. Even if the stiffness of the lining in the walls could be improved by having the umbrella reach down the wall of the tunnel, the steel pipes would provide minimal lateral weight distribution. Because of this, and further investigations done by numerical modeling, the extent of the steel pipe umbrella is decided to cover predominantly the crown of the tunnel. The umbrella is installed at an angle of approximately $150°$ from the center of the tunnel. The angle of $150°$ was also found by Tan (2005) to generally be the preferred angle of coverage.

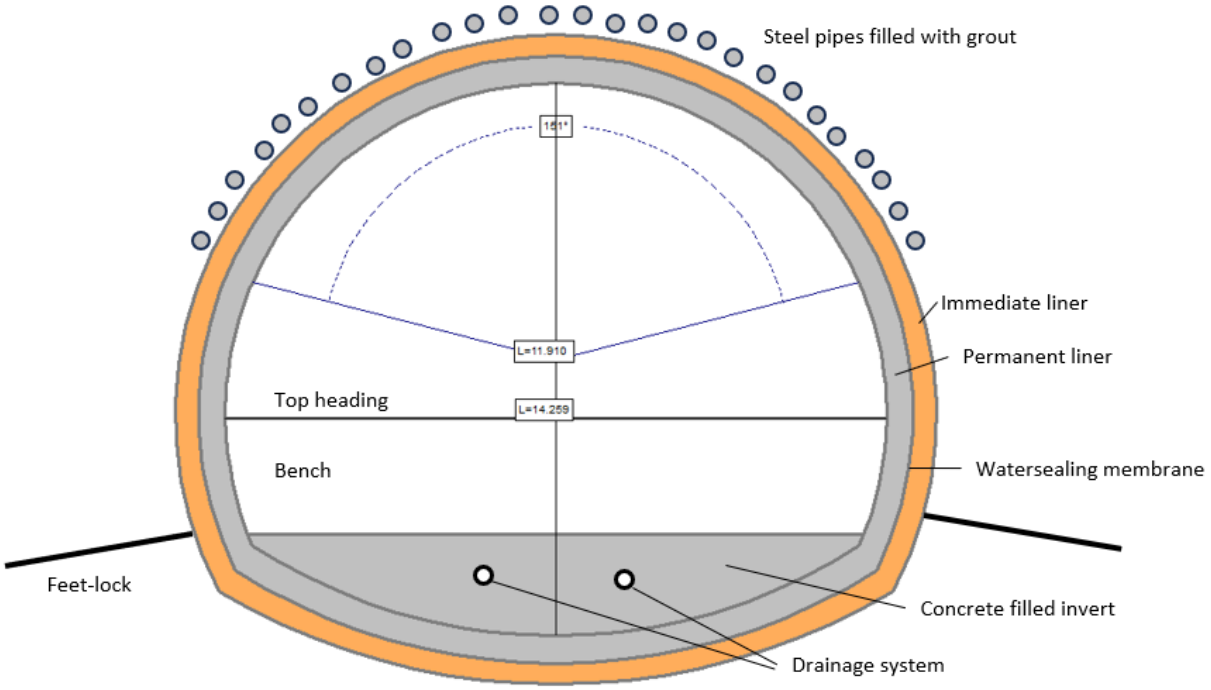

Figure 6.2: Cross section of the planned construction.

Length, overlap and number of pipes

The length of the steel pipes can differ between $10 - 30m$. The most common length for courser-grained soils however is $12 - 15m$ as previously mentioned. The chosen length for the Drammen tunnel would be $15m$. This length is long enough to distribute the weight horizontally in an effective way and at the same time short enough to not be a problem installing. Drilling steel pipes into till can be challenging due to the presence of larger rocks within the soil. The larger rocks can block or deflect the pipes from their path.

The steel pipes are installed at an angle of 5 degrees to the tunnel axis. This is done to make room for the drilling of the next umbrella underneath the first one, with that ensuring the important overlap of the umbrellas. An overlap of $4m$ should be sufficient for a pile length of $15m$. After the pipes are installed they are grouted with concrete. In most ground conditions the grout would pass through the pipes and fill the voids in the ground outside of the pipes as well. By doing this a zone outside of the steel pipes themselves would have improved stiffness and lower permeability.

The steel pipe umbrella system is attained from a manufacturer that has different sizes to choose from. The system chosen for the Drammen tunnel is produced by the American company DSI Tunneling LLC and is named the AT-Pipe Umbrella System. The model best suited for Drammen is the system with a $114mm$ diameter and a wall thickness of $8mm$. This system is suitable for medium-sized tunnels and is considered to be the largest diameter needed for the project. The wall thickness is the thickest possible for the system

to increase the stiffness of the pipes. This choice is made because of the increased difficulties of drilling in till. As a less stiff pipe would bend off from its path easier than a stiffer one. This was experienced at Joberget where pipes of $6.3mm$ were used (Asgeir S. Gylland 2017). The spacing between the holes, center to center, is set as the same as Joberget at $0.4m$. The spacing usually differs from $0.2 - 0.6m$ (Tan 2005). In table 6.2 the specifications of the AT-114 system are listed. Based on the spacing and dimensions of the steel pipe umbrella there is going to be 2.5 pipes per meter.

Table 6.2: Spesifications of the steel pipe umbrella system chosen for the Drammen tunnel.

AT -114	**Value**
Length [m]	15
Weight [kg/m]	21
Diameter [mm]	114
Wall thickness	8
Max elastic momentum [kNm]	23.6
Overlap [m]	4
Inclination	5
Spacing [m]	0.4

Since the piles' length is $15m$ and the excavation of the bench is carried out in sections of approximately $4m$, the installation of the next umbrella will be done after three sections of bench excavations, where the last bench is only $3m$. This was considered when calculating the section length of the bench.

The flexibility of the method is important to remember when designing the umbrella. The fact that it is easy to make changes to the initial plan gives room for starting off conservatively. As construction moves forward assessments can be done and decisions to be more impetuous can be made. The extent of the umbrella, excavation length, and pipe spacing are all variables that could easily be changed to speed up construction time and lower the budget.

6.5 Support

The choosing of support lining for a tunnel constructed with the pipe umbrella method it is crucial that this lining is of the capacity to withstand the confining pressures of the ground around the tunnel. Compared to tunneling in stronger rock, the support for soil and weaker rock masses has to be able to carry loads and prevent displacement rather than reinforce the tunnel profile. Therefore, the method is most commonly used in combination with steel supports, shotcrete, concrete lining, foot piles, jet grouting, and fiberglass face reinforcement (Tan 2005). This lining has to be the first lining installed because the need for support is immediate.

The choice of lining for the Drammen tunnel is steel supports in the form of lattice girders in combination

with reinforced shotcrete. Lattice girders are made of steel and consist of a series of intersecting bars welded together to form a grid-like structure. They are installed transversely across the tunnel and are fairly easy to install and cheap compared to the alternatives. Because the tunnel is fully in soil, in contrast to many other tunnels constructed by this method, a feet-lock should be applied. The feet-lock is made of steel pipes or bolts and is placed in the ground close to the tunnel foot. Its end is securely attached to the bottom of the lattice girders. When the feet-lock pipe is set up, it can bear the weight from the ground above the tunnel foot and minimize the settling of the lattice girders (Chen et al. 2019). The effect of the feet-lock can be seen in figure 6.3. Support of the invert is also needed. Lattice girders in a closed circle could be an option. Reinforced shotcrete, or filling the invert with concrete are also possible solutions. Which choice is the better one depends on the relationship between stability, economy, and environmental impact. The support of the tunnel and the invert in particular will be further studied in chapter 8 which will decide the best option.

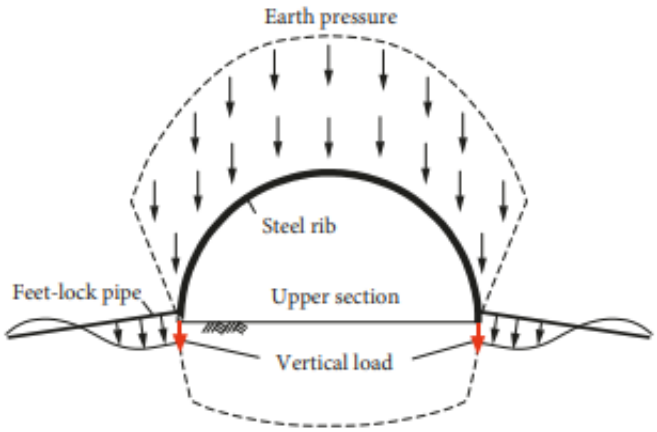

Figure 6.3: The effect of utilizing feet-locks (Chen et al. 2019).

Since the ground conditions are dominated by such compact till the use of bolts could be utilized. normally in soft ground conditions, bolts are not an applicable option but because of the tightly till, it could be an option (Bent Aagaard, verbal communication, 12.04.2023). The type of bolt would need to be a self-drilling bolt as a bored hole would collapse. Drammen till could be strong enough for the effect of bolting. The decision on whether bolting should be used or is even needed at all should be made after further testing with bolts in the specific ground conditions of Drammen.

Face support of tunnels constructed in soil is of utmost importance. The majority of collapses occur at the tunnel face (Spyridis and Proske 2020). Especially in cohesionless soil support of the tunnel face is needed. Soils of high cohesion, such as unsaturated clays, can at the right conditions stand rather stable vertically. This is not the case for the till of Drammen. The support of the Drammen tunnels face will be

done with reinforced shotcrete and face bolts. Face bolts are the most common type of face support in relation to the steel pipe umbrella method (Volkmann and Schubert 2009a).

After the tunnel is fully excavated a permanent concrete lining can be installed. This measure should not be critical if the immediate lining is dimensioned correctly. From a long-term perspective, a concrete permanent lining adds to the safety factors benefit. Therefore, especially in Norway where the construction of soft ground tunnels is a new technology, it is a demand from the contractor.

6.6 Groundwater control

The presence of groundwater can cause serious stability problems while constructing tunnels in soft ground. This is because groundwater causes physical deterioration of soil grains and reduces effective confining stress due to pore water pressure. In situations where tunnel construction is carried out below the groundwater table, the tunnel can act as a drain. As a result, the groundwater table can be lowered, leading to severe surface settlements.

There are various ways of dealing with groundwater-related problems. A common approach is to install a groundwater drainage system to pump water out of the ground and lower the water table, thereby reducing pore water pressure and stabilizing the soil. Grouting, ground freezing, cut-off walls, jet grouting, and geotextiles are also effective methods to control groundwater inflow and stabilize the ground. Each of these techniques has its own advantages and limitations, and the selection of the appropriate method depends on factors such as ground conditions, water table level, and available resources. A combination of different techniques may also be required in some cases to achieve the desired level of groundwater control and tunnel stability (Karimi, Sabetamal, and Ajalloeian 2021).

In the case of the Drammen tunnel, severe problems related to groundwater are not expected on the basis of the preliminary investigations with a permeability of $5.5 \cdot 10^{-7} m/s$ and a porosity of 14%. Despite this prediction, to ensure proper seepage of the tunnel an impermeable membrane should be added between the immediate and permanent lining. The drainage system will lead the water to the membrane through pipes installed parallel to the steel pipes. This way pore water won't build up against the lining. There could also be discussed whether lowering the groundwater should be allowed. The strict demand to not lower the groundwater is related to the concern of disturbing sensitive clay located close to the Drammen city center. If lowering the groundwater at the site actually would affect the soil in the city center is rather unlikely.

7 Analytical and empirical methods

7.1 Employment

When designing a tunnel in soft ground the most common way of assessing tunnel-induced ground deformations is through empirical calculations and numerical modeling. Empirical calculations are self-explanatory based on empirics, meaning they are based on observed real-life data. Because the ground does not always behave alike even for similar ground conditions, it is important to not fully trust the results of the empirical calculations. The results should be considered as a whole and be used together with other calculations done on the project (Jones 2022).

The weight load on a tunnel located in soil is shaped like a cone above the crown of the tunnel (Bent Aagraad, Verbal Communication, 12.04.2023). When doing calculations on the deformations caused by tunneling the weight load is an essential factor. The crown of the tunnel is also one of the areas where displacements can be expected. The invert of the tunnel is also an area where displacement might occur when the whole tunnel profile is located in soil. Since the Drammen tunnel is rather shallow, with a maximum overburden of approximately $27m$, there is decided to use full weight load in the calculations. Meaning the weight load is not shaped like a cone, all weight above the tunnel is regarded as weight affecting the tunnel. In addition to the low overburden, this is done to make more conservative calculations.

The Q-system is the popular choice of empirical method for tunneling in rock. For soft soil tunneling this method is not very useful. Many of the system's parameters do not make sense for soil as they are related to the jointing of rock masses. If the Q-system is used, the result would be ground conditions described as 'exceptionally poor', and heavy support is recommended. The same goes for other rock mass classification systems such as the RMR system and the RMi system.

7.2 Tunnel deformation analysis

The deformation of weak ground initiates approximately half a tunnel diameter ahead of the advancing face and peaks around one and a half diameters behind it. By the time the face reaches its position, about one-third of the overall radial closure of the tunnel has already taken place. Figure 7.1 illustrates the inward deformation of a tunnel in weak ground conditions (Hoek 2007).

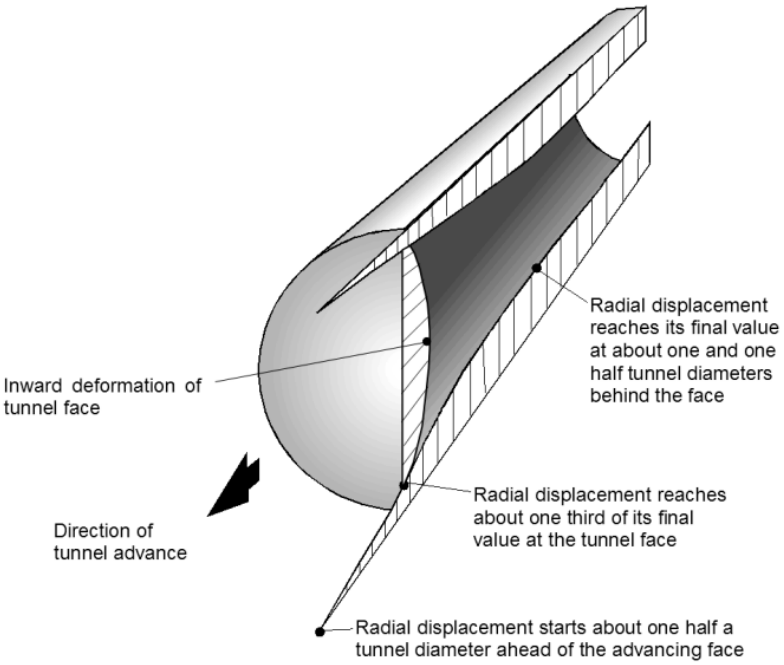

Figure 7.1: Tunnel deformation in weak ground conditions (Hoek 2007).

An analytical model will be used to further investigate the deformation of the ground due to the excavation of a tunnel. This model is significantly simplified and assumes a circular tunnel subjected to a hydrostatic stress field, p_0. This means that the horizontal and vertical stresses are equal, hence $K = 1$. The model is based on the Mohr-Coulomb failure criterion. The till is therefore assumed to be an elastic-perfectly plastic material in which failure is assumed to occur with zero plastic volume change. Support of the tunnel is in the form of internal pressure, p_i. In figure 7.2 the situation is presented. Where r_0, is the radius of the excavated tunnel, and r_p, is the radius of the plastic zone surrounding the tunnel.

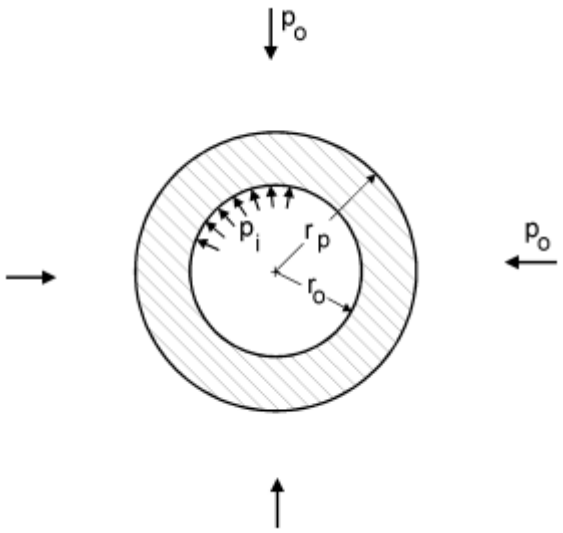

Figure 7.2: The situation assumed for the analytical analysis (Hoek 2007).

The Mohr-Coulombs failure criteria of which the failure of the ground the in model is expressed as:

$$\sigma_1' = \sigma_{cm} + k\sigma_3' \tag{7.1}$$

Where σ_{cm} is the uniaxial compressive strength of the ground and k is the slope of the σ_1' and σ_3'-line. These parameters are defined by (Hoek 2007):

$$\sigma_{cm} = \frac{2c'cos\phi'}{1 - sin\phi'} \tag{7.2}$$

$$k = \frac{(1 + sin\phi')}{(1 - sin\phi')} \tag{7.3}$$

Where σ_1' is the axial stress when the failure occurs, σ_3' is the confining stress, c' is the cohesive strength, ϕ is the friction angle, σ_{cm} is the uniaxial compressive strength, and k is the slope of the σ_1' and σ_3' line.

Given the situation and the Mohr-Coulomb failure criterion the critical support pressure, p_{cr} can be found (Hoek 2007). This is the amount of internal pressure necessary to avoid failure of the ground surrounding the tunnel.

$$p_{cr} = \frac{2p_0 - \sigma_{cm}}{1 - k} \tag{7.4}$$

The model will be set up for the site in Drammen at chainage 54+160, this chainage can be seen in the longitudinal section A.1 and A.2 in the appendix. It is at the beginning of the soil tunnel, where the overburden is low and the most instability problems are expected. The numerical analysis in chapter 8 is also done for 54+160 and the two analyses can be compared. At 54+160 the overburden of the tunnel is $8.5m$, making the surrounding pressure $p_0 = 8.5m * 0.020kg/m^3 = 0.17MPa$. Using the coheison of $5kPa$ and friction angle of $40°$, $k = 4.6$ and $\sigma_{cm} = 0.021$. The critical internal pressure is then calculated and equals $p_{cr} = 0.057MPa$.

If $p_i \geq p_{cr}$ the inward elastic displacement of the tunnel can be found (Hoek 2007):

$$u_{ie} = \frac{r_0(1 + \nu)}{E}(p_0 - p_i) \tag{7.5}$$

Setting $p_i = p_{cr} = 0.057MPa$ the displacement is estimated to be $u_{ie} = 11.4mm$. This amount of radial displacement equals 0.2% percent strain, which can undoubtedly be tolerated for a soil tunnel. From field observations done by Chern, Shiao, and Yu (1998) from the Second Freeway, Pinglin and New Tienlun headrace tunnels in Taiwan around 2% strain can be allowed for tunnels without experiencing stability

problems. This is however only an indication and there are lots of exceptions.

Failure will occur if the internal pressure is less than the critical pressure, $p_i < p_{cr}$. The plastic zone around the tunnel is then given by (Hoek and Marinos 1998):

$$\frac{r_p}{r_0} = (1.25 - 0.625\frac{p_i}{p_0})\frac{\sigma_{cm}}{p_0}^{(\frac{p_i}{p_0} - 0.57)} \tag{7.6}$$

The inward radial displacement for the plastic failure can then be found (Hoek and Marinos 1998):

$$\frac{u_{ip}}{r_0} = (0.002 - 0.0025\frac{p_i}{p_0})\frac{\sigma_{cm}}{p_0}^{(2.4\frac{p_i}{p_0} - 2)} \tag{7.7}$$

Setting $p_i = 0$ for the site in Drammen, the plastic zone around the tunnel would be $r_p = 24.7m$ and the radial displacement would be $0.786m$, which is a strain percent of 13.1%, indicating failure.

7.3 Support analysis

7.3.1 Ground response curve

Ground response curves (GRC) are widely used in geological engineering to estimate the behavior of the surrounding ground during tunneling. These curves provide insights into the relationship between ground movements and the applied loads on the tunnel. The curves represent the relationship between ground settlement or convergence and the corresponding applied load or displacement of the support system. They assist in the design process, to select appropriate support types, determine optimal spacing, and evaluate the overall stability of the excavation (Alejano et al. 2009).

The GRC is found by plotting the tunnel wall displacement, found by equation 7.8, towards the support pressure, p_i. (Aygar and Gokceoglu 2013) .

$$u_{ip} = \frac{r_0(1+\nu)}{E}(2(1-\nu)(p_0 - p_{cr})(\frac{r_p}{r_0})^2 - (1-2\nu)(p_0 - p_i) \tag{7.8}$$

The GRC for the site in Drammen can be seen in figure 7.3.

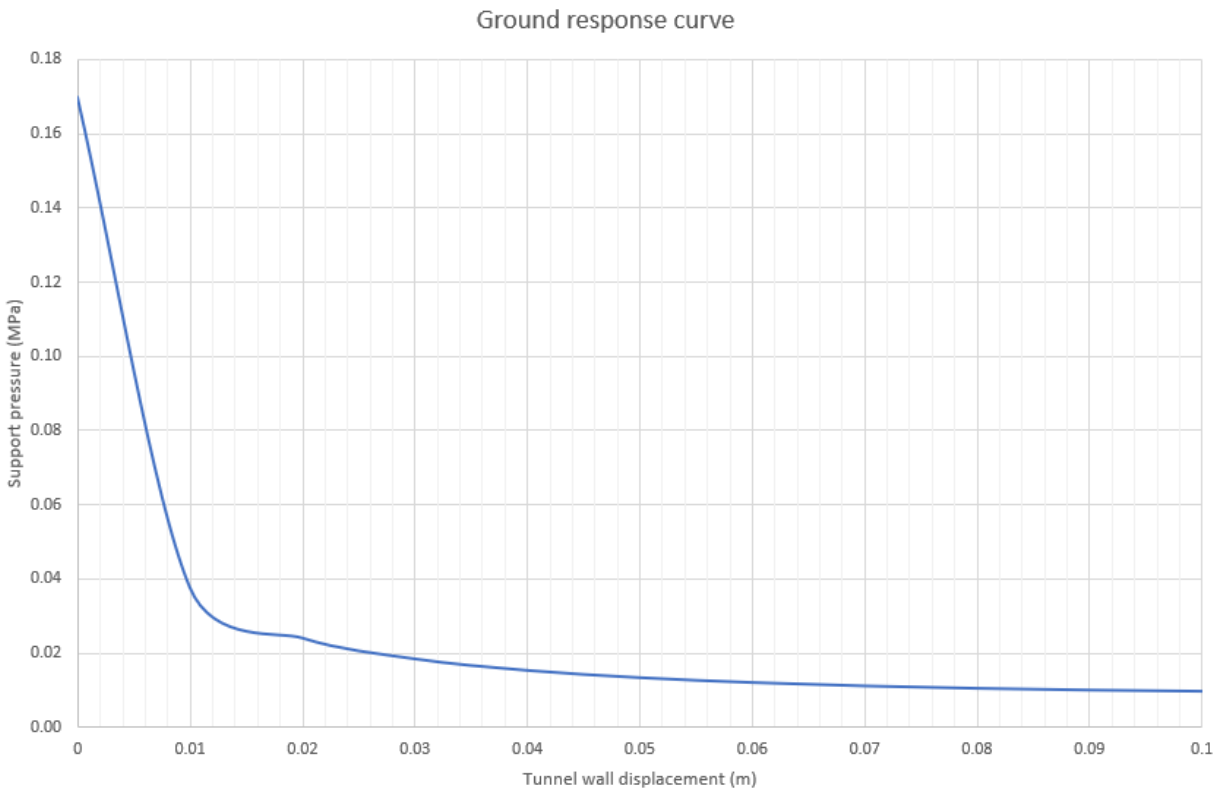

Figure 7.3: Calculated ground response curve of the Drammen site.

The curve can be seen to begin at the value of $0.17MPa$, which is when the support pressure equals the surrounding pressures. As the support pressure decreases the tunnel wall displacements increase fast. A support pressure close to the surrounding pressure is needed.

7.3.2 Longitudinal displacement profile

The longitudinal displacement profile (LDP) is used to optimize the installation of support systems with specific displacement capacity or determine the appropriate timing for stiff support installation in tunnel design. This profile represents the variation of closure or displacement along the tunnel's length. Prior to the face advancing past a certain point, a portion of the maximum radial displacements occurs at the tunnel boundary. As the tunnel progresses beyond this point, the tunnel boundary continues to displace (P. Zhang et al. 2008). This phenomenon is illustrated in figure 7.1. To plot the longitudinal displacement profile the Vlachopoulos and Diederichs- equations are used (Vlachopoulos and M. S. Diederichs 2013).

$$u_{im}\left(\frac{u_{if}}{u_{im}} \cdot e^{\frac{x}{r_0}}\right), x < 0 \tag{7.9}$$

$$u_{im}\left(\frac{u_{im}}{3} \cdot e^{-0.15\frac{rpm}{r_0}}\right), x = 0 \tag{7.10}$$

$$u_{im}(1-(1-\frac{u_{if}}{u_{im}})\cdot e^{(\frac{-3x}{r_0})(\frac{2r_{pm}}{r_0})}), x>0 \tag{7.11}$$

Where equation 7.10 is used to find u_{if}. Equation 7.9 and 7.11 is thereafter plotted as functions of, x, the distance from the tunnel face.

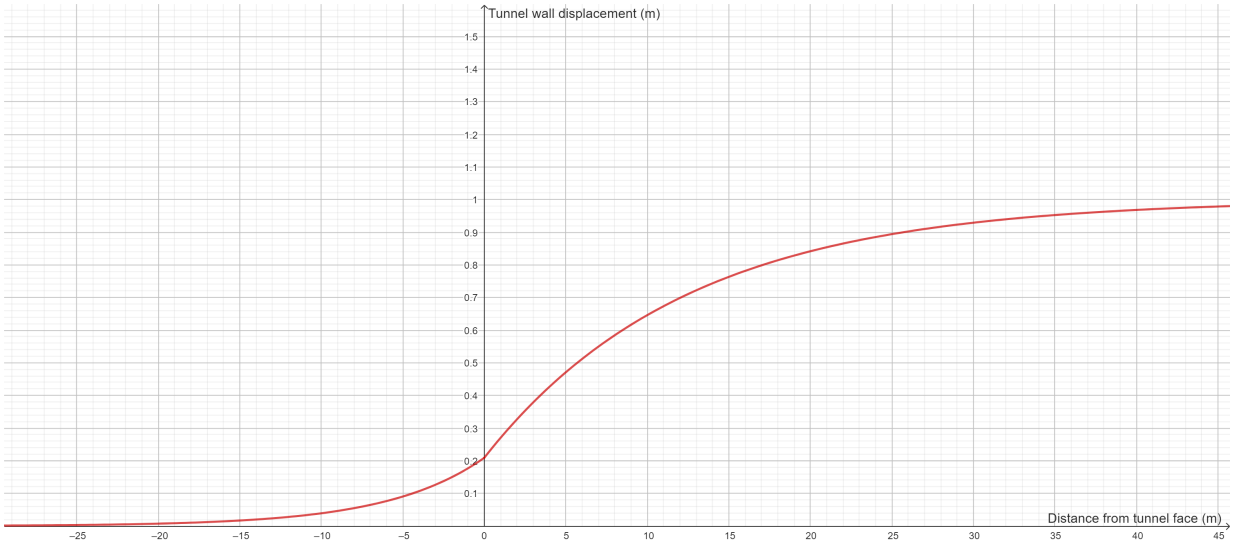

Figure 7.4: LDP for the site in Drammen.

the displacements can be seen to start approximately $23m$ ahead of the tunnel face. At the tunnel face, the displacement is $0.2m$. The need for immediate support of the tunnel is further highlighted.

7.4 Volume loss

Volume loss is a significant consideration in tunneling projects, particularly in soft ground conditions. It refers to the reduction in ground volume that occurs during the excavation of a tunnel. The concept of volume loss is closely related to the behavior of the surrounding soil or rock mass and the effectiveness of the chosen tunneling method and support system. Managing volume loss is crucial for the overall stability and long-term performance of the tunnel and its surrounding environment. Excessive volume loss can lead to the settlement of adjacent structures, the ground surface, and potential risks to the tunnel structure itself.

While volume loss plays a significant role in estimating ground movements during the design phase of tunneling, it is often challenging to calculate and predict accurately. This parameter is commonly determined based on past experience, making it difficult to predict the precise impact of volume loss when project parameters such as soil conditions, tunnel depth, or surrounding sensitivity change. According to Minh Ngan Vu (2015), the relationship between volume loss and the cover-to-diameter (C/D) ratio was

investigated specifically for shallow tunneling scenarios. Through empirical data relationships for different ground conditions were made. The graph for sandy ground conditions is found in figure 7.5. On the premise of the Drammens sites till consists of mainly sand this graph is considered a good fit.

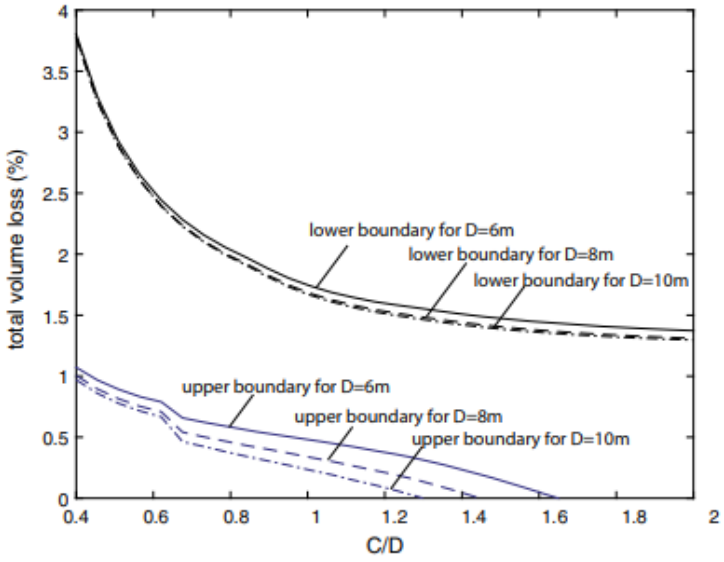

Figure 7.5: Graph of the relationship between volume loss and the relationship C/D for sand (Minh Ngan Vu 2015).

At 160+54 in Drammen, the cover distance, which is the distance from the ground to the center of the tunnel is $14.5m$ and the diameter is $11.91m$. This equals $C/D = 1.2$ which the graph estimated to be a volume loss between $0.1 - 1.5\%$, the average is then 0.7%.

7.5 Surface settlement

The settlements induced on the surface by tunneling can be calculated using Peck's empirical equation. In 1969, Peck proposed a settlement trough that exhibits a double-curved shape. The reversed Gaussian error function curve, illustrated in figure 7.6, represents the settlement trough observed above real tunnels. However, this approximation tends to be more accurate for clays than for coarse-grained soils such as sands and gravels. The settlement, S, at a particular offset from the tunnel centreline can be determined, as well as the maximum displacement S_{max} (Q. Zhang et al. 2019).

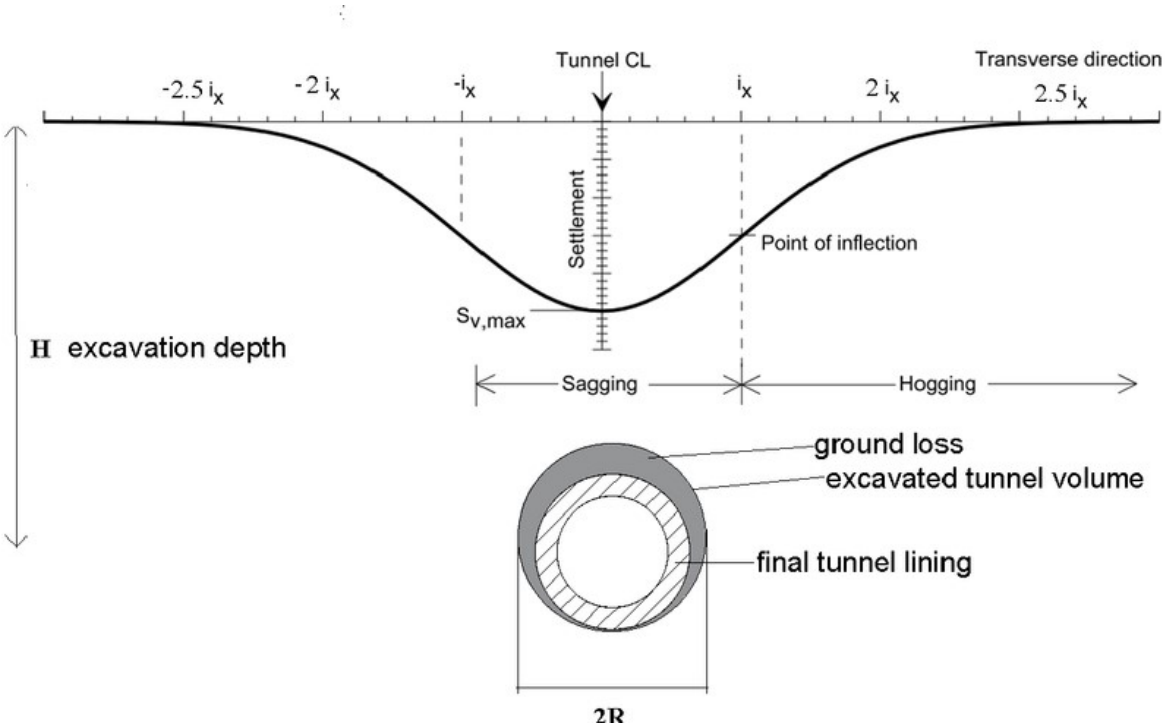

Figure 7.6: Surface settlement profile after Peck(1969) (Masosonore 2018)

Peck's equation is given by (Q. Zhang et al. 2019):

$$S(x) = S_{max} \cdot exp(\frac{-x^2}{2i^2}) \tag{7.12}$$

Where, S_{max} is the maximum settlement measured above the tunnel axis, i is the trough width parameter that represents the standard deviation in the original Gaussian equation, x is the horizontal distance from the centerline, and V_s is the area enclosed by the settlement trough (per meter length of tunnel).

Peck's settlement profile is graphed for four different chainages on the route of the tunnel. The volume loss of the tunnel is assumed to be 0.7% as found in the chapter above. Knowing the volume loss also the volume trough can be found using equation 7.14 (Masosonore 2018). Further, S_{max} can be found using equation 7.13 (Masosonore 2018). i in equation 7.13 is defined as $i = K \cdot z$, where K is the trough width constant, and z is the depth. By recommendation of Norconsult (2018a) is $K = 0.4$.

$$V_s = \frac{V_L \pi D^2}{4 \cdot 100} \tag{7.13}$$

$$S_{max} = \frac{V_s}{\sqrt{2 \cdot \pi} i} \tag{7.14}$$

In figure 7.7, the settlement profile for sections 54+160, 54+260, and 54+360 is plotted. In the appendix A.1 and A.2 a longitudinal section can be found to see the exact locations of the sections. Note that these calculations do not take into account any ground improvement or other favorable conditions, such as the bedrock. Therefore they can only be considered as a first approximation to surface settlement.

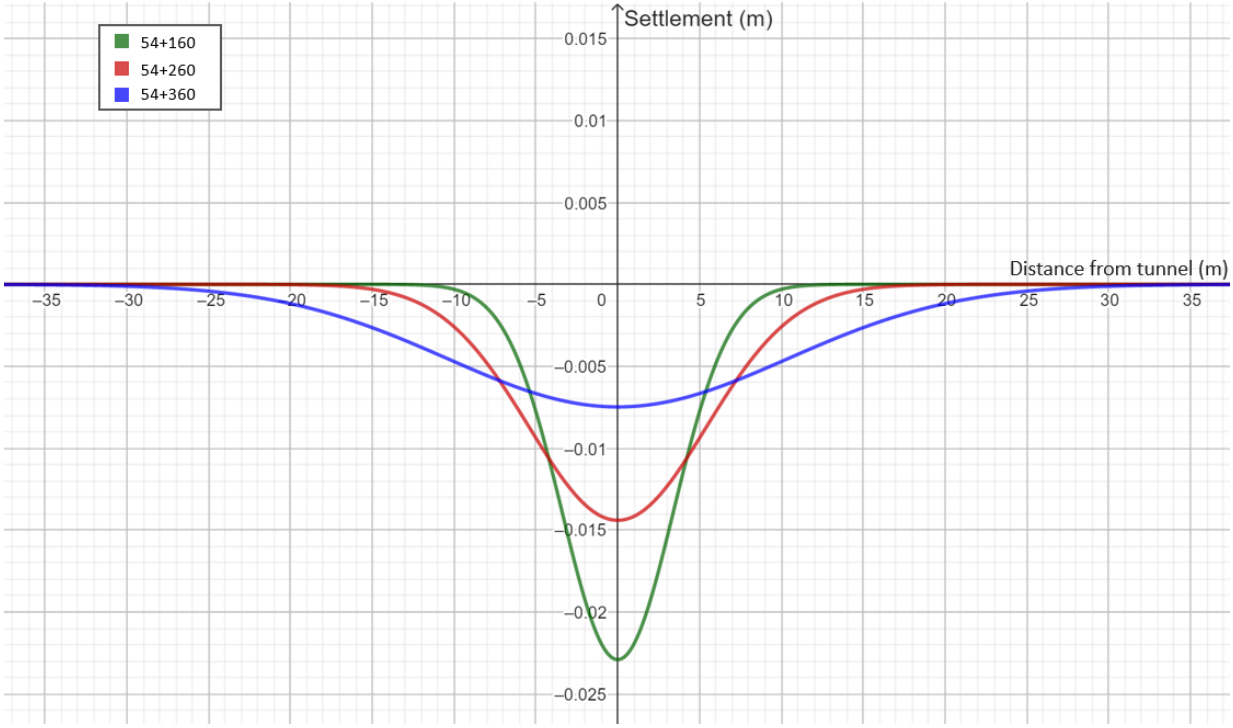

Figure 7.7: Surface settlement profile for Drammen.

In table 7.1 a comparison of the overburden, settlement, and trough width at the different sections is presented. The largest surface settlements occur at the beginning of the tunnel where the overburden is low.

Section	Depth (m)	i	S_{max} (mm)
54+160	8.5	3.4	22.9
54+260	13.5	5.4	14.4
54+360	26	10.4	7.5

Table 7.1: Volume loss and volume trough at different ground settlements.

8 Numerical modeling

8.1 Introduction to numerical modeling

Numerical modeling involves using mathematical equations and computational techniques to simulate and analyze a specific process. It is usually an important tool for geological engineers when designing underground structures such as tunnels and caverns. By discretizing the geological domain into a grid or mesh and solving governing equations, numerical models provide estimations of the change caused. Since numerical models never will reflect the real world it is important to have accurate input variables. These input variables consist of geological data, material properties, and external forcing factors. Model validation is also crucial for ensuring the accuracy and reliability of the model. While there is a challenge to recreate the real world in a model, numerical modeling is a powerful tool that supports informed decision-making in various geological applications. Within the field of geology, numerical modeling is used for tunneling, slope stability, hydrogeology, geotechnical engineering, petroleum reservoir engineering, geological hazard assessment, climate change studies, and geological resource exploration.

There are various forms of numerical modeling, the most common are the boundary element method, the finite volume method, the finite difference method, and the finite element method. The finite element method and the finite difference methods are the best suited for modeling tunnels. In addition, there are 2D and 3D numerical modeling. The difference between the methods is mainly the complexity, a 3D model is way more complex and requires a bigger model, more time to build, debug, and run, and additionally increased time to interpret the results. The advantages of 3D modeling are that there is no need to make as many assumptions as it is necessary for 2D modeling. The common approach is as pointed out in the introduction to start with the simplest methods of calculation first and gradually increase complexity (Jones 2022).

8.2 RS2

RS2 (version 11.015) was the software used to perform the numerical modeling of this study. The program is made for 2D finite element analysis of geological applications, in both rock and soil. The software is commonly used to model tunnel and support design, underground and surface excavations, slope stability, embankments, dynamic analysis, foundations, consolidation, and groundwater seepage (Rocscience 2023b).

8.3 Finite Element Method

The program used for the modeling done in this study is based on the numerical finite element method.

The finite element method (FEM) is a numerical technique employed to conduct finite element analysis (FEA) for predicting the behavior of structures and analyzing various physical phenomena. In most cases, solving the partial differential equations (PDEs) analytically is impossible due to the complexity of the geometries. Instead, numerical methods can be utilized to approximate and solve these PDEs through a process known as discretization. By subdividing the complex domain into finite elements, which are small, countable pieces, the behavior of each element can be described using simpler and manageable equations. Although the solutions obtained through FEM are approximations, they provide solutions to help understand complex problems (Zienkiewicz, Taylor, and Zhu 2005).

The finite element method is a technique that is based on fundamental principles of equilibrium, compatibility, constitutive behavior, and boundary conditions to formulate a set of equations. These equations represent the physical behavior of a system and its forces, material properties, and geometric constraints. The equations are then put into a matrix, and solved, typically through inversion. The unknowns are then found. The unknowns are the stresses, strains, and displacements within the system (Jones 2022).

8.4 Modeling of the steel pipe umbrella

The biggest challenge in modeling the scenario of utilizing the steel pipe umbrella method for the Drammen tunnel in 2D is the recreation of the steel pipe umbrella. Since there is no direct way of implementing such a stability measurement as steel pipes or spilling an estimation of the effect it has must be made. Three ways of doing this are (Tan 2005):

- All the material properties in a strip above the crown of the tunnel are combined using weighted averages and an equivalent rock mass strength is used.
- Only the steel pipes are modeled using beam elements. While the grout and rock mass make up a strip around the crown of the tunnel composed of weighted averages of the material properties.
- Both the steel pipes and the grout are modeled as beam elements around the crown of the tunnel.

In a study done by Tan (2005), these three methods of modeling a steel pipe umbrella are assessed and compared. The result of the study found that the method of equivalent material estimated twice as much surface displacement and over twice as much crown displacement. It should be noted that these results came from a comparability study on a spesific project that could have an influence on the result. A

notable finding from the study is however that the method of equivalent material is the more conservative choice. And for that reason, this method will be used in the continuation of this study. This method however is a crude estimation and is not suitable for detailed design proposes. Hoek (2000) specifies that when designing the steel pipe umbrella, most tunnel engineers often rely on field experiences or adopt conservative methods. For this purpose, the equivalent material method can be employed as a suitable alternative.

The properties of the improved strip of material can be found by calculating by multiplying the strength of each component, till, steel, and grout, by their respective cross-sectional areas. The resulting products are then summed, and the total sum is divided by the overall area (Hoek 2000).

Since the steel pipe umbrella is installed at an angle and is overlapping, the thickness of the reinforced zone varies. The thickness of the improved material layer is assumed to have equal strength to the height at which the overlap occurs. With an overlap of $4m$, installment angle of $5°$, and a length of $15m$, this equals a thickness of approximately $0.96m$.

Area of the soil:

$0.96m \cdot 1m = 0.96m^2$

Area of the steel pipe (2.5 steel pipes/m):

$((\pi \cdot (114mm/2)^2) - (\pi \cdot ((114mm - 8mm \cdot 2)/2)^2)) \cdot 2.5 = 0.0067m^2$

Area of grout:

$(\pi \cdot ((114mm - 8mm \cdot 2)/2)^2) \cdot 2.5 = 0.00189m^2$

In chapter 8.6, table 8.3 later in this section the calculations for the parameters of the improved material layer are found.

8.5 Setup of model

There is made three models of the Drammen tunnel; two cross sections; 54+160 and 54+340, and one longitudinal section of the tunnel. The setup is based on conceptual design drawings, seismic profiles, and reports provided by Veidekke, the contractor of UDK02. A longitudinal section with chainages of the tunnel is found in figure A.1 and figure A.2 in the appendix.

8.5.1 Cross sections

One of the cross-sections is at 54+160, early in the construction. At this point, the overburden of the tunnel is $8.485m$, which is almost as low as it gets. The greatest stability problems of the tunnel are for this reason expected to be found at this area of the tunnel's route. The profile of the tunnel is a circular horseshoe shape with a height of $11.91m$, the dimensions of the cross-section were found in Norconsult (2018a). A more or less circular shape of the tunnel is preferred in weak ground conditions because the supporting liner distributes its capacity even in a circle.

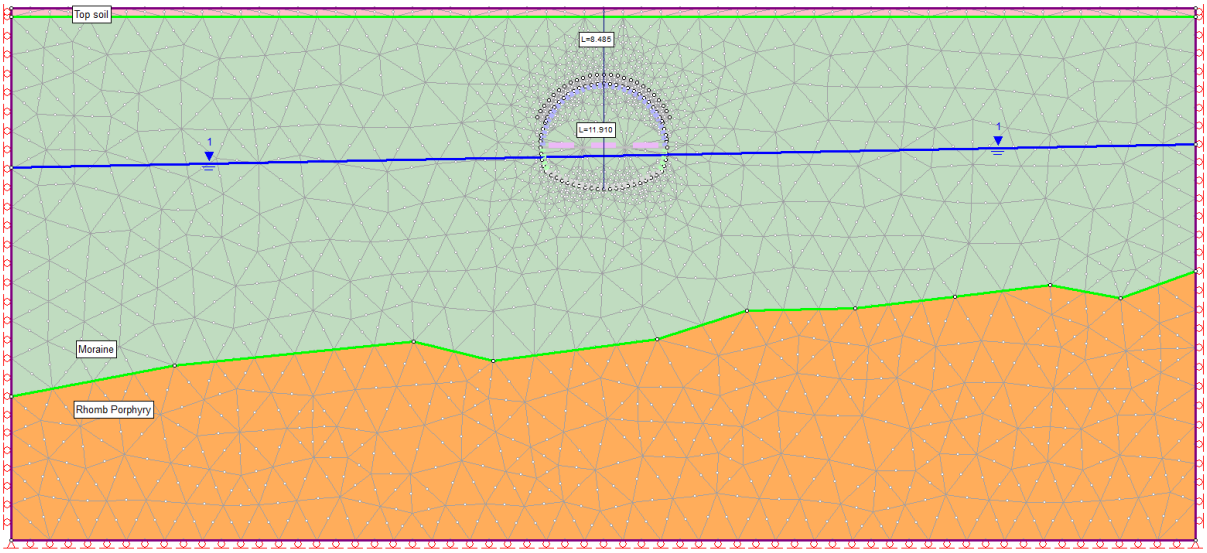

Figure 8.1: Cross section model at 54+160.

Underneath in figure 8.2 and 8.3 is more detailed figures of the sectioning of the model. The improved strip of material can be seen in grey at a $151°$ angle in the crown of the tunnel. The first stage is the in-situ stage where no excavating has been completed. The second stage is after the excavation of the top heading illustrated in figure 8.2. Notice that the support, lattice girder in blue and wire mesh in purple, is installed in this stage. The feet-lock will not be modeled, because it is hard to obtain its effect accurately. The third stage, viewed in figure 8.6, is after the excavation and completion of support measures for the tunnel bench. The remainder of the tunnel wall is supported by lattice girder, and the invert of the tunnel is supported by wire mesh. The permanent liner of concrete is also added at this stage by the use of a composite liner. A composite liner is in RS2 a liner that consists of more than one support measure. At what stage the second liner is installed is optional.

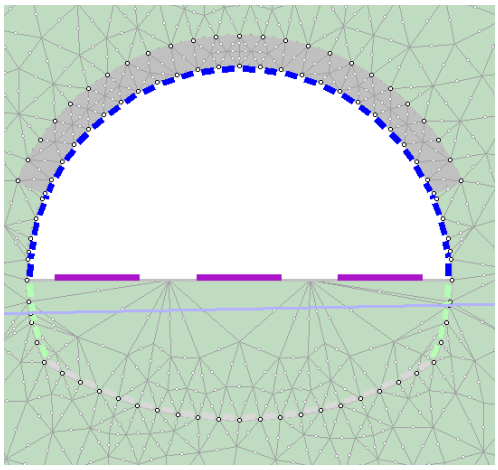

Figure 8.2: Excavated heading at 54+160.

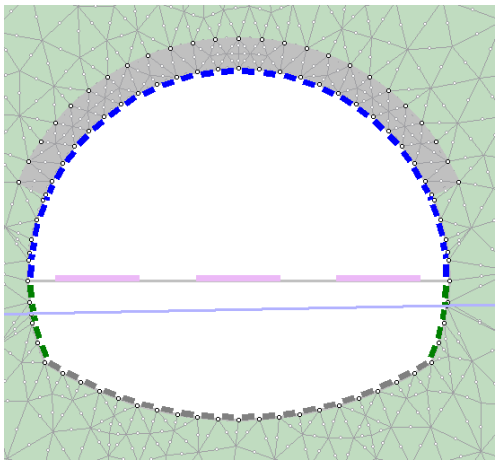

Figure 8.3: Excavated bench at 54+160.

The second cross-section is at 54+340, towards the end of the construction. Here the bottom part of the tunnel is located in the rhomb porphyry. The overburden at this point is $25.045m$ and the groundwater level is at the top of the tunnel profile.

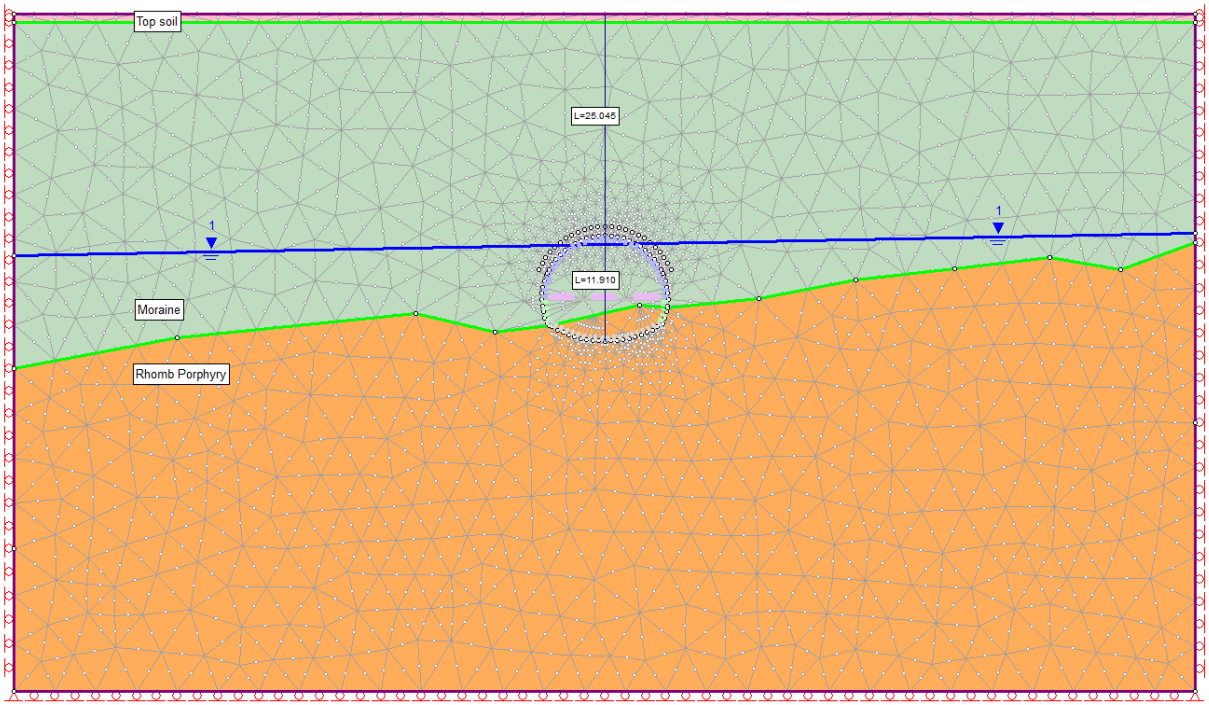

Figure 8.4: Cross section model at 54+340.

The stages of the model at 54+340 can be seen in figures 8.5 and 8.6. The measures of support are initially chosen to be the same for the two cross-sections.

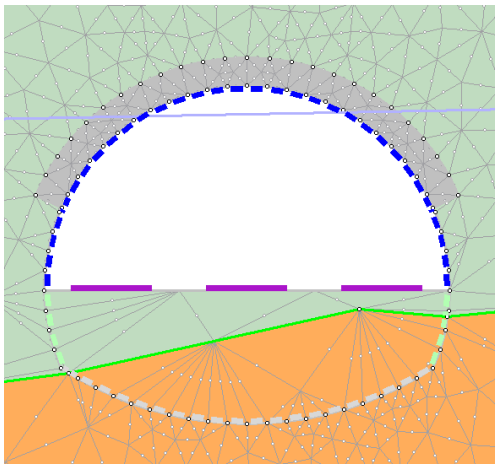

Figure 8.5: Excavated heading at 54+340.

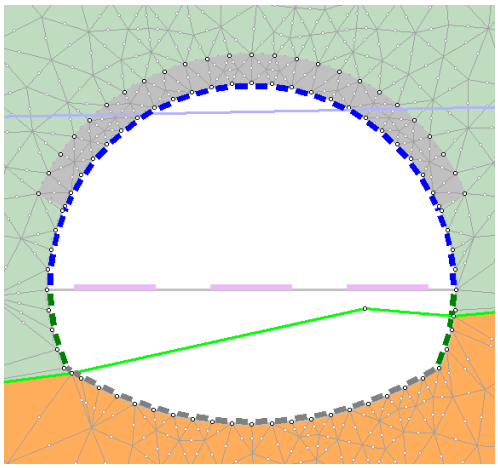

Figure 8.6: Excavated bench at 54+340.

8.5.2 Longitudinal profile

There is an inevitable problem modeling a tunnel's longitudinal section in 2D. In 2D the walls and arching effect of a tunnel are not present, meaning the excavation into the plane is in theory infinite. Also, the liner option in RS2 makes no sense to use in a longitudinal section. However, with the use of internal pressure to account for the liners and set displacement to account for the beam effect a reasonable model can be archived. The main purpose of this model is to study the tunnel face stability. Because the model is quite crude the values of deformation should not be used directly but be considered estimates (Trinh, Broch, and Lu 2010).

As mentioned, when modeling a tunnel longitudinal section in 2D the beam effect will occur. The beam effect refers to the phenomenon where the surrounding soil or rock mass behaves as a beam-like structure due to the presence of the tunnel. When a tunnel is excavated, the soil or rock mass around it undergoes significant changes in stress distribution. The tunnel creates a cavity, which redistributes the stresses in the surrounding ground. The primary mechanism that supports the tunnel is the arching action of the soil or rock mass. In 2D-modeling this effect is not present as there are no tunnel walls or surrounding ground. The overlying ground of the tunnel in the model behaves as a beam fixed on both ends, hence the beam effect, this causes unrealistic high displacements of the tunnel roof (Myhre 2014).

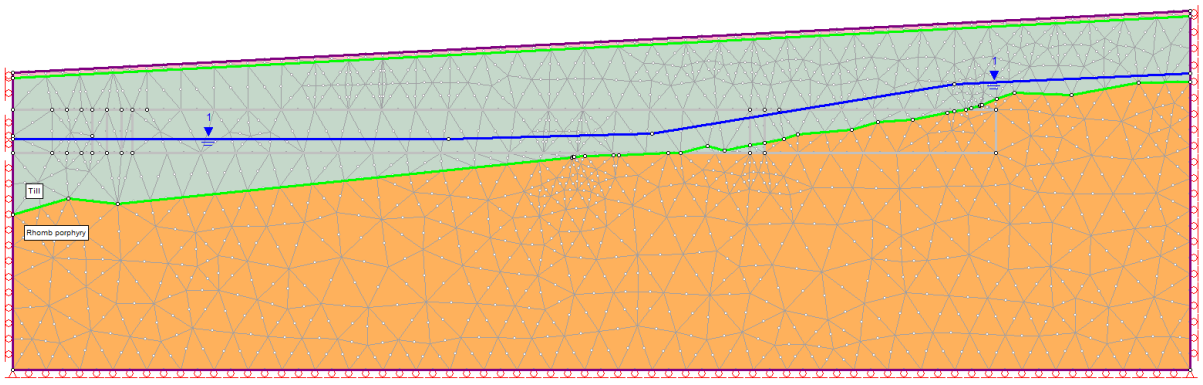

Figure 8.7: Setup of the longitudinal section.

In figure 8.7 the setup of the longitudinal section is found. It covers the entire length of the tunnel which makes the model bigger than the models of the cross sections. Only the beginning of the tunnel is investigated. The tunnel face stability is studied from chainage 54+162, this is the chainage where the third steel pipe umbrella is installed. From there the stability is modeled at all bench excavations before the fourth steel pipe umbrella is installed. This area is chosen because the greatest face stability problems are expected where the tunnel overburden is at its lowest.

8.5.3 Mesh and boundaries

For the models, it is chosen a graded 6-noded triangle mesh, with a number of 90 nodes on external. In order to perform a detailed analysis, particularly focusing on the tunnel excavation area, a mesh with suitable resolution is chosen. The deformation is simulated with a tolerance level of 0.001, ensuring precision in the results. Additionally, a maximum iteration count of 5000.

The external boundary is selected to be 7 times the size of the excavation, this is based on recommendations from Rocscience. The boundary surface is determined based on measurements of the actual ground surface, while other external boundaries are deliberately selected to minimize their influence on the numerical analysis results. The surface boundary is assigned free restraint, allowing for movement in all directions. The bottom boundary of the model is only permitted horizontal movement, whereas the vertical boundaries are only permitted vertical movement. However, the lower corners of the model are restrained both horizontally and vertically. The specific mesh and boundary conditions are illustrated in figure 8.1 and figure 8.4 for the cross-section and figure 8.7 for the longitudinal section.

8.5.4 In-situ stresses

The field stress for the models is chosen to be gravitational field stress. This means that the vertical stress of the model varies with depth. Commonly, a gravitational stress field is the better choice for models close to the ground surface because the gravitational forces are usually a dominant factor determining the vertical stresses in the ground. The vertical stresses are given by: $\sigma_v = \gamma h = \rho g h$. The horizontal stresses are decided by the horizontal/vertical-stress ratio, K. This parameter is given by: $K = \frac{\sigma_H}{\sigma_V}$. And can also be expressed using the friction angle through Jakys (1948) simplified equation (Leen et al. 2013):

$$K = 1 - \sin\phi \tag{8.1}$$

When calculating the coefficient of lateral earth pressure for Drammen $K = 0.357$. This expression is best suited for normally consolidated soils (Leen et al. 2013). Queiroz, Roure, and Negro Jr (2006) states that the more over-consolidated the soil is the higher K is. Because the till is assumed to be over-consolidated to some extent given it's from a glacial ice-contact moraine the value of K is rounded up to $K = 0.4$. Later in the chapter, a stress field analysis will be performed to see how K changes the results of the model.

8.5.5 Groundwater modeling

A steady-state finite element seepage analysis is performed to evaluate the distribution of pore water pressure within the system. The analysis considers the groundwater boundary condition defined in the model. Default values for tolerance and the maximum number of iterations are utilized in RS2. The boundary condition for the total head is assumed to be situated at the groundwater table at the external side boundaries.

8.6 Material parameters

The RS2 software offers the capability to perform analyses using both elastic and plastic materials. In an elastic material, no failure occurs, and deformations can not be attained. The analysis of the Drammen tunnel is therefore done using a plastic model. A plastic model allows for yielding and permanent displacement of the material when it is stressed during excavation. After the material yields the residual parameters and dilatation angle account for its strength. The dilatation angle is the measure of volume increase during the shearing of a material. Soft ground conditions are associated with low dilatation angles, while brittle material tends to have high dilatation angles. The residual strength of materials also depends on their quality. Strain-softening is assumed for average quality rock mass, while soft ground such as till

is assumed to behave elastoplastic; meaning the strength parameters stays the same after yielding. The behavior of materials after failure can be seen in figure 8.8 (Rocscience 2023c).

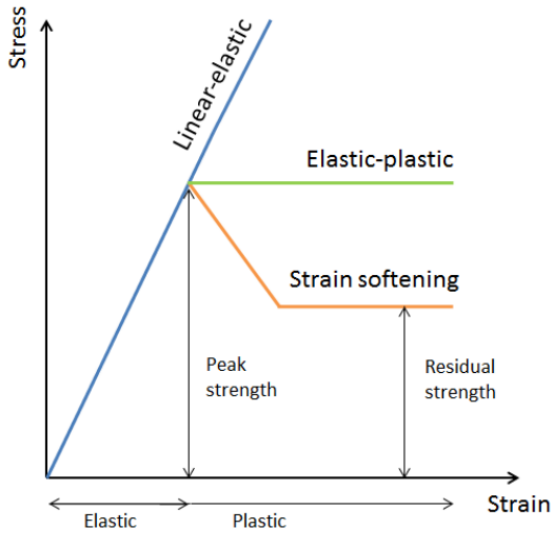

Figure 8.8: The post-failure behaviors of different materials (Hoek 2007).

8.6.1 Till

The soil parameters of the till at the site of the Drammen tunnel are based on the Mohr-Coloumb model. It is linearly elastic until reaching peak strength and becomes perfectly plastic after failure. Its strength is defined by the Mohr-Coulomb failure criterion, found in equation 8.2. Where τ is the shear strength, σ is the normal strength, ϕ is the friction angle, and c is the cohesion. The stiffness of the soil is defined by Hooke's law through the stiffness parameters; Young's modulus and Poisson's ratio. The values for the parameters are found through laboratory testing and other methods further elaborated in chapter 4, they are found in table 8.1 below.

$$\tau = \sigma \cdot \tan \phi + c \tag{8.2}$$

A drained behavior is expected by the till. This means that excess pore pressure are going to dissapate during the time of construction and reach steady-state. According to Anagnostou and Kovari (1996), a rule of thumb is that soils with a permeability higher than $10^{-6} - 10^{-7} m/s$ will behave as drained. The till of Drammen has a permeability of $5.5 \cdot 10^{-5} m/s$ which is above the rule of thumb. As found in chapter 4 the porosity is set to be 14%.

Since the till is assumed to behave elastoplastic the residual values for the strength parameters of the

Table 8.1: Parameters of the till.

Parameter	Value
Unit weight [kg/m^3]	20
Young's Modulus [MPa]	77
Poissons Ratio	0.3
Tensile Strength [MPa]	0
Friction Angle	40
Cohesion [MPa]	0.005

friction angle and cohesion are the same as before failure is reached.

8.6.2 Rhomb porphyry

The Rhomb porphyry of Drammnen is assumed to behave as a plastic material. The generalized Hoek-Brown model is used to describe the rock mass. This failure criterion is the most commonly used to describe hard rock masses. The criterion is initially based on the properties of intact rock. However, it is then modified by applying reduction factors that consider the characteristics of joints within the rock mass. This adaptation is done to better suit the behavior exhibited by the rock mass as a whole (Rocscience 2023c). The generalized Hoeak-Brown criterion can be found in equation 8.3.

$$F_s = \sigma_1 - \sigma_3 - \sigma_{ci}(m_b \frac{-\sigma_1}{\sigma_{ci}} + s)^a \tag{8.3}$$

Where σ_1 and σ_3 are maximum and minimum principal stresses at failure, σ_{ci} is the uniaxial compressive strength of an intact piece of the rock, m_b is the Hoek-Brown constant of the rock mass, and s and a are constants depending on the rock characteristics.

Because laboratory test of the rock mass has not been available certain parameters have been estimated by empirical tables and graphs. These estimation tools are incorporated into RS2 as a parameter calculator.

The parameter calculator takes the intact UCS (σ_{ci}), GSI, m_i, and disturbance factor, D, as inputs. From these values m_b, s and a are attained. The empirical tools to find the UCS, GSI, and disturbance factor are found in figure 8.9. The Hoek-Brown constant, m_i, is 20 ± 5 for porphories. The parameters used to describe the rhomb porphyry can be found in table 8.2. The unit weight and Poisson's ratio were known from Norconsult (2018a).

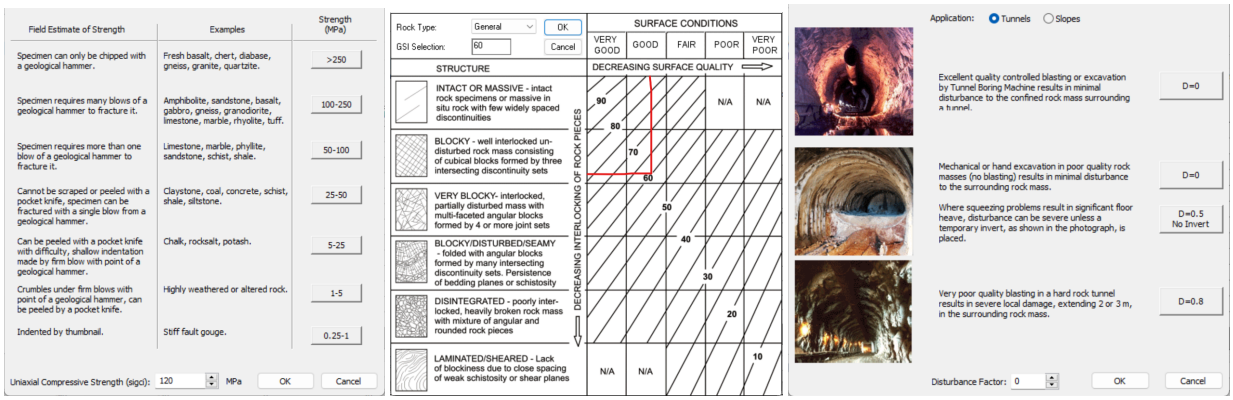

Figure 8.9: Empirical tools to find values for UCS, GSI, and the disturbance factor, D.

Table 8.2: Parameters of the rhomb porphyry.

Parameter	Peak	Residual
Unit weight [kN/m^3]	27	
Young's modulus [MPa]	22000	
Poisson ratio	0.18	
UCS	120	
The Hoek-Brown constant [m$_i$]	20	
Geological Strength Index [GSI]	60	
Disturbance factor [D]	0	
Modulus ratio [MR]	400	
Hoek-Brown constant [m$_b$]	4.79302	0.82085
Hoek-Brown constant [s]	0.011744	0.000419
Hoek-Brown constant [a]	0.502841	0.522344

8.6.3 Steel pipe umbrella

The modeling of the improved layer imitating the steel pipe umbrella was accounted for in chapter 8.4. The calculations of the compilation of the materials, till, steel, and grout are found in table 8.3. This improved layer is as the till based on the Mohr-Coulomb failure criteria but has a plastic failure that allows for yielding, meaning the residual strength is not the same as peak strength.

Table 8.3: Calculations of the parameters of the steel pipe umbrella.

Parameter	Till ($\cdot 0.96m^2$)	Steel ($\cdot 0.0067m^2$)	Grout ($\cdot 0.0189$)	Sum	Improved layer ($Sum/0.9856m^2$)
Unit weigth [kg/m^3]	19.2	0.5226	0.4347	20.16	**20.46**
Young's modulus [MPa]	73.92	1407	945	2425.92	**2461**
Poisson's ratio	0.288	0.002	0.0028	0.2928	**30**
Tensile [MPa]	0	2.38	0.0945	2.4745	**2.5**
Friction angle [°]	38.4	High	0.72		**40**
Cohesion [MPa]	0.0048	1.34	0.567	1.9	**1.93**

The residual strength is assumed to be $\frac{2}{3}$ of the peak values according to Trinh (2014), stated in (Langåker 2014).

The dilatation angle for noncohesive soils that has a friction angle of 30 or greater can be estimated as follows (Hong 2012):

$$\beta = \phi - 30 = 40° - 30 = 10° \tag{8.4}$$

8.7 Support

The tunnel is supported by lattice girders and wire mesh as an immediate lining at every excavation stage. Both the lattice girders and wire mesh include a $0.4m$ thick layer of sprayed-on concrete. The lattice girders are of the 3-bar kind of the bar size $26/34mm$, and the section depth of the girders is $175mm$. This is the lattice girder featured in RS2 that is most similar to the AT-Pipe Umbrella System chosen. The wire mesh has a diameter of $12mm$. In the stage after bench excavation, the permanent lining is also established. The permanent liner consists of a $0.4m$ thick layer of concrete that covers the entire profile.

The thickness of the liners at $0.4m$ is an initial assumption, based on a design presented by Norconsult in Norconsult (2018a). Later, in the chapter on the support analysis, the thickness of liners will be examined as well as other support measures.

Further specifications of the support liners can be found in tables 8.4, 8.5, and 8.6.

Lattice girders

Lattice girder, 3-bar, #115, Bar size: 26, 36mm, selected in RS2.

Table 8.4: Parameters of the lattice girder support used in the model.

Reinforcement	Value
Spacing [m]	0.4
Section depth [m]	0.175
Area [m^2]	0.00197
Moment of inertia [m^4]	1.04e-04
Young's modulus [MPa]	210000
Poisson's ratio	0.25
Compressive strength [MPa]	400
Tensile strength [MPa]	400

Wire mesh

Wire mesh, Canda type, #12, selected in RS2.

Table 8.5: Parameters of the wire mesh support used in the model.

Reinforcement	Value
Spacing [m]	0.6
Section depth [m]	0.012
Area [m^2]	0.000113
Moment of inertia [m^4]	1.02e-09
Young's modulus [MPa]	200000
Poisson's ratio	0.25
Compressive strength [MPa]	400
Tensile strength [MPa]	400

Concrete

Table 8.6: Parameters of the concrete support used in the model.

Concrete	Value
Thickness [m]	0.4
Young's modulus [MPa]	30000
Poisson's ratio	0.15
Compressive strength [MPa]	40
Tensile strength [MPa]	3

8.8 Stability analysis

When analyzing the stability of the Drammen tunnel the total displacement attained from the numerical modeling is of interest because the till has a ductile behavior. When a material behaves ductile displacement is the best indicator of its stability (Trinh, Broch, and Lu 2010). The total displacement is defied by: $\sqrt{X^2 + Y^2}$, where X is the displacement in the horizontal direction and Y is the displacement in the vertical direction for every node in the mesh.

Determining how much deformation is to be accepted is a complex matter. Because tunnels behave differently an exact critical value would not be precise. Despite that, there are some correlations made;

According to Sakurai (1983), the evaluation of tunnel stability can be based on the strain observed in the surrounding rock mass. The strain is determined by the ratio of tunnel convergence to tunnel diameter. He found that a critical strain of approximately 2% serves as the threshold distinguishing between stable and unstable tunnels. But exceptions of stable tunnels with as high strain as 10% were encountered in the study (Hoek 1999).

Li and Zeng on the other hand claimed that the maximum total displacement for a shallow tunnel at a depth between $10 - 50m$ in soft ground conditions is $0.002 - 0.005m$ (Su, Su, and Vlachopoulos 2021).

Often other factors such as long-term stability are just as important. Because of the low water content and the tight-packed till of Drammen, it is considered to be a good environment for long-term stability. Based on experience Bent Agaard has stated that around $30 - 40mm$ of total displacement can be allowed for in the long run (Benrt Aagaard, verbal communication, 06.06.2023).

8.8.1 Cross sections

To express the need for support for the Drammen tunnel, the full excavation of the tunnel was modeled without any support at all. The model did not converge, which indicates failure. The results can be found in figure 8.10 and 8.11. The maximum total displacement for both chainages is over $31m$. This is of course a unrealistic scenario but the need for support is clearly conveyed.

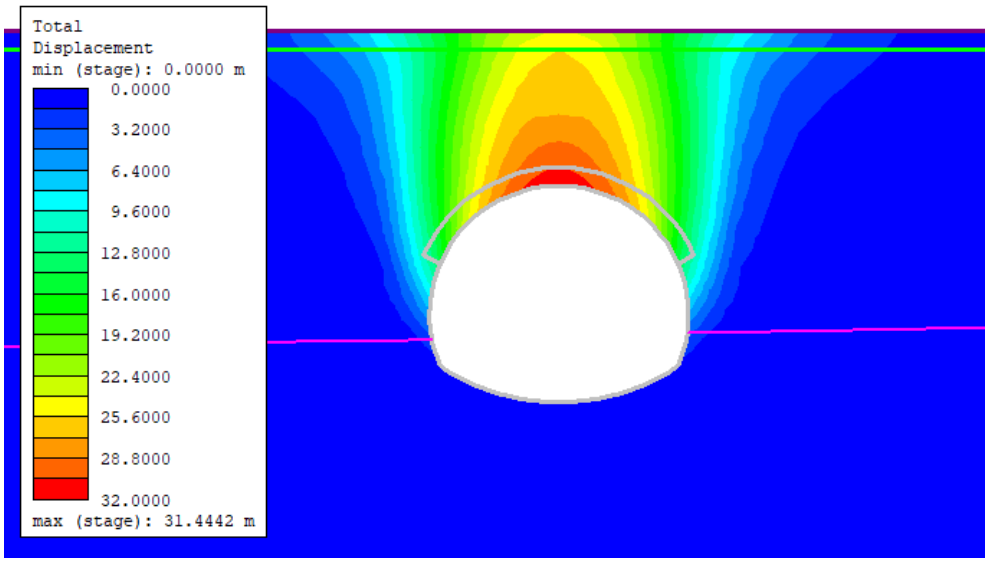

Figure 8.10: 54+160 without any support.

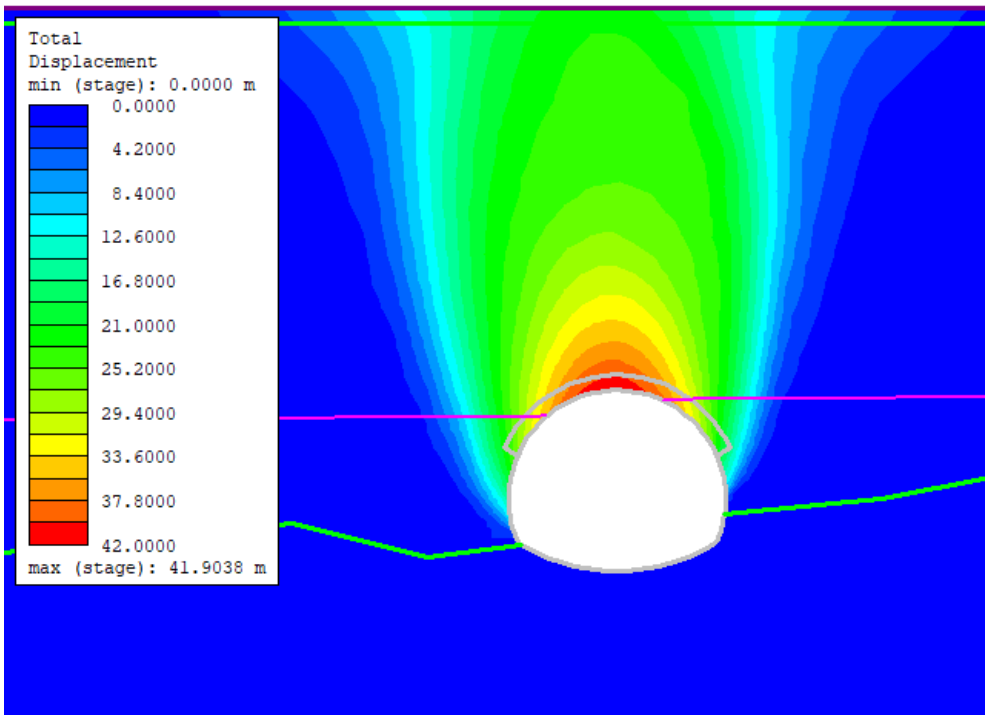

Figure 8.11: 54+340 without any support.

In figure 8.12 and 8.13, only the steel pipe umbrella is added in the form of the improved material layer. The displacements are significantly less but still unacceptable. As previously stated, the steel pipe umbrella is inadequate to support a tunnel in itself. It is the interaction of the steel pipe umbrella and the lining that is effective. Neither one of the models did converge in this analysis as well, again indicating failure.

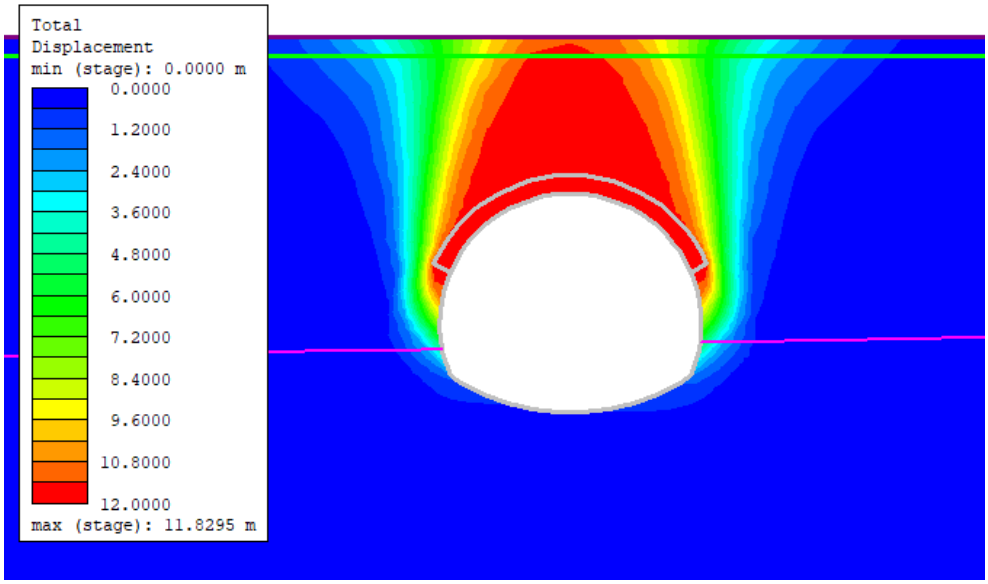

Figure 8.12: 54+160 only supported by improved layer over crown representing the steel pipe umbrella.

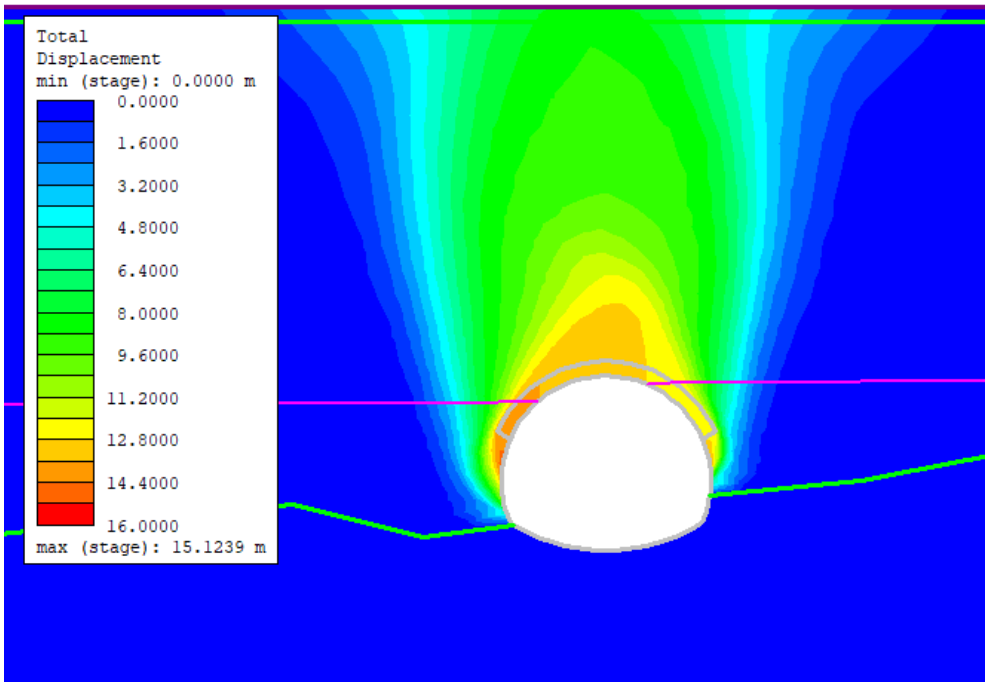

Figure 8.13: 54+160 only supported by improved layer over crown representing the steel pipe umbrella.

Modeling of the planned execution of the excavation of the tunnel at 54+160 is shown in figure 8.14 and 8.15. Here the liners are included, the maximum total displacement for the top heading is $41.4mm$, and the maximum total displacement of the bench is $41.3mm$. Meaning the tunnel is on the verge of being a stable tunnel. The vertical displacements are the largest induced after the excavation, with a maximum equalling the maximum total displacement of $41.3mm$.

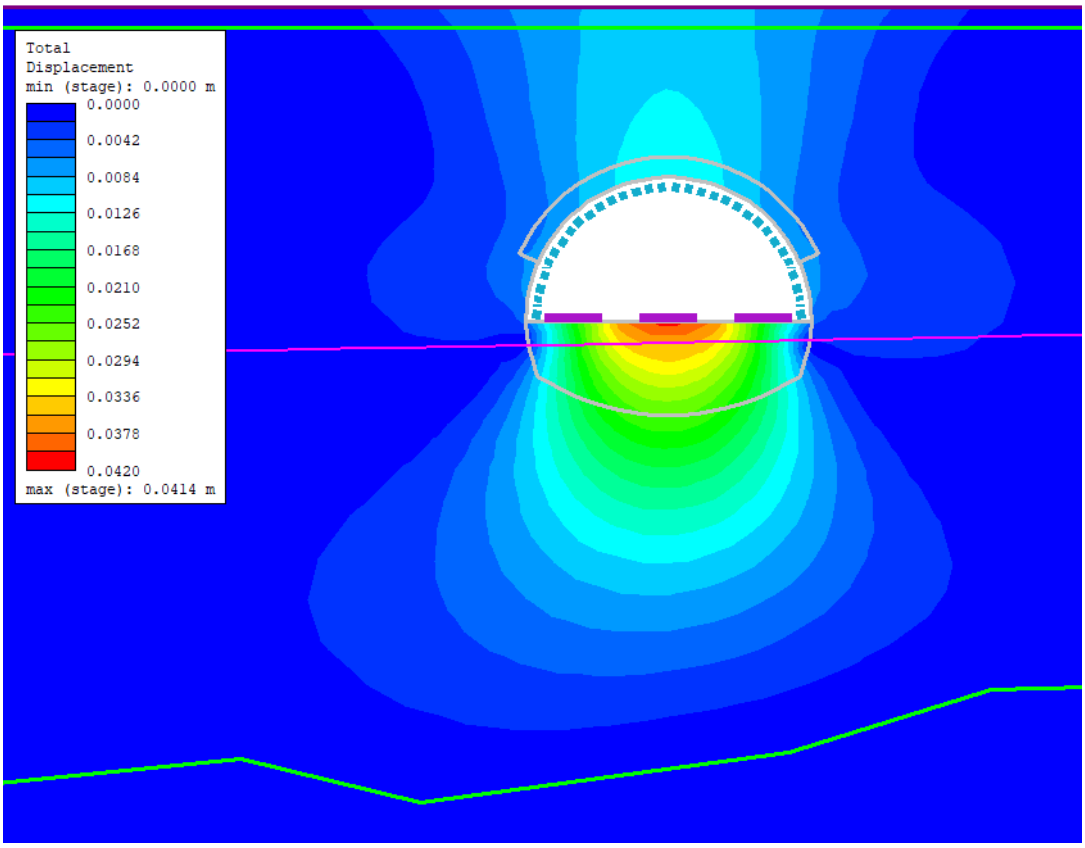

Figure 8.14: Modeled excavation of the tunnel's top heading at 54+160.

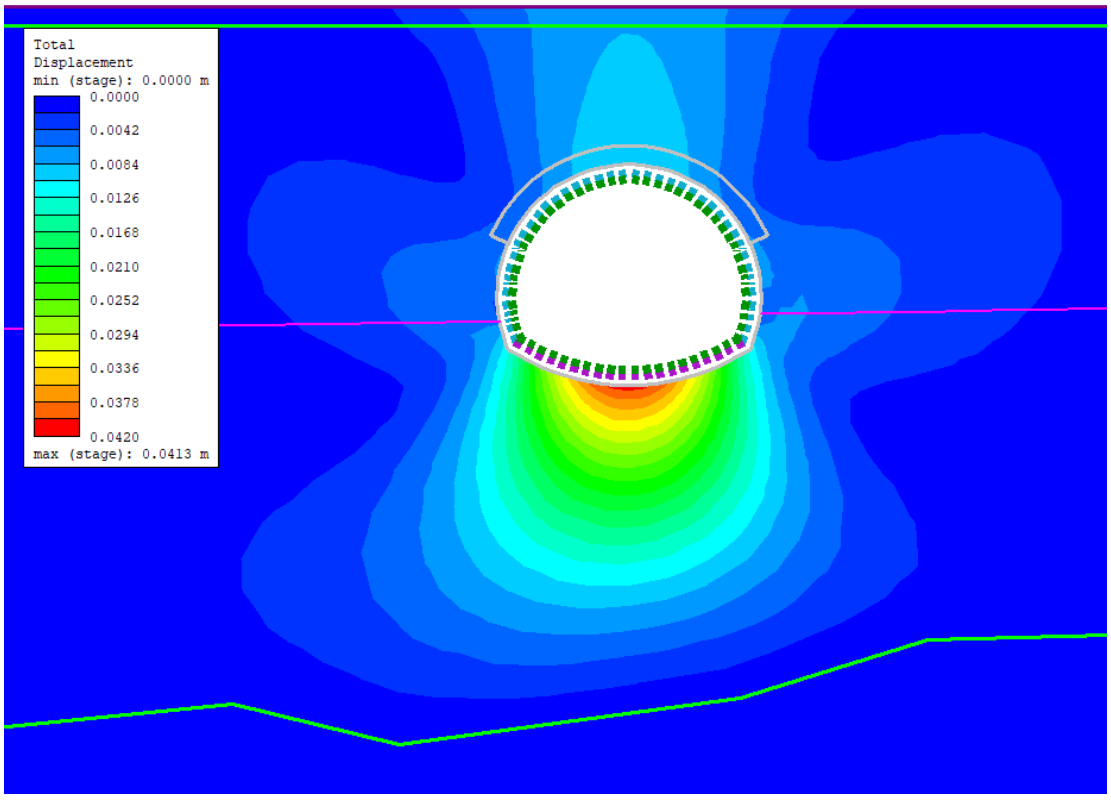

Figure 8.15: Modeled excavation of the tunnel's bench at 54+160.

In figure 8.16, the displacement and yielded elements around the tunnel are displayed. Yielded elements appear where all the elements connected to a node are yielded, failure at this point occurs. As seen in the figure, some shear failure occurs in the invert of the tunnel. This is where the pressure of the soil is the greatest. In figure 8.17 the deformation contour and vectors of the fully excavated tunnel can be seen. The pressure is applied from both over and under the tunnel whereas the walls experience outward displacement. One can also see that there is some settlement of the ground above the tunnel deformation.

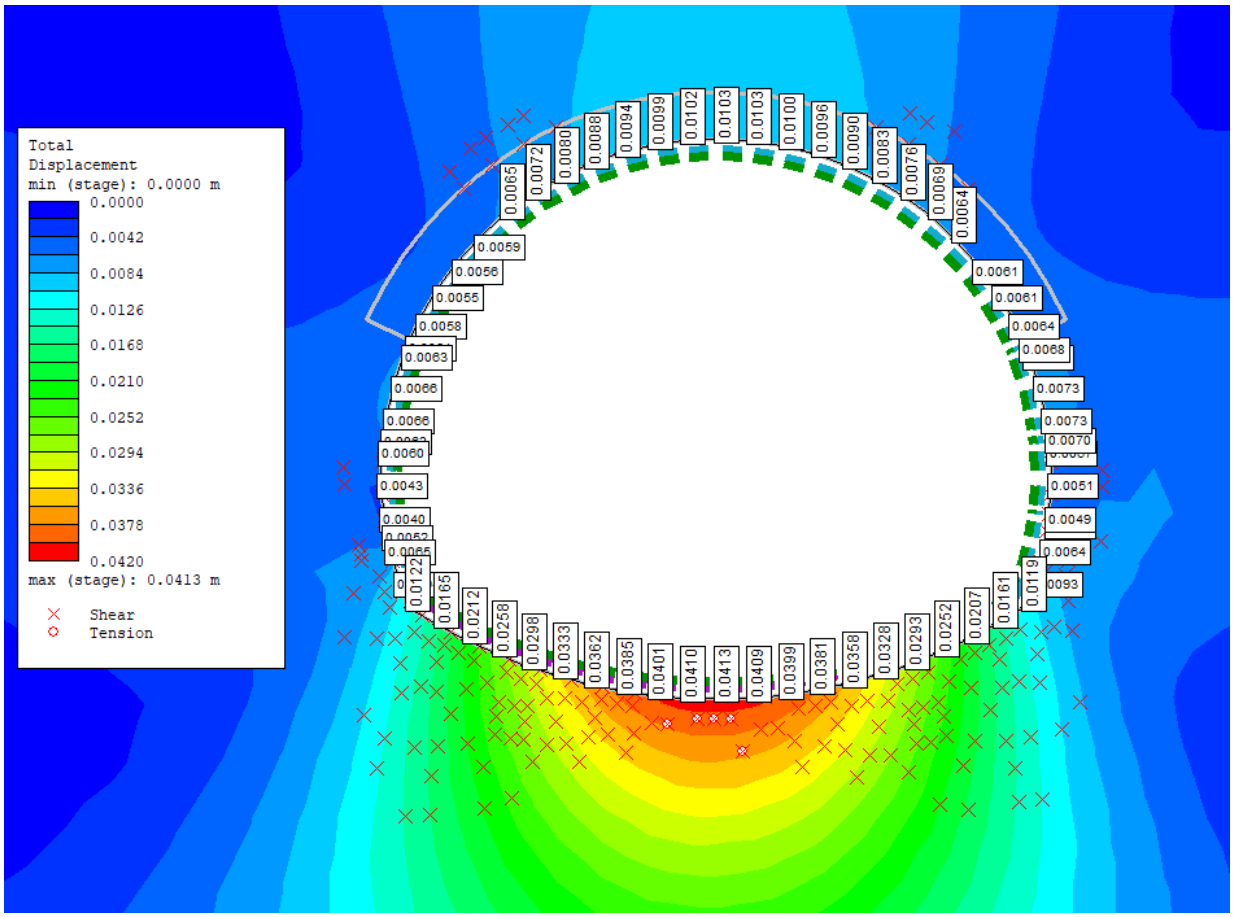

Figure 8.16: Displacements and yielded elements of the bench excavation at 54+160.

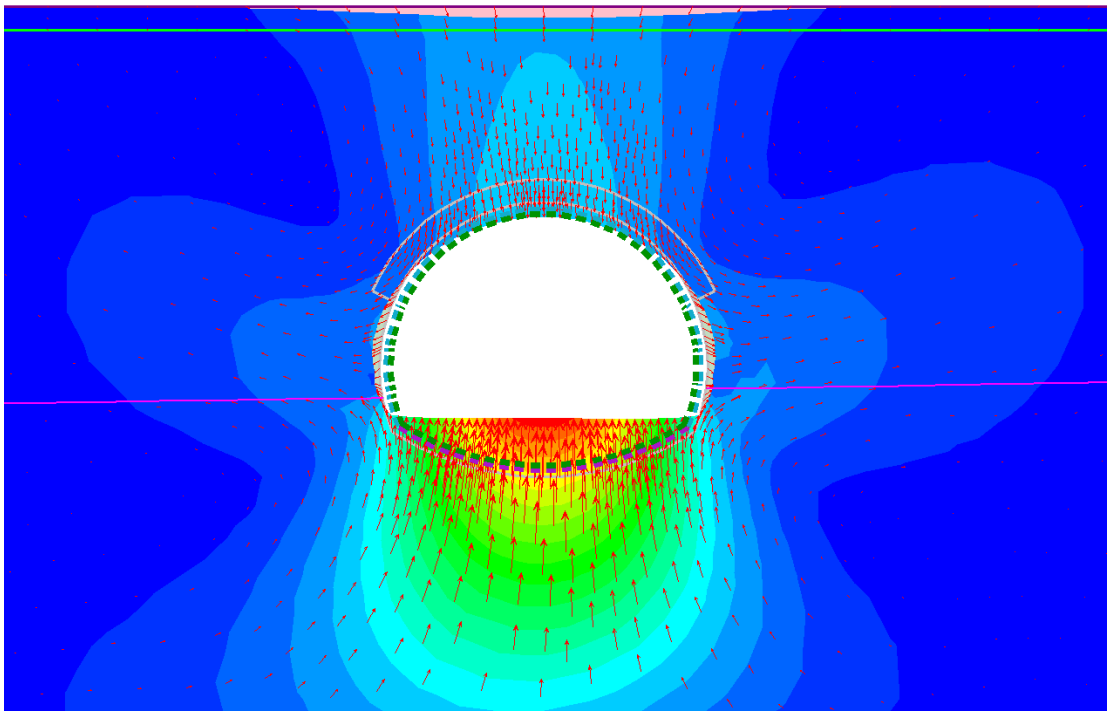

Figure 8.17: The displacement contour and vectors of the bench excavation at 54+160.

Filling the invert with concrete is a common support measure and was proposed by Norconsult in their planning of the Drammen tunnel (Norconsult 2018a). As well as reinforcing the invert it is practical for making a flat surface for the train tracks. A drainage system can also be installed within the concrete. In figure 8.18, this scenario is modeled. The displacement is reduced from $41.3mm$ to $38.3mm$.

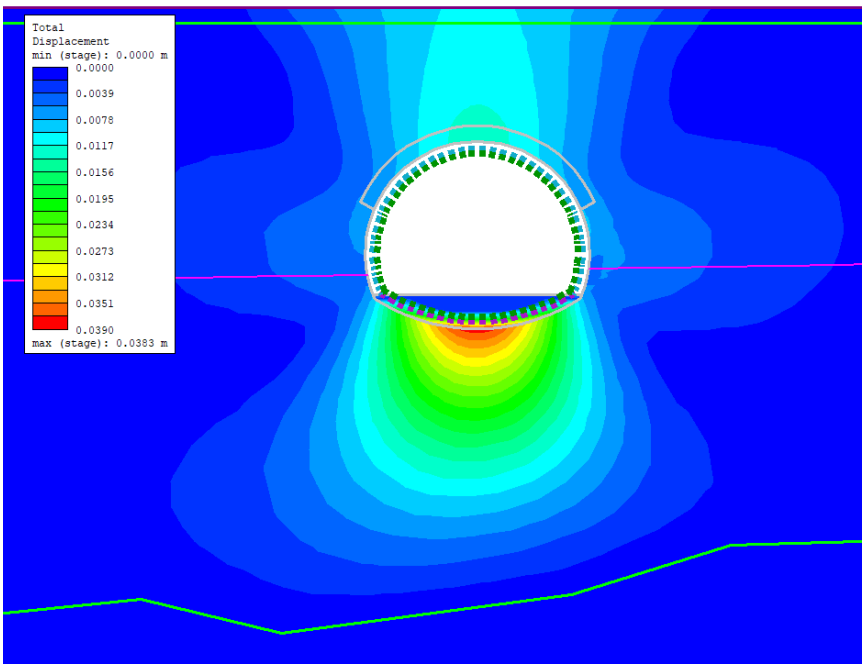

Figure 8.18: Modeled excavation of the tunnel's bench at 54+160 when the invert is filled with concrete.

The planned excavation of the tunnel's top heading and bench at 54+340 is viewed in figures 8.19 and 8.20. Section 54+340 is as expected more stable than 54+160 because of the sole being placed in bedrock. The displacements tend a bit toward the left because of the slope of the bedrock, which allows for some more pressure on the left side wall. The compact bedrock in the sole does not allow for uplift such as the till does. Below the excavation of the top heading, there is a maximum displacement of $56.7mm$. The soil has the potential to come underneath the stiff support lining and this creates high pressure on a small area causing large displacement. The maximum displacements of the bench where the arch is closed, are smaller than both the heading and 54+160's bench at $30.5mm$.

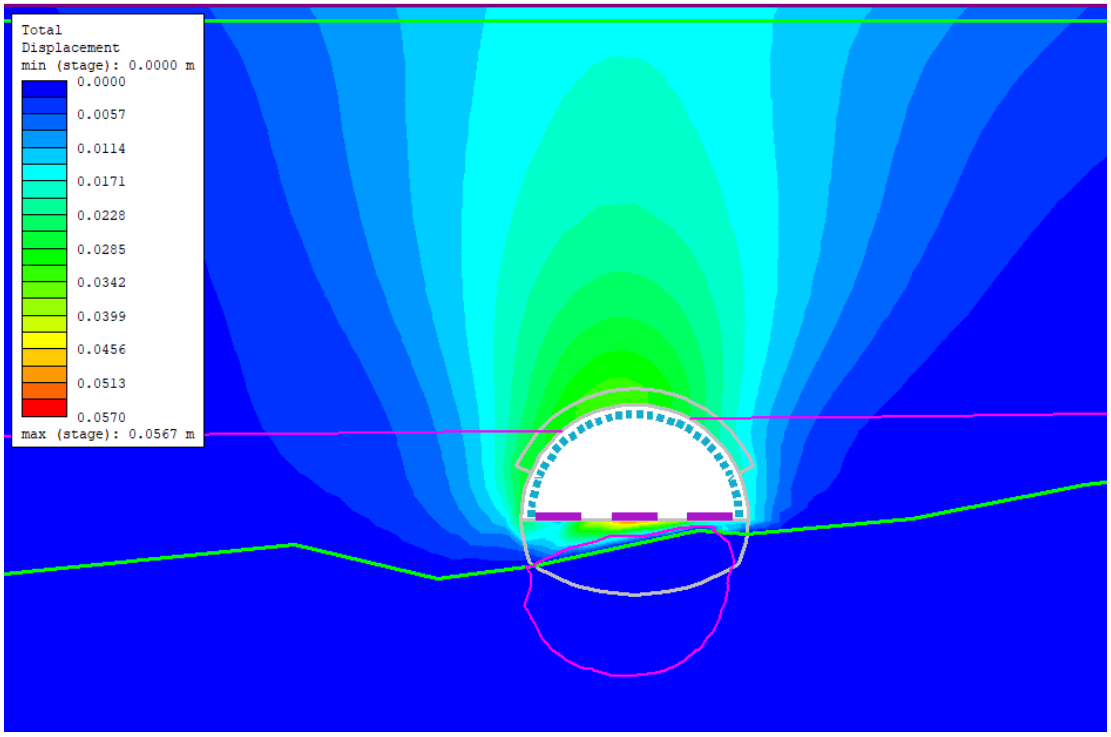

Figure 8.19: Modeled excavation of the tunnel's top heading at 54+340.

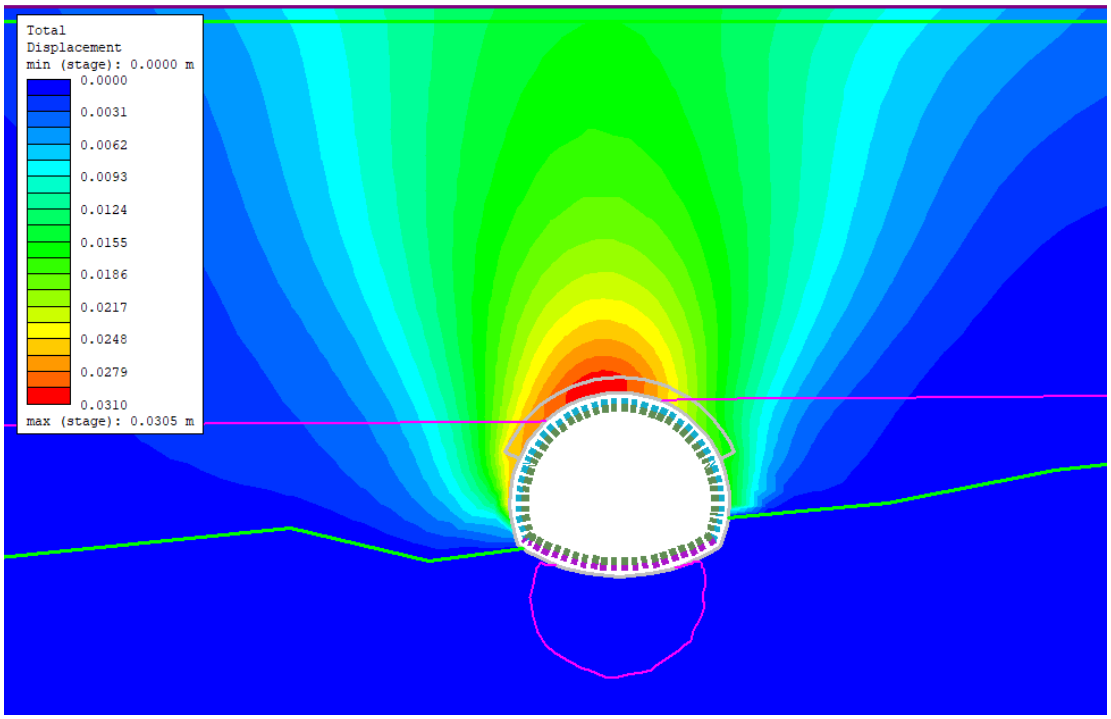

Figure 8.20: Modeled excavation of the tunnel's top heading at 54+340.

In figure 8.21 the displacement and yielded element around the profile of the tunnel at chainage 54+340 can be seen.

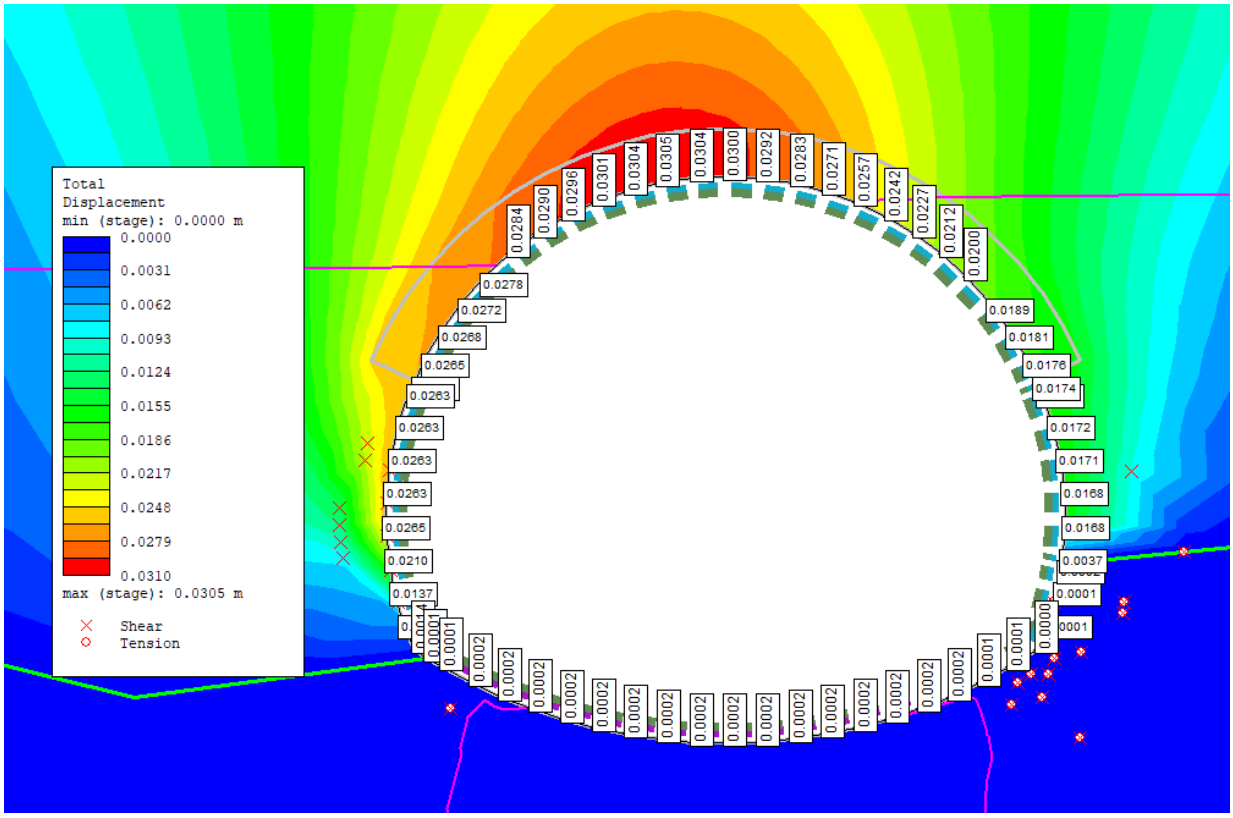

Figure 8.21: The displacement contour and vectors of the bench excavation at 54+160.

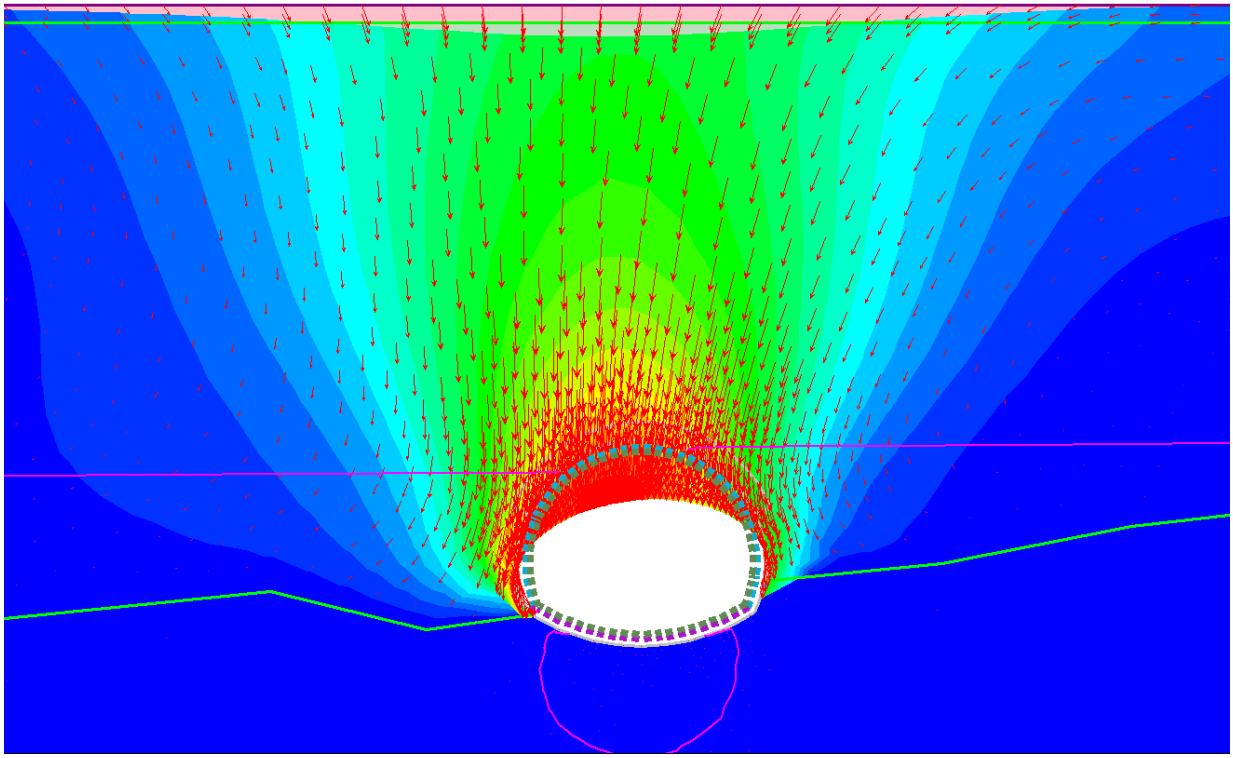

Figure 8.22: The displacement contour and vectors of the bench excavation at 54+340.

The displacement contour and vectors are viewed in figure 8.22. It can be seen that all the vectors now are facing downwards and the settlement of the ground surface is broader.

8.8.2 Longitundinal section

To account for the beam effect the displacement of the tunnel's crown and invert the displacements are fixed. To get all the focus towards the face of the tunnel the fixed values are set to be $1mm$ of maximum displacement (Trinh, Broch, and Lu 2010). The maximum vertical displacement in tunnels is expected to be limited to approximately 1.5 times the tunnel diameter from the tunnel face (Hoek 2007). This distance is typically where the highest radial displacement occurs. Therefore the fixed displacement starts $18m$ behind the tunnel face, the fixed area of the tunnel can be seen as blue arrows in the figures.

Between the set displacement and the tunnel face internal pressure is added to account for the liners. Further, in front of the tunnel face is the steel pipe umbrella represented also as internal pressure. $0.18MPa$ is used as internal pressure for the lattice girders and $0.3MPa$ is used as internal pressure for the support of the invert. For the steel pipe umbrella, a pressure of $0.09MPa$ is used. These pressures were calculated from the approximates of support characteristics found in Hoek and Kaiser (1995).

In figure 8.23 the excavation has reached chainage 54+166, this is the first bench excavation after the third

steel pipe umbrella has been installed. Exactly this chainage was chosen since the cross-section of 54+160 is approximately in the same area, and the beam effect is made sure to be handled this far into the tunnel when displacements are fixed. The following figures 8.24, and 8.25 show the tunnel face stability after reaching respectively chainage 54+170, and 54+174.

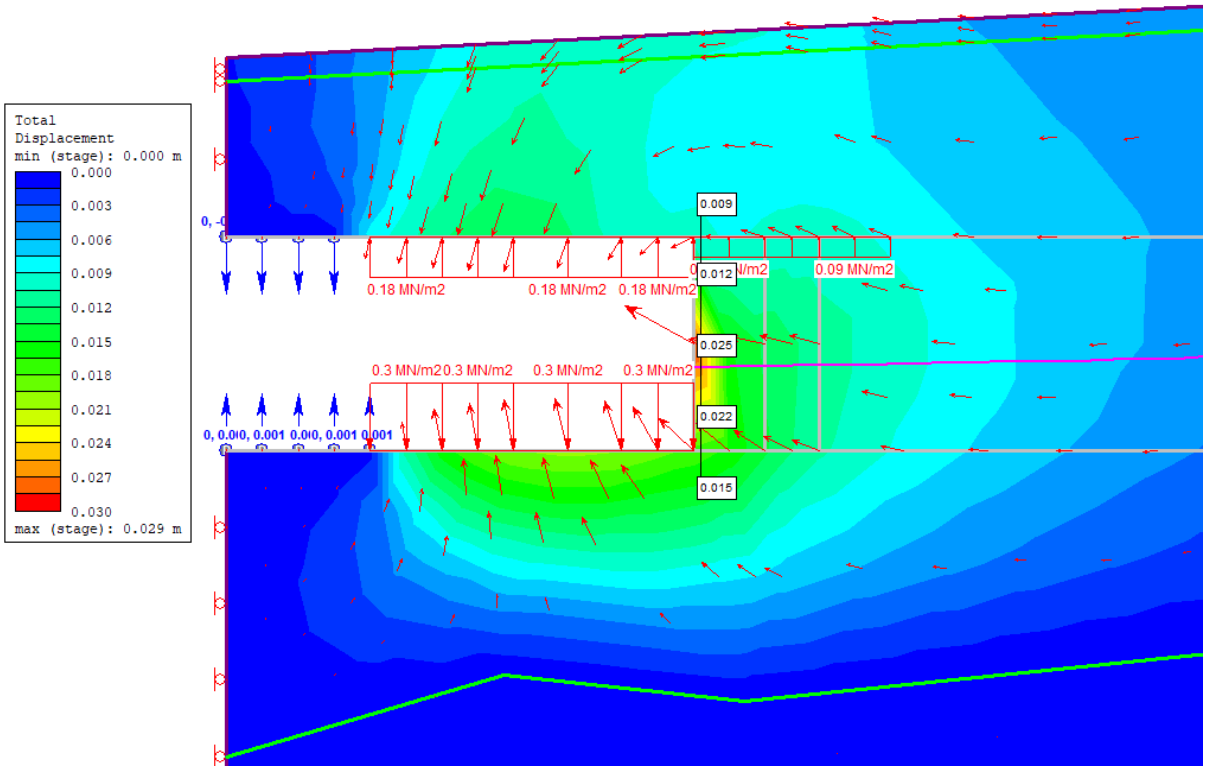

Figure 8.23: Tunnel face stability when construction has reached 54+166.

The maximum total displacement of the longitudinal sections is all located at the tunnel face as expected. The values vary from $29mm$ to $42mm$. These are acceptable displacements according to Trinh, Broch, and Lu (2010), considering no support measures are installed at the tunnel face. This will of course be implemented in reality. As the excavations proceed the displacements increase. This is due to the fact that the tunnel face has less and less coverage under the steel pipe umbrella until a new one is established. At 54+174 the fourth steel pipe umbrella is due to be installed.

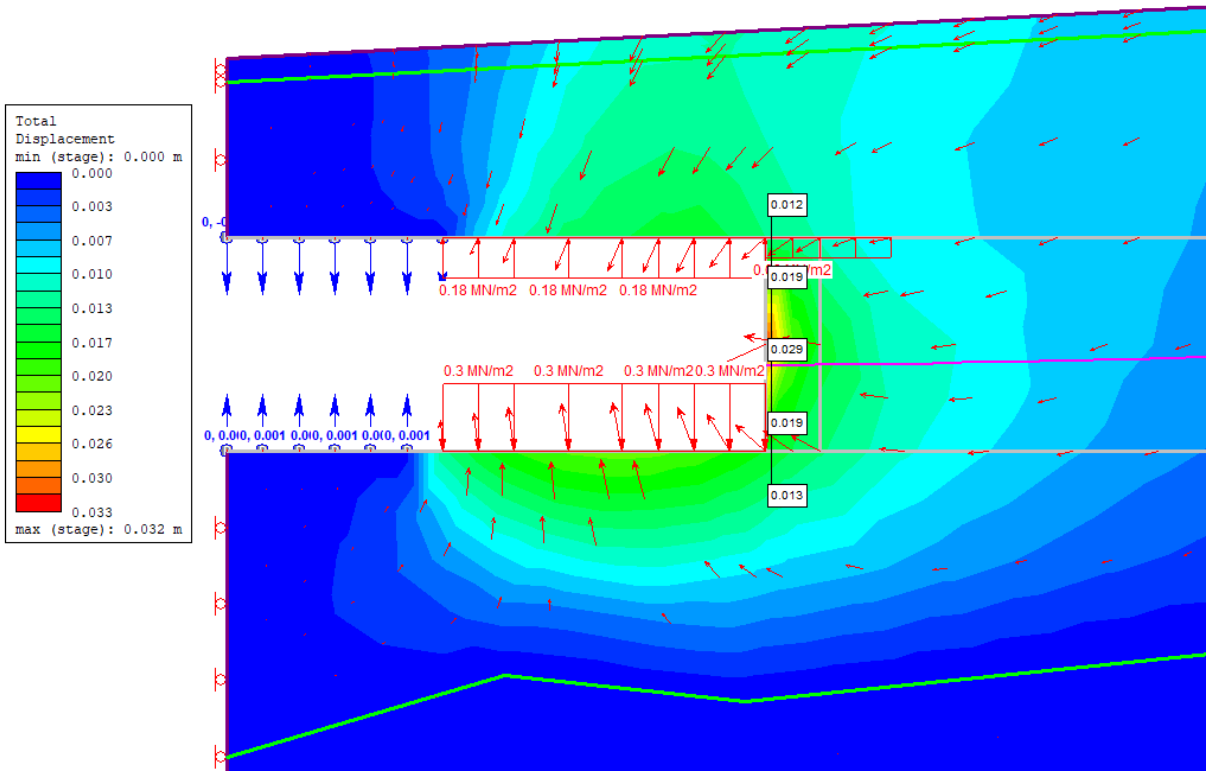

Figure 8.24: Tunnel face stability when construction has reached 54+170.

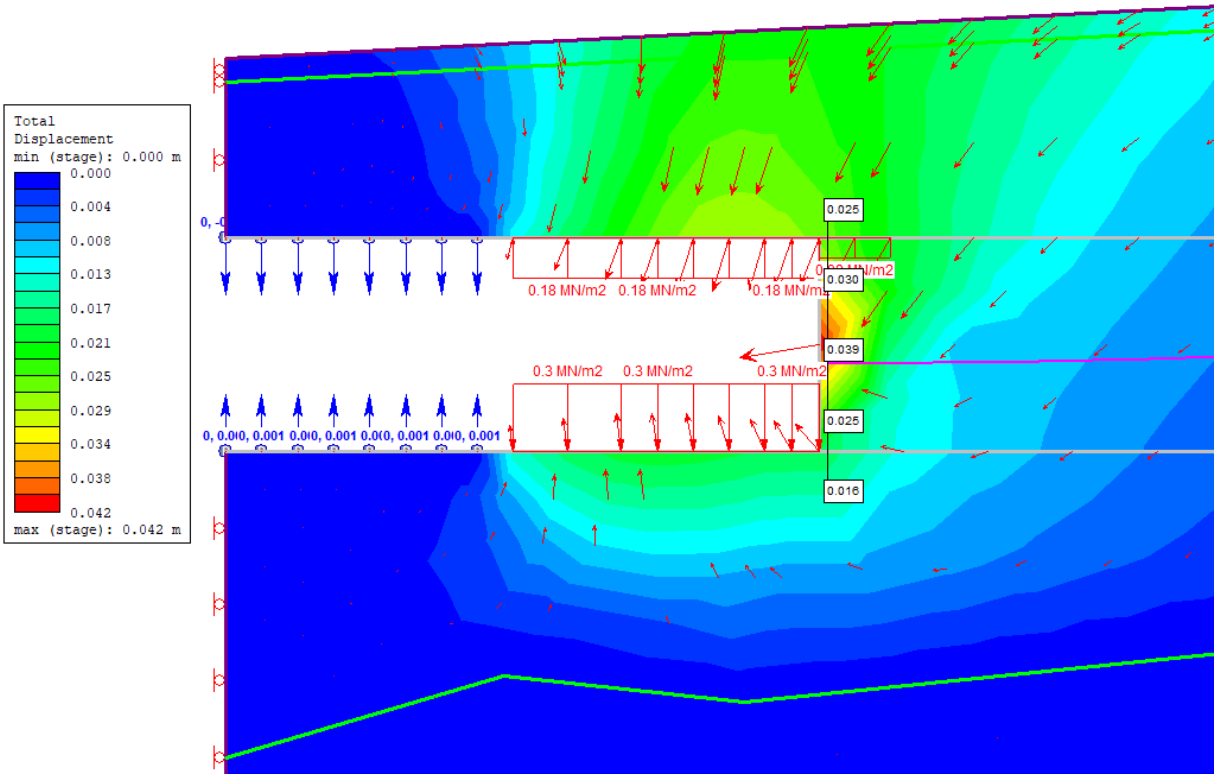

Figure 8.25: Tunnel face stability when construction has reached 54+174.

8.9 Groundwater analysis

It is considered more plausible that there is little groundwater to be found rather than more than expected. A model of the tunnel at the same chainages has been modeled without any groundwater present. This is also useful if there were to be decided to lower the groundwater level to increase stability.

In figure 8.26 and 8.27 the results from the models of 54+160 without any groundwater present is presented. The maximum displacement of the top heading is $41.1mm$, and the maximum displacement of the bench is $40.7mm$. These are slightly smaller displacements compared to when the groundwater was present. As well as that there are fewer yielded elements.

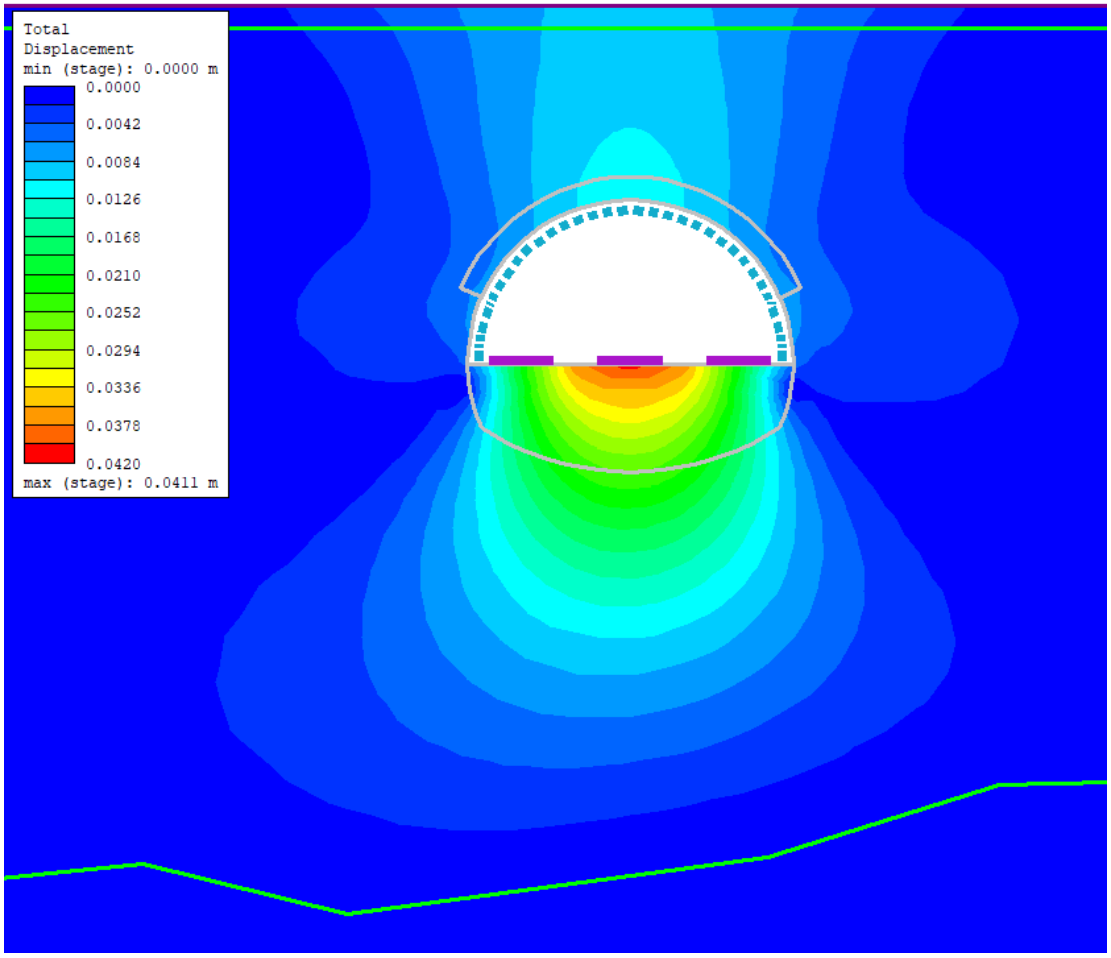

Figure 8.26: Modeled excavation of the tunnel's top heading at 54+160 without present groundwater.

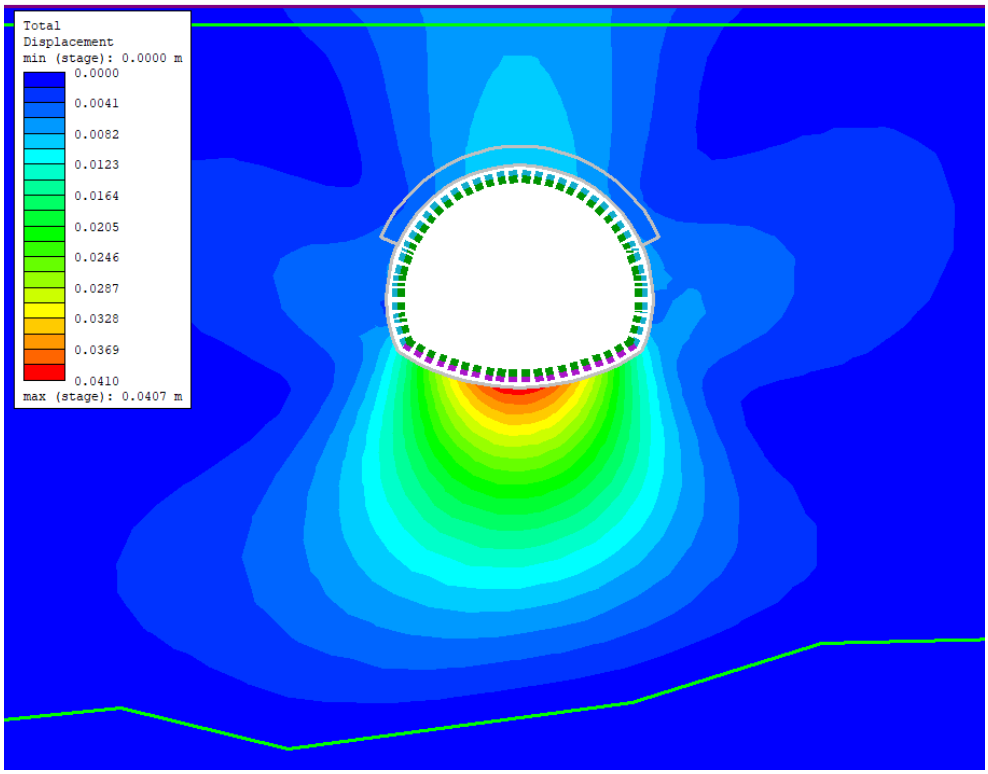

Figure 8.27: Modeled excavation of the tunnel's bench at 54+160 without present groundwater.

The models of 54+340 without present groundwater are viewed in figure 8.28 and 8.29. The displacement at this section is significantly smaller with a displacement of $34.3mm$ for the top heading. The potential for uplift is less when there is an absence of groundwater. $37.1mm$ is the maximum total displacement of the bench.

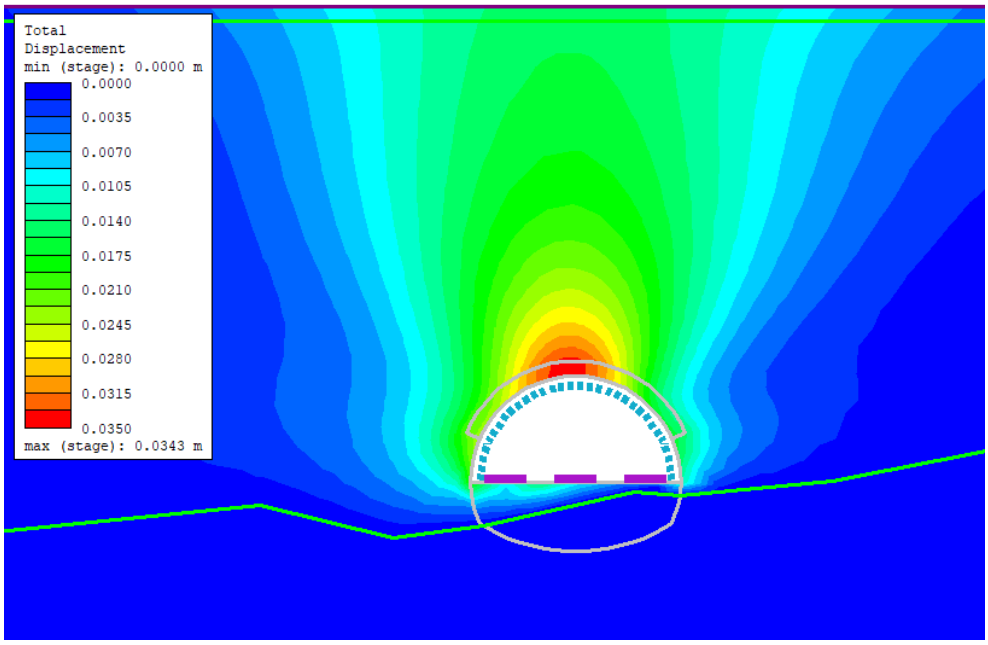

Figure 8.28: Modeled excavation of the tunnel's top heading at 54+340 without present groundwater.

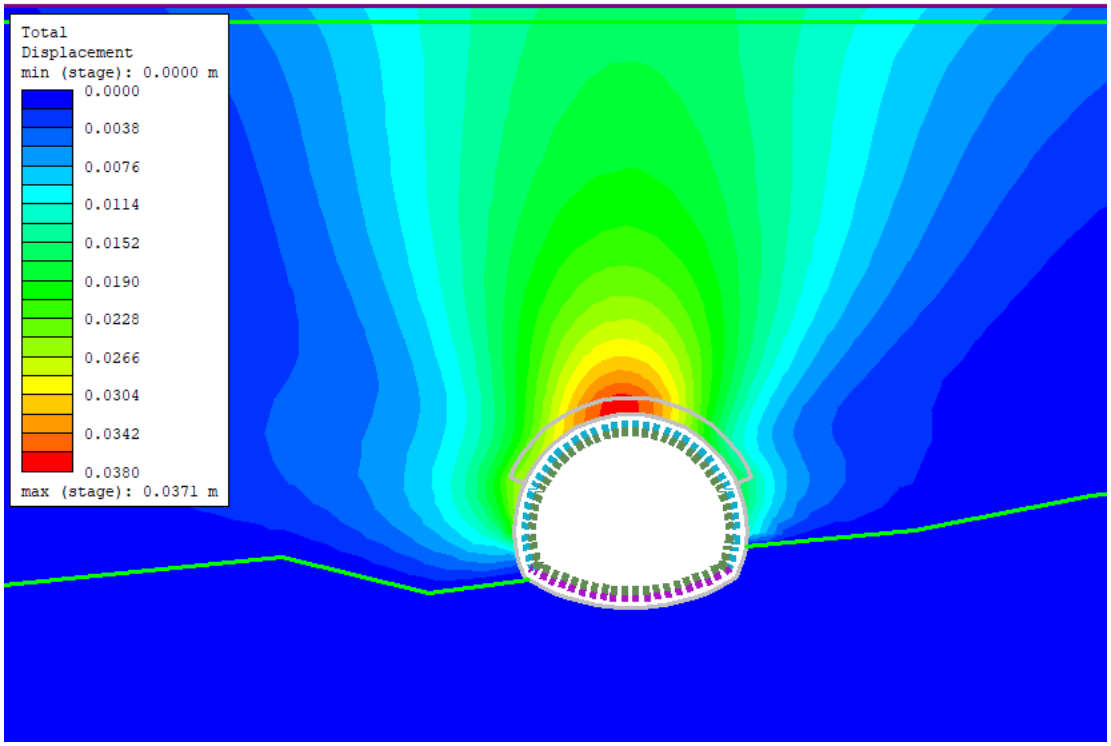

Figure 8.29: Modeled excavation of the tunnel's bench at 54+340 without present groundwater.

Even though it is assumed unlikely that the groundwater raises above the assumed level it has been modeled the scenario of the groundwater level being above the improved layer. The results of this can be seen in figure 8.30. The maximum total displacement continues to increase with the rising groundwater table. The amount of yielded elements also increases sufficiently. This is due to the pore water pressure decreasing the effective stresses. Thus pushing the stress situation closer toward failure, determined by the Mohr-Coulombs failure criterion. The seepage force becomes greater. When groundwater infiltrates the ground towards the tunnel face, it exerts a seepage force that separates the soil particles. This force is directly proportional to the hydraulic gradient and acts in the direction of flow, consequently leading to instability (Jones 2022).

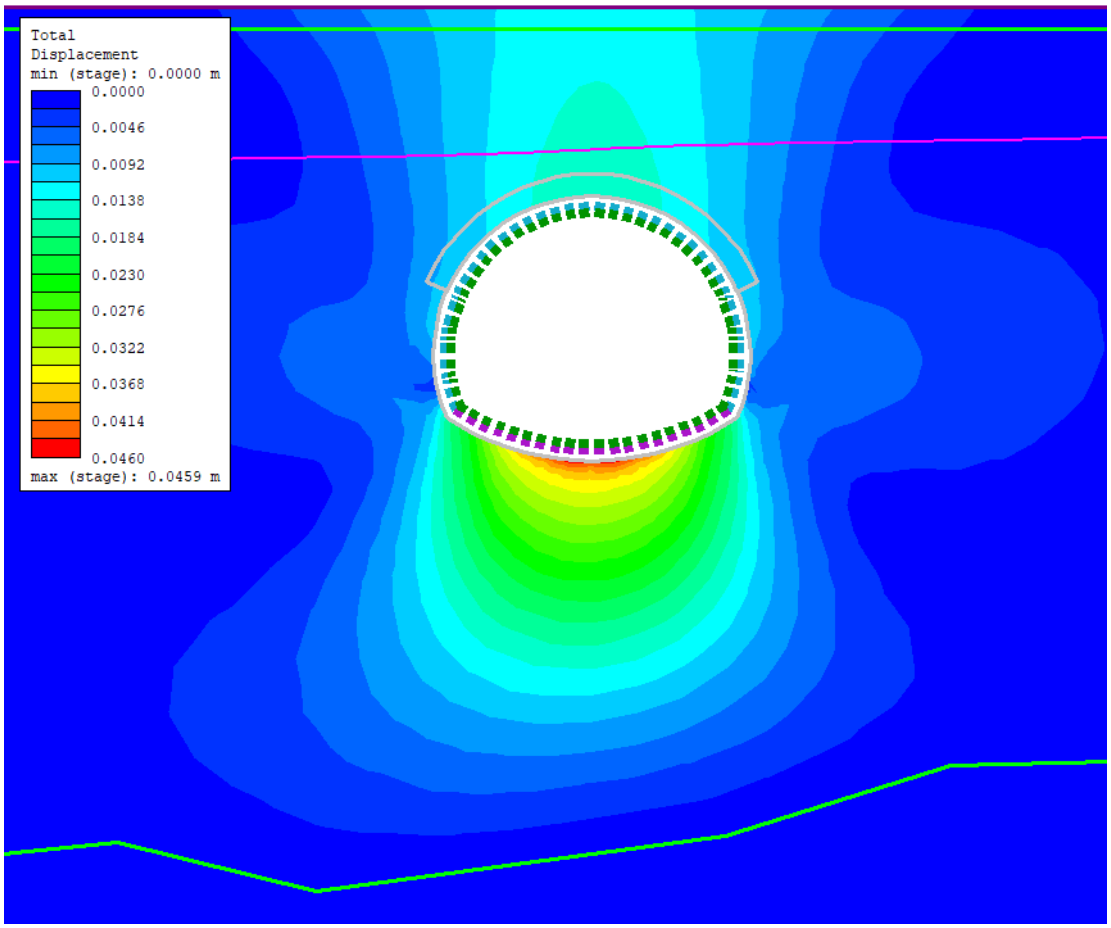

Figure 8.30: Modeled excavation of the tunnel's bench at 54+340 without present groundwater.

8.10 Parameter study

The accuracy of parameters used in a numerical model is crucial to obtain functional results. The parameters influence can differ from model to model. Therefore, there is done a parameter analysis to investigate the influence of the assumed most important parameters; the Young's modulus, cohesion, and friction angle. These parameters are initially found through preliminary investigations and laboratory tests. Several uncertainties follow. The samples on which the tests are performed might not be the most descriptive of the soil or rock as a whole. As well, are often averages of parameter values used, which also can be misleading. Because of this, the influence of the parameters is important to know.

The parameter analysis is done by only changing the parameter of questioning while keeping all the other parameters the same. The model of the cross-section 54+160 is used, with groundwater, the improved layer, and both liners present.

Table 8.7: Results from the analysis of the Young's modulus.

E-modulus (MPa)	E-modulus of improved layer (MPa)	Total displacement (mm)
50	2435	60
60	2445	51.4
70	2455	44.9
80	2464	39.9
90	2474	36
100	2484	32.7
110	2494	30
120	2503	27.8
130	2513	25.8
200	2583	17.4

Young's modulus

The Young's modulus was tested from $50MPa$, which is a reduction of approximately 30% of the obtained value of $77MPa$, to $200MPa$, which is an increase of approximately 185%. The large increase in the Young's modulus could describe the soil if it had been through further ground improvement. When the Young's of the soil modulus change, so does the composition of the improved layer, this accounted for when the analysis was carried out. In table 8.7 the resulting values for both the Young's modulus for both the till and steel pipe umbrella , and the resulting total maximum displacemnet can be seen. In figure 8.31 the results of total maximum displacement are graphed towards the respective value of Young's modulus.

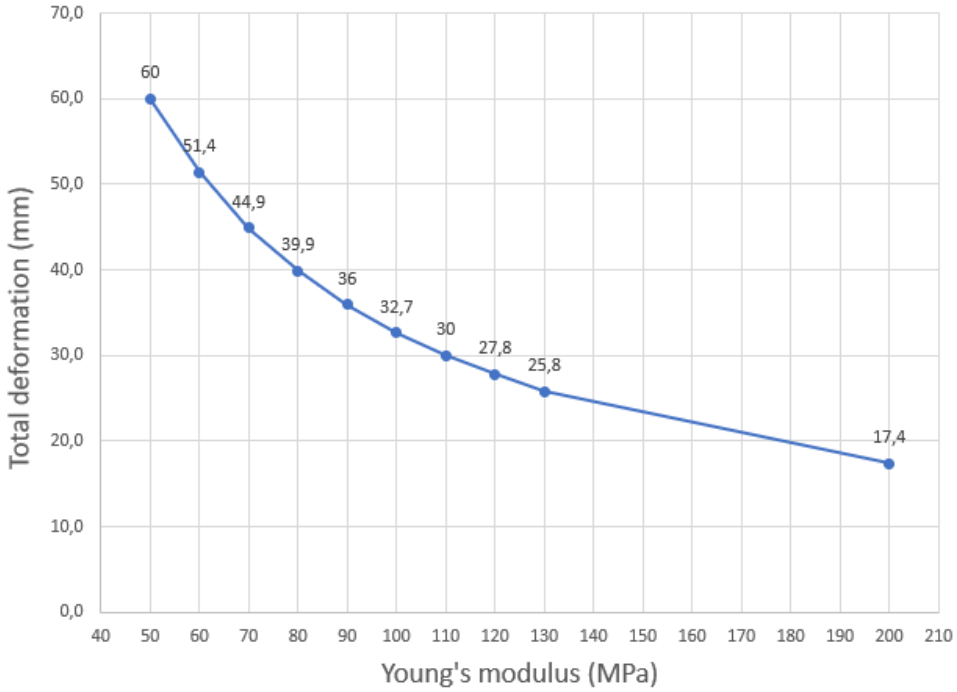

Figure 8.31: Value of the Young's modulus graphed towards the induced maximum total displacement.

Cohesion and friction angle

Drained soils stability depends strongly on the drained cohesion and friction angle, whereas undrained soils depend more on the undrained shear strength (Jones 2022). The influence of these parameters where therefore investigated in this parameter analysis. Both parameters' influence is plotted in the same graph, found in figure 8.32.

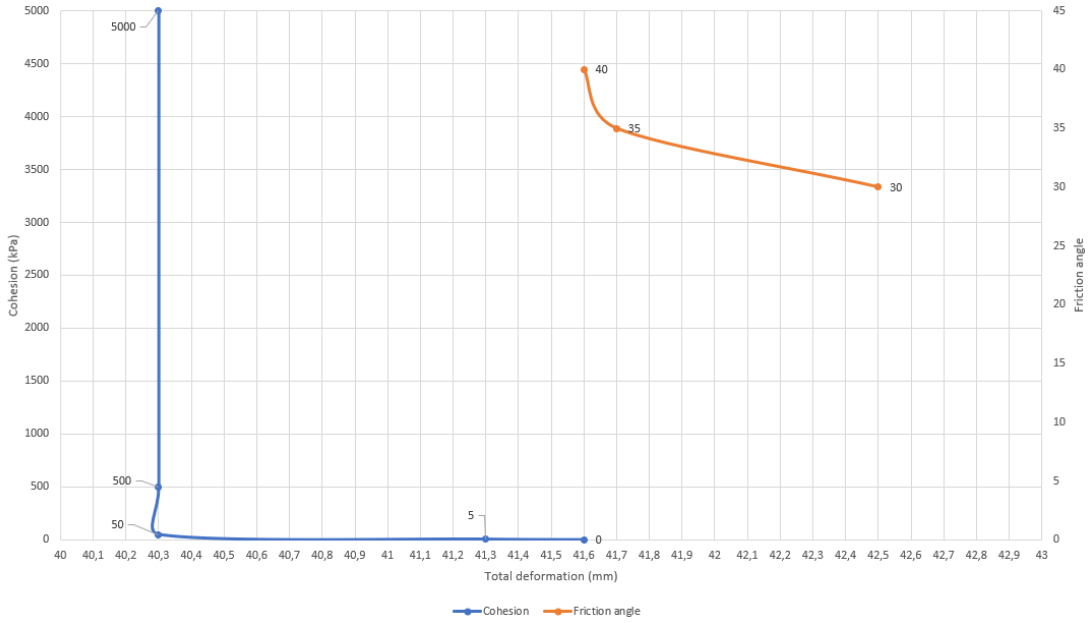

Figure 8.32: Results of the parameter analysis done for the cohesion and the friction angle.

The cohesion was tested at 5, 50, 500, and $5000kPa$. While the friction angle was tested at 30, 35, and 40. The change of these parameters was done separately.

8.11 Stress analysis

The field stress is as previously mentioned in chapter 8.5.4 a gravitational stress field. While the vertical component is easily calculated, the horizontal field stress component is more of a variable. It is given by: $\sigma_H = K \cdot \sigma_V$. In the previous models ran the value K has been equal to 0.4, as estimated through Jakys equation and statements of Queiroz, Roure, and Negro Jr (2006). However, the value of K can be found to be different. According to Queiroz, Roure, and Negro Jr (2006), the parameters of K are the least investigated and most overlooked parameter. Also stating that a typical interval for Quartenary glacial deposits is between $0.6 - 1$.

As proved by the grain size distribution curves the soil of the Drammen site is dominated by sand. The value of K for sand can vary from $0.25 - 1.0$ (Janbu and Hjeldnes n.d.). Based on this information the stress analysis has been done testing values from $0.3 - 1.0$. The results of the analysis are found as a graph

in figure 8.33.

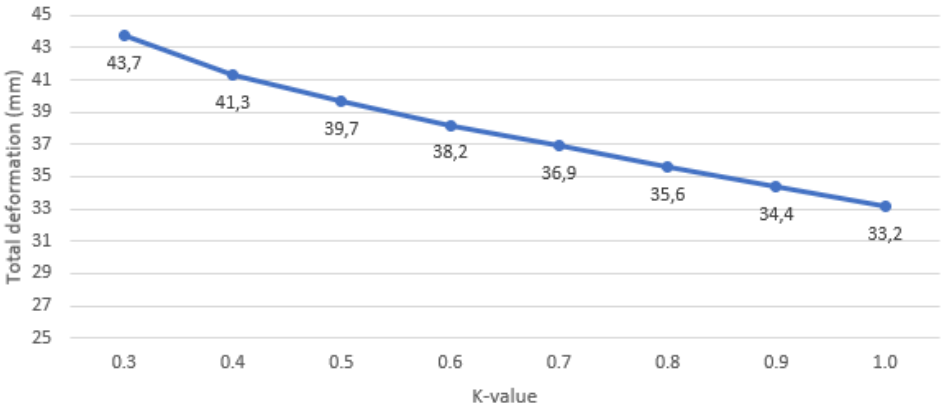

Figure 8.33: The value of K graphed towards the total displacement of the tunnel.

The maximum total displacement of the tunnel is regarded as the most important displacement value. Despite this, the change of K induces an unproportionate change in the displacement along the profile of the tunnel. In figure 8.35 the absolute value of the horizontal displacements along the tunnel profile when $k = 1$ can be seen, and in figure 8.34 the same can be seen when $k = 0.4$. When K decreases the vertical stress becomes increasingly larger than the horizontal stresses. This causes the shear forces of the walls to increase and the horizontal displacement of the walls increase while the horizontal displacement of heading and invert decrease.

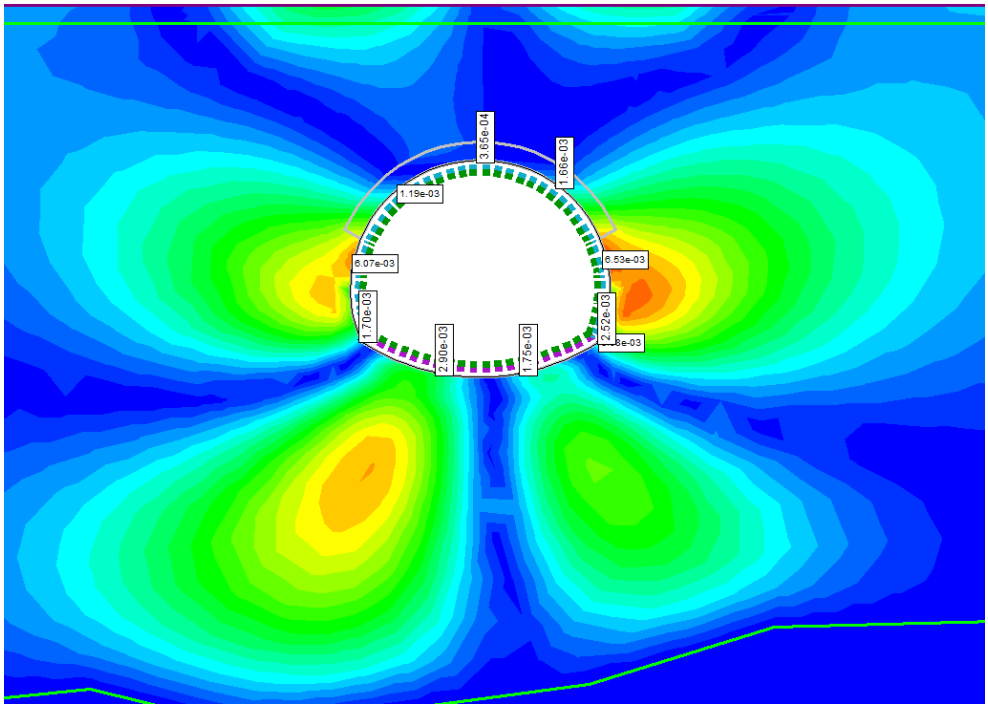

Figure 8.34: The horizontal displacement distribution around the tunnel when $k = 0.5$.

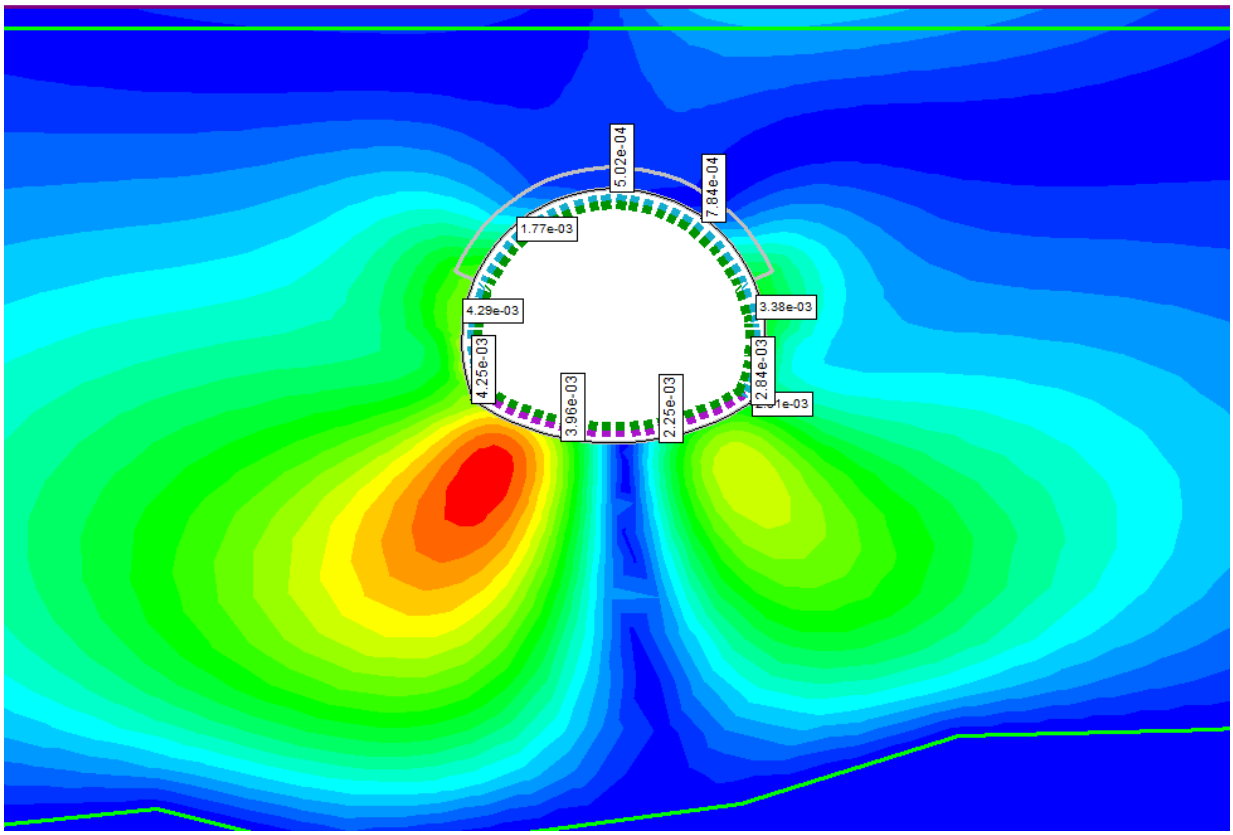

Figure 8.35: The horizontal displacement distribution around the tunnel when $k = 1$.

8.12 Support analysis

Since the support of the tunnel is essentially decided, the support analysis is done on the thickness of the liner. The initial thickness is $0.4m$ for both the immediate and permanent lining. To investigate how the thickness of the liner affects the results of the model an increase and decrease of $5, 10, 25, 50$, and 75% of the liner thickness tested. The change of thickness applies to both the immediate and the permanent liner. The result of the analysis is viewed in figure 8.36 as a graph.

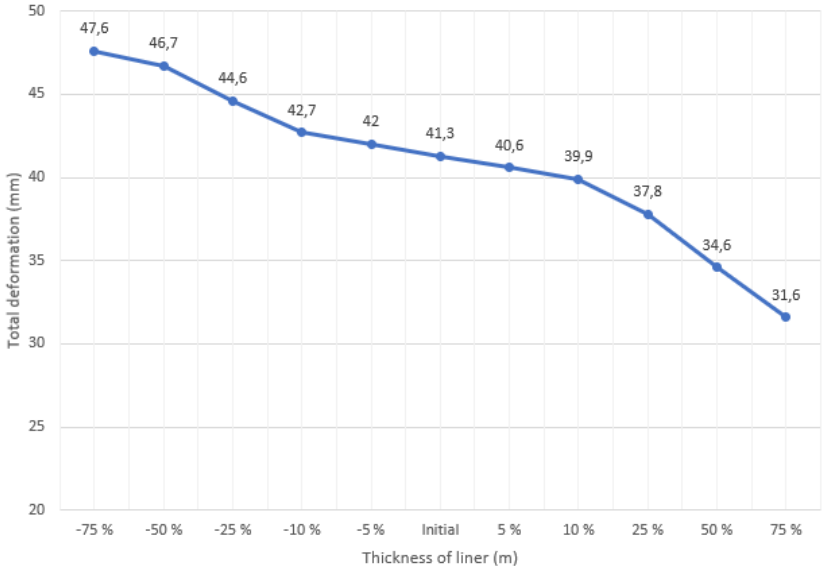

Figure 8.36: The thickness of the liner graphed towards the total displacement of the tunnel.

Experiences from international projects have proved that bolts can be effective even in soft ground conditions. The bolts have to be self-drilling because if a hole was to be drilled it would likely collapse. To see if bolts could have a significant impact on the stability of the tunnel, bolts were added to the model. In figure 8.37 the setup of the excavation with bolt can be seen. Bolts are added all around the profile. The bolts chosen were fully bonded, meaning the bolt is divided into the elements of the model and act independently of each other (Rocscience 2023a). They are *Dextra Geotec self-drilling anchor R38* of $4m$ length and spacing of $1m$. The parameters of the bolts can be seen in table 8.8.

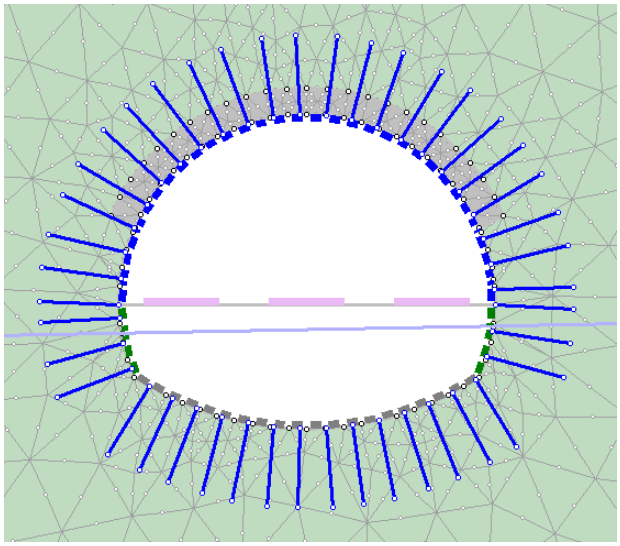

Figure 8.37: Setup of the model featuring bolts as support.

Table 8.8: Parameters of the bolt Dextra GEOTEC Self Drilling Anchor R38.

Bolt	**Value**
Bolt diameter [mm]	38
E-modulus [MPa]	45000
Tensile capacity [MN]	0.5
Residual tensile capacity [MN]	0
Out-of-plane spacing [m]	1

When running the model with the bolts the maximum total displacement was $39.3mm$, which is a decrease of $2mm$.

8.13 Limitations

Numerical modeling of tunnels in 2D is an approximation. When modeling we are assuming an unknown as an input instead of obtaining it as an output. The stress distribution is determined in advance and applied to the tunnel lining at the beginning of the final stage, which significantly influences the results. Consequently, 2D analysis of tunnels is, at best, semi-empirical, and, at worst, predetermined. Although 2D numerical models can be adjusted to find a maximum settlement, volume loss, or lining stresses. It is rare to obtain all simultaneously (Jones 2022).

It is as stated crucial to handle the results of numerical analyses with care. The variability in input data introduces uncertainty, so relying solely on a single analysis is foolish. When doing numerical analysis one should instead perform multiple parametric studies, systematically varying input parameters within a credible range. This approach helps to understand how sensitive the design is to these different parameters. According to Hoek and M. Diederichs (2006) assessing the design's acceptability based on the sensitivity to changes in input parameters can be more useful than relying on a single calculated displacement value or an obtained factor of safety (Hoek and M. Diederichs 2006).

9 Discussion

9.1 Reliability of parameters

When designing a complex construction, such as a tunnel, the understanding of the ground conditions is essential. This knowledge is acquired through preliminary investigation. The preliminary investigations should be thorough to prevent as much uncertainty as possible. Geotechnical parameters found are later used for calculations of the stability of the tunnel, and dimensioning of support measures. As proved in the parameter analysis of the numerical modeling certain parameters influence the stability significantly. The Young's modulus was such a parameter emphasizing the importance of valid parameters.

When performing geotechnical investigations there are several factors to consider to obtain values that describe the area of interest as accurately as possible. As geology rarely is isotropic, there are usually differences in characteristics within the same rock or sediment. This means that the locations where to take samples or measurements have to be carefully considered. When constructing a tunnel the locations of interest are through the planned route of the tunnel, surrounding areas should also be investigated but less frequently. As some of the tests done to acquire geotechnical parameters are dependent on physical specimens the state of the specimen facilitates another uncertainty. Getting a sample from the ground in the state of in-situ is near impossible.

When doing calculations such as numerical modeling one can only use one value to describe a material. In these cases usually, the averages of obtained values are used. Averages can often be reasonable values but not always. As one parameter have to be brought down to one single value provides for uncertainty. Empirical formulas are often used to acquire parameters that can't be found directly. Certain formulas are more documented than others and the degree of unreliability differs. There can also be multiple formulas giving different values. In these cases the choice of picking the better option for your spesific project is important.

The prediction of groundwater is an example of an unreliable parameter for the project of the Drammen tunnel. The preliminary investigations indicated that the groundwater table was located in the middle of the tunnel profile. Based on this information the tunnel support measures were divided into chambers that could be drained before excavation. In reality, hardly any water was encountered at all, and the attempts to drain the chambers were abandoned. Following the wrongly predicted groundwater table, more jet grouting was done than necessary, increasing the cost and the emissions of the project. For this thesis, the water table was assumed to be where the preliminary investigations initially placed it.

9.2 Comparison of the analytical and numerical results

When comparing the results of the analytical solutions and the numerical modeling it is important to remember that the calculations are done at different stages of the design process. The analytical solutions are crude estimations calculated as a first approach to the problem. Several simplifications regarding the characteristics of the ground conditions are made. The tunnel is assumed to be circular in a hydrostatic stress field. Drained or undrained behavior is not taken into account, and neither is groundwater at all. The difference between undrained and drained ground behavior is a crossroad when designing tunnels in soft ground. Also, geological structures such as rock boundaries, slopes, and joints are taken into account. Despite leading to somewhat unassertive solutions these calculations give an indication of how the ground should react to the construction. These indications are useful to consider when more precise calculations are carried out.

The tunnel deformation analysis uses the Mohr-Coluombs failure criterion to estimate the deformation of the tunnel walls and find the radius of the plastic zone surrounding the tunnel. Cohesion and friction angle, the strength parameters for drained soils, are used to find a value for the uniaxial compressive strength of the till. A sufficient internal pressure to withstand the external forces is then found, this value was found to be $0.057MPa$. With the calculated critical internal pressure the displacement of the walls was found to be $11.4mm$. This value is not far from the displacement found in the walls in the numerical modeling. Here the displacement in the walls ranges from $5 - 13mm$. Both the numerical modeling and the analytical solutions indicate a failure when no support measures are applied.

Through plotting the wall displacement towards the support pressure, the ground response curve was found. The curve starts off at the point where $p_i = p_0 = 0.17MPa$. The linear-elastic behavior of the rock can be seen until the support pressure reaches its critical value of $0.057mm$. After this point failure and the plastic deformation begins. The curves give an indication of how heavy the lining of the tunnel needs to be.

The longitudinal displacement profile was found using the equations of Vlachopoulos and M. S. Diederichs (2013). The profile reveals that a displacement of $0.2m$ will occur at the tunnel face if the tunnel was to be excavated unsupported. This profile does not take into account the steel pipe umbrella, and that the tunnel face is dived into sections. It can be observed the displacement is not only large at the tunnel face, displacements actually start approximately $22m$ ahead of the tunnel face. This is confirmed by the numerical model, but it also shows that with the support of the steel pipe umbrella the displacement at the tunnel face is not concerning. The value of K in the numerical model also decreases the displacement at the tunnel face. Both the model and the LDP indicates failure if no support is installed, as the tunnel wall

displacement reaches $1m$.

Peck's surface settlement equation is the empirical solution that stood out the most compared to the numerical modeling. Peck's equation estimated a settlement of $22.9mm$ at 54+160. The numerical model gave a settlement of $7.7mm$ at 54+160. Chainage 54+360 can be compared to the chainage of 54+340 where numerical modeling was done. Peck's equation gave a settlement of approximately $7.5mm$, while the numerical modeling gave a settlement of $15.3mm$. Hence, Peck's equation gives a larger settlement when the overburden is low and the numerical modeling indicates the opposite. The reason for this could be that Peck's equation doesn't take as many variables into account and is constructed to fit most tunnels, not all. The equation is also known to be a better fit for clays than sand which could have an impact (Masosonore 2018). Consequently, the results of the numerical modeling are assumed to be more accurate. What the curves of Peck do reflect is that the tunnel is more unstable where the overburden is lower, this is information that was brought into further calculations on the project.

Volume loss is used in the surface settlement prediction performed. This parameter in itself was found through an empirical chart to be 0.7%. The value was close to Norconsults' predicted value of 0.5%. After the numerical modeling was done the volume loss obtained in the models could be found by dividing the area of the excavation, being $22m^2$, with the change of the original area. In the model at chainage 54+160, the volume loss was 0.36%. At chainage 54+340 the volume loss is 2.6%. The change in the models' area was $-0.0784048m^2$ and $-0.564177m^2$ respectively. With the exception of the value for chainage 54+340, the values seem to be plausible and within the range of the empirical chart. All intent tends to the volume loss being bigger as the overburden increases.

9.3 Stability

Based on the numerical modeling the tunnel is on the verge of being described as stable using the steel pipe umbrella method. Given the cautious approach of the methods utilized, the decision leans towards characterizing the project as feasible. Further calculations and even more cautious approaches are however recommended. By doing this and with the right procedures the displacements and settlements should be acceptable. The calculation done on the project has been on purpose on the conservative side to further add to the safety factor. Pointing out the design of the steel pipe umbrella in RS2 where the decidedly most conservative method was chosen. Also, the effect of grouting and the feet-lock was not taken into account.

Displacement in the invert of the tunnel generally causes the largest displacements. Excavating a tunnel causes the ground to "fall" into the tunnel from all angles. The crown of the tunnel is reinforced better

than the invert by its superior arch and the steel pipe umbrella. Also, the feet-lock would in reality take on some of the engating forces. When doing numerical modeling for tunnels surrounded by soil it is quite common that the result shows a large displacement in the invert. In reality, this has proven to not be as big of a problem as the model indicates (Bent Aagaard, verbal communication, 06.06.2023). According to Aagaard, the largest displacements usually are expected in the lower parts of the walls (Bent Aagaard, verbal communication, 06.06.2023). If the large displacement of the invert is to be excluded the displacement along the profile at chainage 54+160 is barely surpassing $10mm$.

Specifically, the largest displacements in the numerical analysis were found in the invert of the top heading. Of course, at this point in construction, the tunnel is not fully supported, again, the feet-lock is not considered, and it won't be in that state for long. Taking this into account, a bit more displacement is allowed for, as far as it doesn't affect further construction. There are however measures that should be utilized to further improve stability after the excavation of the top heading. The displacement in the invert can be minimized by implementing a temporary invert of the top heading. The parabola shape of an invert distributes the uplifting forces better than a straight invert. To be even more careful the excavation could be divided into even more sections. The top heading could for example be split into two parts, and/or the invert could be excavated as an individual section.

Through numerical modeling, the influence of the most important parameters was studied. The presence of groundwater is undoubtedly not wanted. Groundwater makes the ground more sensitive to failure and the tunnel face is considerably less stable. Pumping and drainage will also add to the cost of the project. The groundwater table is however not supposed to be higher than initially modeled.

Out of the rest of the parameters tested, the Young's modulus clearly was the most influential. A reduction to $50MPa$ made the displacement increase to $60mm$, which in the designing phase is too much. Even though lots of preliminary investigations were performed, the Young's modulus was conducted from just two boreholes. Considering the importance of this parameter more tests should have been performed. The influence of cohesion and friction angle was also tested. The results from the testing of different cohesions were interesting. With just some cohesion the stability of the tunnel improves, and when this improved stability is achieved there is no difference if the value is further increased. For $50 - 5000kPa$ there is no difference in displacement. From $0 - 50kPa$ displacement decrease from by $1.3mm$. Stability increases as expected with the friction angle. Notably, the difference from $40 - 35°$ is $0.1mm$ of displacement, and the difference from $35 - 30°$ is $0.8mm$. Either one of these parameters seems to influence the stability of the tunnel significantly. Considering the significance of these parameters in drained conditions, it was anticipated that the differences would be more substantial.

Subsequently, the study focused on the impact of the K-value of the applied stress field. It was observed that the relationship between the K-value and the total maximum displacement was nearly linear. The rate of decrease was approximately $0.8mm$ per 0.1 increase in K. Hence, it is advantageous to have an isotropic stress field.

An analysis of the thickness of the lining was then conducted. The results revealed that lining thickness definitely does affect the maximum displacement, but perhaps not as much as first anticipated. The difference in reducing thickness with 10% and increasing the thickness with 10% was approximately $2.8mm$. The relationship between reducing/increasing the thickness is close to linear. The use of bolts was also applied to the model. The effect of bolting $3m$ bolts with a spacing of $1m$ was a reduction of $2mm$ displacement. Proving the measure can increase the stability, the question is however if it is considered efficient enough. Conceivably the use of bolts could be implemented if it is required by the displacements.

Stability of the tunnel face was investigated in the model of longitudinal sections. The values obtained indicate a stable tunnel face when support measures are applied. The most effective support measure for the face of a soft ground tunnel is the use of face bolts. This is also the cheapest alternative (Volkmann and Schubert 2009b). To ensure the stability of the tunnel face, sprayed-on concrete can also be utilized if needed.

To further investigate the stability of the tunnel 3D modeling should be carried out. As there are even more details necessary to conduct a 3D model this is the natural next step. Because of increased complexity, it is more difficult to recreate an accurate model of the scenario. If the model is successful, a further understanding of how the ground will react to excavation will be obtained. In particular effect of the steel pipe umbrella would be an advantage to have modeled in three dimensions. The simplifications that were done to model the two-dimensional steel pipe umbrella would then certainly be reduced.

9.4 Final design

After studying the ground conditions and the construction of the Drammen tunnel using the steel pipe umbrella method the proposed final design and order of construction will be as follows;

- Construction is carried out using a steel pipe umbrella of the dimensions described in chapter 4.
- Grouting through the steel pipes should be attempted before excavation is started. This can increase the strength of the soil surrounding the tunnel.
- The cross-section of the tunnel is to be divided into two sections; a top heading and a bench. After excavating the heading feet-locks are installed on both sides of the tunnel. The top heading should

also be excavated with an invert as proposed previously in this chapter. The excavation length of the top heading is $1m$ before immediate lining is applied. After four rounds of top-heading excavations the excavation of the bench is carried out.

- If groundwater is encountered, a drainage system leading the water out of the tunnel should be installed.
- The immediate lining consists of lattice girders in crown and walls, and wire mesh in the invert. Sprayed-on concrete is then applied around the entire profile with a thickness of minimum $0.4m$.
- To secure the face of the tunnel face bolts and sprayed-on concrete when needed is utilized.
- After three rounds of bench excavations, where the last one is $3m$ the next steel pipe umbrella is installed. The last bench excavation is shortened to $3m$ to ensure a $4m$ overlap of the steel pipe umbrellas.
- When the entire tunnel is fully excavated a waterproofing membrane is applied before permanent lining is installed. The permanent lining consists of concrete elements with a thickness of $0.4m$. At least the length of the tunnel being totally surrounded by till, the invert is to be filled with concrete to reduce heaving.
- Monitoring of both displacements of the tunnel profile and at the ground surface is also to be carried out to ensure control of the induced displacements. This is also done so that assessments of up-scaling or down-scaling of the construction can be done. For example, the section length could increase if the displacements are lower than expected.

9.5 Cost and emissions

When planning to construct a tunnel there are several factors to consider. First and foremost the tunnel has to be safe, hence stability of the tunnel is priority one. Secondly, it is desirable to construct the tunnel as cost-effective as possible and to keep emissions of the project as low as possible. There are many ways for utilizing emission-friendly measures for a given construction. However, there is no doubt that usually, the method itself is where there are the most emissions to save. In terms of emissions, it is clear that the jet grouting method has a greater environmental impact. This method involves considerably more use of concrete and machinery over an extended period, in contrast to the steel pipe umbrella method.

It is clear that the use of the steel pipe umbrella method would cost less than reinforcing the ground by jet grouting. The reason for this conservative choice of construction method was probably the assessment of

risk. One could question whether the safety factor has been set too high for this project. The feasibility of constructing the Drammen tunnel using the steel pipe umbrella method has been assessed as possible through this thesis. An estimate of the cost based on the information accessible follows.

9.5.1 Jet grouting method

The contract of UDK02 as a whole had a value of 1,8 billion NOK (Backer 2021). Of course, this included the $540m$ of cut-and-cover tunnel being built. The soft ground tunnel however costs more than the cut-and-cover tunnel. Therefore, to estimate the price of just the soft ground tunnel the price is cut in half, becoming 600 million. Even when cut in half the price is most likely underestimated

Over 2000 boreholes with an average length of $30m$ were drilled to establish the jet grout structure. Accounting for an area of approximately $40,000m^3$ (Backer 2021). The cost of jet grout is $6700\text{NOK}/m^3$, thus the jet grouting alone cost 268 million NOK. For excavating the tunnel after jet grouting is finished the cost is $2500 - 3000\text{NOK}/m^3$ for the heading and $1200 - 1300\text{NOK}/m^3$ for the bench and invert (Einar Helgasson, written communication, 24.04.2023).

9.5.2 Steel pipe umbrella method

When estimating the cost for the steel pipe umbrella method, cost of the Joberget tunnel is used based on Aagaard et al. (2017). The cost of the tunnel as a whole was $425,000\text{NOK}/m$ for the Joberget tunnel. Since the method would be more challenging at the Drammen site, considering the entire tunnel is located in till for $150m$, and the cross-section is larger, the cost for the Drammen tunnel is rounded up to be $500,000\text{NOK}/m$. Adjusted for inflation to the year of 2022 it becomes $627.261\text{NOK}/m$. Cost of the entire soft ground tunnel of $290m$ would then be approximately 182 million NOK. This is less than a third of the price for the underestimated cost of the current tunnel constructed using the jet grout method.

9.6 Future work and recommendations

The stability analysis resulted in the tunnel being declared stable if constructed correctly. To get another perspective a stability analysis through 3D modeling is recommended. More trustworthy values for parameters are needed. Several of the parameters used in the numerical modeling is found through empirical equations and other estimations which will never be true values of the ground. The increased safety factor is a cause of uncertainties in these parameters. More resources should be put into getting reliable parameters and a detailed investigation of possible options for constructing tunnels. By following up on these suggested recommendations, it is possible, or even likely, that tunnel construction could be cheaper with less emissions.

10 Conclusion

As part of the new double-track railway from Drammen to Kobbervikdalen the Drammen tunnel is being constructed. $290m$ of this tunnel is being constructed as a soft ground tunnel. The tunnel is located in glacial till and rhomb porphyry, and the water table was in the preliminary investigations assumed to be located between the middle and upper part of the tunnel's profile. Veidekke has a total enterprise on the project and has chosen to build the tunnel through extensive reinforcement of the ground by jet grouting. This approach is expensive and time-consuming. The project is also likely over-dimensioned. Therefore, the possibility of constructing the soft ground tunnel by using the steel pipe umbrella method is assessed in this thesis.

To evaluate if the steel pipe umbrella method is a feasible solution for the construction of the Drammen tunnel, the following methodology was employed. Starting by investigating the area of interest and its ground conditions. Through gathered information and laboratory work, an understanding of the ground conditions including the groundwater situation was obtained. Based on the knowledge of the ground conditions and comparisons to similar projects an initial design of the steel pipe umbrella and the construction of the tunnel was prepared. Thereafter, analytical and empirical calculations were made before more complex calculations were carried out through numerical modeling. After the calculations were done and adjustments were made the final design was proposed.

It was found feasible to construct the Drammen tunnel using the steel pipe umbrella method. Granted enough caution during construction. The sectioning is of importance and support has to be established immediately after excavation. The tunnel's face is divided into a heading with an invert and a bench. Feet-locks are also established. Excavation lengths are held short. Due to the large relative displacement of the invert, it should be filled with concrete for the first $150m$ of the tunnel. Avoiding groundwater is found to be of utmost importance and a lowering of the groundwater should be considered. Based on there being possible sensitive clay some distance away this was not allowed for.

Analytical, empirical, and numerical calculations were done for the tunnel. The calculations usually were similar, with some exceptions. Generally, the numerical models were more trusted as the scenarios are better described, but the analytical and numerical solutions did provide valuable indications. The largest displacements were found in the invert of the tunnel. This is common for numerical analysis of tunnels surrounded by soil, but through experience, the displacements are often smaller. Also, the factor of the feet-lock was not accounted for in the model. Considering the displacements surrounding the profile, the values indicate a stable tunnel.

To save expenses and the environment preliminary investigations should be more detailed. Geotechnical parameters are of great importance when planning construction. By achieving more precise designs, it may be possible to avoid overly cautious construction choices. If the tunnel were constructed using the steel pipe umbrella method it would have been much cheaper and stood for less emission. There should be a stronger emphasis on obtaining precise geotechnical data in order to enhance the accuracy of the models and avoid over-dimensioning of tunnel projects.

References

Aagaard, B. et al. (2017). "The Joberg tunnel. Successful tunnelling in moraine". In: *Proceedings of the World Tunnel Congress 2017 – Surface challenges – Underground solutions*. Bergen, Norway: Publisher Name.

Aagaard, B. (2020). *Forelesning om løsmassetunneler gitt i faget ingeniørgeologi videregåede kurs, løsmasser*.

AG, R. G. (2015). *Pipe Umbrella*. URL: https://www.rodio.ch/rodio-geotechnik-ag/pipe-umbrella-rodio-geotechnik-ag.html (visited on 09/10/2022).

Alejano, L. et al. (2009). "Ground reaction curves for tunnels excavated in different quality rock masses showing several types of post-failure behaviour". In: *Department of Natural Resources and Environmental Engineering, ETSI Minas. Campus Lagoas-Marcosende s/n, University of Vigo, 36280 Vigo, Spain*.

Ali, A., Y. W. Chiang, and R. M. Santos (2022). "X-ray Diffraction Techniques for Mineral Characterization: A Review for Engineers of the Fundamentals, Applications, and Research Directions". In: *MDPI*.

Alpan, I. (1970). "The geotechnical properties of soils". In: *Earth-Science Reviews* 6.1, pp. 5–49. ISSN: 0012-8252.

Anagnostou, G. and K. Kovari (1996). "Face Stability Conditions with Earth-Pressure-Balanced Shields". In: *Tunnelling and Underground Space Technology* 11.4, pp. 415–424.

Andreassen, F. (1999). "OSLOFJORDTUNNELEN - ERFARINGER FRA FRYSING OG DRIVING GJENNOM FRYSESONEN". In.

Asgeir S. Gylland, B. A. (2017). *E39 Joberget løsmassetunnel - Rørskjerm - Erfaringsrapport*. Tech. rep. Sweco.

Aygar, E. B. and C. Gokceoglu (2013). "Analytical solutions and 3D numerical analyses of a shallow tunnel excavated in weak ground: a case from Turkey". In: *Tunnelling and Underground Space Technology* 35, pp. 113–122.

Løsmassetunnel Drammen (2021). Fjellsprengningskonferansen 2021.

UTGRAVING OG SIKRING AV NORGES STØRSTE OG MEST SPEKTAKULÆRE LØSMASSETUNNEL (2022). Fjellsprengningskonferansen 2022.

BaneNor (2012a). *UVB-02-V-21150 km 54,140-54,431 Temporary support and jet grouting-Plan view and longitudinal section 2 of 2, Blueprint*.

– (2012b). *UVB-02-V-21150 km 54,140-54,431 Temporary support and jet grouting-Plan view_and longitudinal section 1 of 2, Blueprint*.

– (2021). *Vestfoldbanen (Drammen – Larvik) UDK02 Kulvert og Løsmassetunnel Geoteknikk/Kulvert Jet Grouting Compartment 2 Final Report*. Tech. rep. BaneNor.

Box jacking (2022). URL: https://www.jackedstructures.com/box-jacking.html (visited on 12/16/2022).

Brede, N. K. (2022). "Drivemetoder og grunnforhold for løsmassetunneler i Norge". NTNU.

Chapuis, R. P. (2012). "Estimating the in situ porosity of sandy soils sampled in boreholes". In: *Engineering Geology* 141-142, pp. 57–64.

Chen, L. et al. (2019). "Vertical Load and Settlement at the Foot of Steel Rib with the Support of Feet-Lock Pipe in Soft Ground Tunnel". In: *School of Highway, Chang'an University, Xi'an 710064, Shannxi Province, China*. Ed. by F. Aslani.

Chern, J. C., F. Y. Shiao, and C. W. Yu (1998). "An empirical safety criterion for tunnel construction". In: *Proceedings of Regional Symposium on Sedimentary Rock Engineering*. Taipei, China, pp. 222–227.

Dash, M. (2012). *The Epic Struggle to Tunnel Under the Thames*. URL: https://www.smithsonianmag.com/history/the-epic-struggle-to-tunnel-under-the-thames-14638810/ (visited on 11/15/2022).

Dywidag-Systems (2010). *AT-pipe Umbrella System*. Brochure. URL: http://www.dywidag-norge.no/wp-content/uploads/2015/04/DSI-ALWAG-Systems-AT-Pipe-Umbrella-System-en.pdf.

Eidesen, J. M. (2013). "Metodikk for driving og sikring gjennom svakhetssoner ved Rogfast". MA thesis. NTNU.

FREEZING 120 MBSL IN THE OSLOFJORD SUBSEA TUNNEL (2022). URL: https://www.geofrost.no/no/artikler/grunnfrysing-i-oslofjordtunnelen/ (visited on 10/18/2022).

GEOFROST (2022). *Om grunnfrysning*. URL: https://www.geofrost.no/no/om-grunnfrysing/ (visited on 10/12/2022).

Gheibi, A. and A. Hedayat (n.d.). "The Relation between Static Young’s Modulus and Dynamic Bulk Modulus of Granular Materials and the Role of Stress History". In: *Geotechnical Earthquake Engineering and Soil Dynamics V*, pp. 373–382.

Google (2023). *Google maps*. URL: https://www.google.com/maps/@64.248077,15.6682714,5.45z?entry=ttu (visited on 03/12/2023).

Gylland, A. S. (2012). "Strindheimtunnelen - Stabilitetsanalyse og vurderinger av påhugget ved dagsone vest". MA thesis. NTNU.

Hæstad, N. and L. Backer (2020). *UDK 02 Kulvert og Løsmassetunnel – tekniske utfordringer og gjennomføring av totalentreprise*. Presentation. Tunneldagene i Drammen Conference. Veidekke and Bane NOR.

Halvdorsen, S. (1977). *Morener; dannelse, klassifikasjon og egenskaper*. Norges landbrukshøyskole.

Hansen, H. (2016). *Da tyskerene måtte sitt Waterloo i de trønderske leirmassene ved Lerkendal*. Strinda historielag.

E6 Trondheim Stjørldal, parsell Trondheim, dagsone vest, spesielle utfordringer krever spesielle løsninger (2011). Fjellsprengningskonferansen 2011.

Hoek, E. (1999). "Support for very weak rock associated with faults and shear zones". In: *Distinguished Lecture for the Opening of the International Symposium on Rock Support and Reinforcement Practice in Mining*. Kalgoorlie, Australia.

– (2000). "Numerical Modelling for Shallow Tunnels in Weak Rock - Unpublished notes". In: *Rocscience*.

Hoek, E. (2007). *Practical Rock Engineering*. Spon Press.

Hoek, E. and M. Diederichs (2006). "Empirical estimation of rock mass modulus". In: *International Journal of Rock Mechanics and Mining Sciences* 43.2, pp. 203–215.

Hoek, E. and P. Kaiser (1995). "Support of Underground Excavation in Hard Rock". In.

Hoek, E. and P. Marinos (1998). "Predicting tunnel squeezing problems in weak heterogeneous rock masses". In: *Tunnelling and Underground Space Technology* 13.3, pp. 263–273.

Hong, W.-K. (2012). "Hybrid Composite Precast Systems". In: *Journal of Constructional Steel Research* 69.1, pp. 1–12.

ISO 17892-4:2016 Geotechnical investigation and testing – Laboratory testing of soil – Part 4: Determination of particle size distribution (2016). International Organization for Standardization. ISO 17892-4:2016.

Jakobsen, P. D. (2014). "Estimation of Soft Ground Tool Life in TBM Tunnelling". Faculty of Engineering Science and Technology, Department of Civil and Transport Engineering. Thesis for the degree of Philosophiae Doctor. Trondheim: Norwegian University of Science and Technology.

Janbu, N. and E. Hjeldnes (n.d.). "Principal Stress Ratios and Their Influence on the Compressibility of Soils". In: *International Society for Soil Mechanics and Geotechnical Engineering Journal* ().

Jetgrunn (2022). *Jetpeler*. URL: http://www.jetgrunn.no/index.php?option=com_content&view=article&id=25&Itemid=108 (visited on 10/07/2022).

Jones, B. (2022). *Soft Ground Tunnel Design*. Taylor and Francis group LLC.

Karimi, S., M. Sabetamal, and R. Ajalloeian (2021). "Groundwater control in tunnelling through soft ground". In: *Tunnelling and Underground Space Technology* 107, p. 103652.

D18 SYKKELVEI KRONSTADTUNNELEN – KRYSSLØSNING I LØSMASSER (2022). Fjellsprengningskonferansen 2022.

Langåker, M. Ø. (2014). "Joberget Tunnel - Analysis of stability and support design for tunneling in soil". MA thesis. Norwegian University of Science and Technology.

Leen, J. et al. (2013). "Assessment of K_0 correlation to strength for granular materials". In: *Journal of Civil and Environmental Engineering*.

"Loess in Europe—its spatial distribution based on a European Loess Map, scale 1:2,500,000" (2007). In: *Quaternary Science Reviews*.

Marita RamsvikKyrre Kjellevold, E. A. o. R. S. ((2022). *Grav raste ned i tunnelen. – Ikke noen ønskelig situasjon.* URL: https://www.bt.no/nyheter/lokalt/i/G3Ldgm/grav-raste-ned-i-tunnelen-ikke-noen-oenskelig-situasjon (visited on 03/17/2023).

Masosonore, M. C. (2018). *Consequences of tunneling by the New Austrian Tunneling Method (NATM) in urban areas on ground surface*. Tech. rep. University of Science and Technology Houari Boumediene.

Minh Ngan Vu Wout Broere, J. B. (2015). "Volume loss in shallow tunneling". In.

Myhre, S. H. (2014). "Holmestrandtunnelen: Ingeniørgeologisk analyse av stabilitet og sikring for tunneldriving gjennom løsmasser". MA thesis. Institutt for geologi og bergteknikk, Tekniske geofag.

NGI (2022). *Vestfoldbanen, (Drammen) - Larvik, UDK02 Kulvert og Løsmassetunnel, Geoteknikk/Kulvert, Datarapport supplerende grunnundersøkelser*. Tech. rep. BaneNor.

NGU (2023a). *BERGGRUNN - Nasjonal Berggrunnsdatabase*. URL: https://geo.ngu.no/kart/berggrunn_mobil/ (visited on 03/18/2023).

– (2023b). *Rombeporfyr*. URL: https://www.ngu.no/om-geologi/rombeporfyrs (visited on 02/18/2023).

Norconsult (2017). *InterCity-prosjektet, VESTFOLDBANEN, DRAMMEN - KOBBERVIKDALEN, SAMLERAPPORT - GEOFYSISKE OG HYDROGEOLOGISKE FELTUNDERSØKELSER I STRØMSÅSEN*. Tech. rep. BaneNor.

– (2018a). *InterCity-prosjektet, VESTFOLDBANEN, DRAMMEN – KOBBERVIKDALEN, LØSMASSETUNNEL RAPPORT (med kostnader)*. Tech. rep. BaneNor.

– (2018b). *Vestfoldbanen Drammen - Kobbervikdalen, UDK 02 Kulvert og Løsmassetunnel, Totalentreprise, Vedlegg E, del II, Fagrapport hydrogeologi UDK 02*. Tech. rep. BaneNor.

norgeibilder (2023). *BERGGRUNN - Nasjonal Berggrunnsdatabase*. URL: https://www.norgeibilder.no/ (visited on 03/18/2023).

Palmstrom, A. (n.d.). "A SHORT INTRODUCTION TO THE GEOLOGICAL HISTORY OF NORWAY". In: *NFF* ().

Queiroz, P. I. B. d., R. N. del Roure, and A. Negro Jr (2006). "Bayesian Updating of Tunnel Performance for K0 Estimate of Santiago Gravel". In: *Journal of Geotechnical Engineering*.

Railsystem (2022). *Cut and cover*. URL: https://railsystem.net/cut-and-cover/ (visited on 10/23/2022).

Ramberg, I., I. o. N. G. F. Bryhni, and A. Nøttvedt (2007). *Landet blir til: Norges geologi*. Norsk geologisk forening.

Rocscience (2023a). *Fully bonded*. Retrieved May 5, 2023, from https://www.rocscience.com/help/rs2/documentation/rs2-model/support-2/bolts/define-bolt-properties/fully-bonded.

– (2023b). *Geotechnical Software for Rock and Soil | Rocscience*. Retrieved April 28, 2023, from https://www.rocscience.com/.

– (2023c). *Strength Properties*. Retrieved May 20, 2023, from https://www.rocscience.com/help/rs2/documentation/rs2-model/material-properties/define-material-properties/strength-properties.

Sakurai, S. (1983). "Displacement Measurements Associated with the Design of Underground Openings". In: *Proc. Int. Sympo. Field Measurements in Geomechanics*. Zurich, pp. 1163–1178.

Spyridis, P. and D. Proske (2020). *Revised Comparison of Tunnel Collapse Frequenciesand Tunnel Failure Probabilities*. Tech. rep. ASCE.

Su, Y., Y. Su, and N. Vlachopoulos (Feb. 2021). "Tunnel Stability Analysis in Weak Rocks Using the Convergence Confinement Method". In: *Rock Mechanics and Rock Engineering* 54.

Subsurfwiki (2023). *P-wave modulus*. URL: https://subsurfwiki.org/wiki/P-wave_modulus (visited on 05/12/2023).

Svensson, A. (2014). "Estimation of Hydraulic Conductivity from Grain Size Analyses". MA thesis. CHALMERS UNIVERSITY OF TECHNOLOGY.

Tan, W. L. (2005). *Numerical analysis for shallow tunnels in weak ground supported by umbrella arch method*. Tech. rep. Nanyang Technological University, Singapore.

Trinh, Q., E. Broch, and M. Lu (2010). "2D versus 3D modelling for funnelling at a weakness zone". In: *Rock Engineering in Difficult Ground Conditions – Soft Rocks and Karst*. Ed. by D. Vrkljan. SINTEF, Trondheim, Norway; NTNU, Trondheim, Norway. London: Taylor & Francis Group.

Vlachopoulos, N. and M. S. Diederichs (2013). "Improved Longitudinal Displacement Profiles for Convergence Confinement Analysis of Deep Tunnels". In: *Tunnelling and Underground Space Technology* 38, pp. 112–123.

Volkmann, G. and W. Schubert (2009a). *Effects of Pipe Umbrella Systems on the Stability of the Working Area in Weak Ground Tunneling*. Tech. rep. Graz University of Technology.

– (2009b). "Effects of Pipe Umbrella Systems on the Stability of the Working Area in Weak Ground Tunneling". In.

Volkmann, G. and W. Schubert (Jan. 2011). "Advantages and specifications for pipe umbrella support systems". In: *14th Australasian Tunnelling Conference 2011: Development of Underground Space, Proceedings*, pp. 619–629.

WSP (2022). *Cut and cover*. URL: `https://www.wsp.com/en-us/services/cut-and-cover-tunneling` (visited on 10/23/2022).

Zhang, P. et al. (2008). "Determination and verification of the longitudinal deformation profile in a horseshoe shaped tunnel using two-stage excavation". In: *Proceedings of the 5th International Conference and Exhibition on Mass Mining*. Luleå University of Technology. Luleå, Sweden: Luleå University of Technology.

Zhang, Q. et al. (2019). "Surface Settlement Induced by Subway Tunnel Construction Based on Modified Peck Formula". In: *Springer Nature Switzerland AG*.

Zienkiewicz, O., R. Taylor, and J. Zhu (2005). *The Finite Element Method: Its Basis and Fundamentals*. Butterworth-Heinemann.

A Longitudinal section

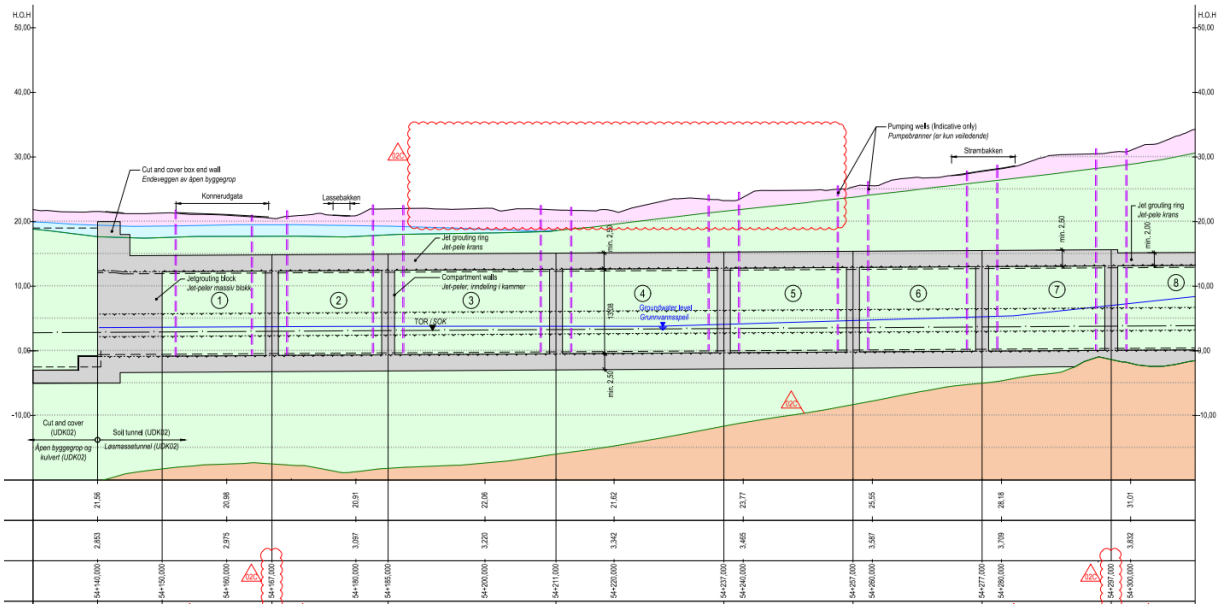

Figure A.1: Longitudinal section of the Drammnen tunnel from 54+140 to 54+300 (BaneNor 2012b).

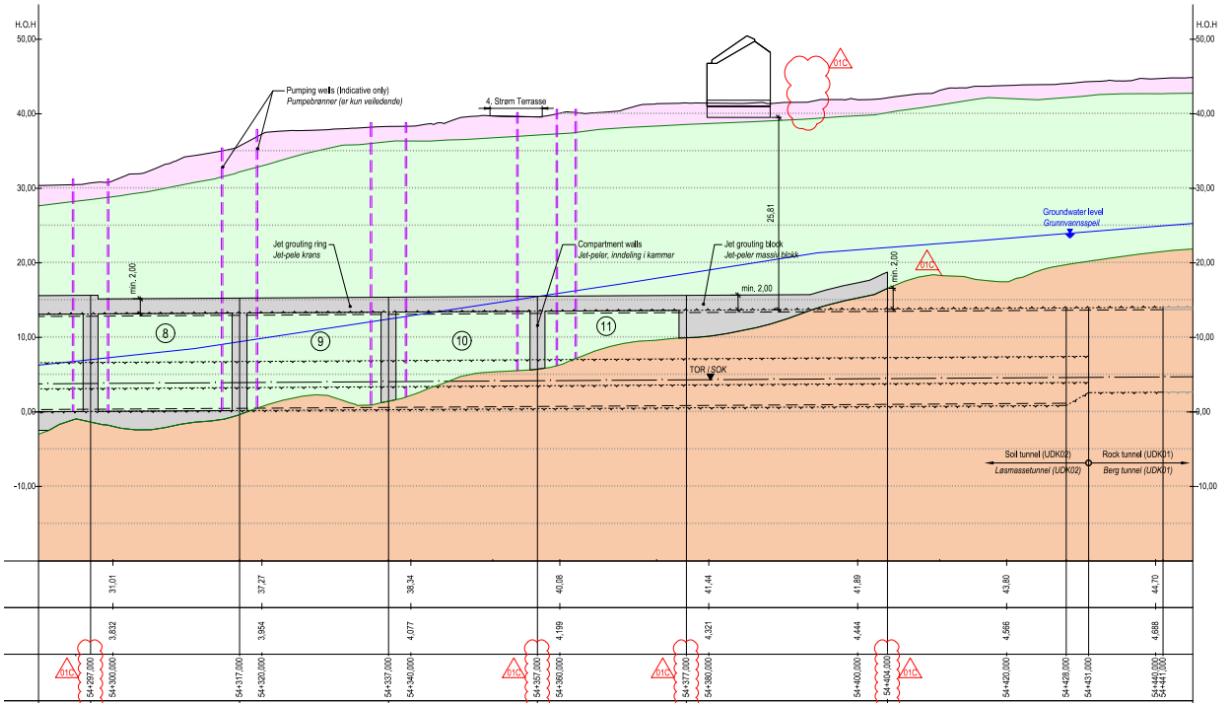

Figure A.2: Longitudinal section of the Drammnen tunnel from 54+300 to 54+404 (BaneNor 2012a).

B Geotechnical Parameters

Overview of core sample boreholes

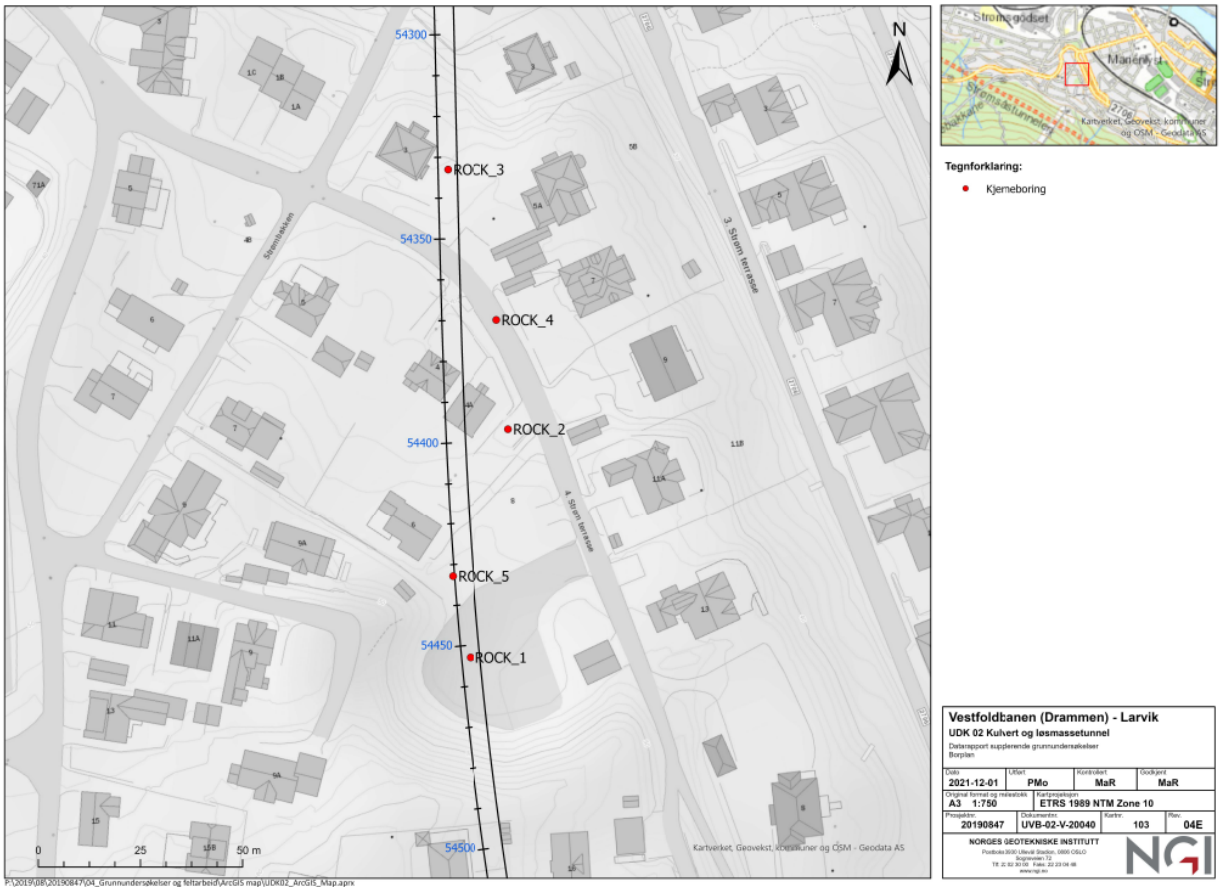

Figure B.1: Overview of the boreholes used for core samples of the rhomb-porphyry (NGI 2022).

Overview of preliminary investigations

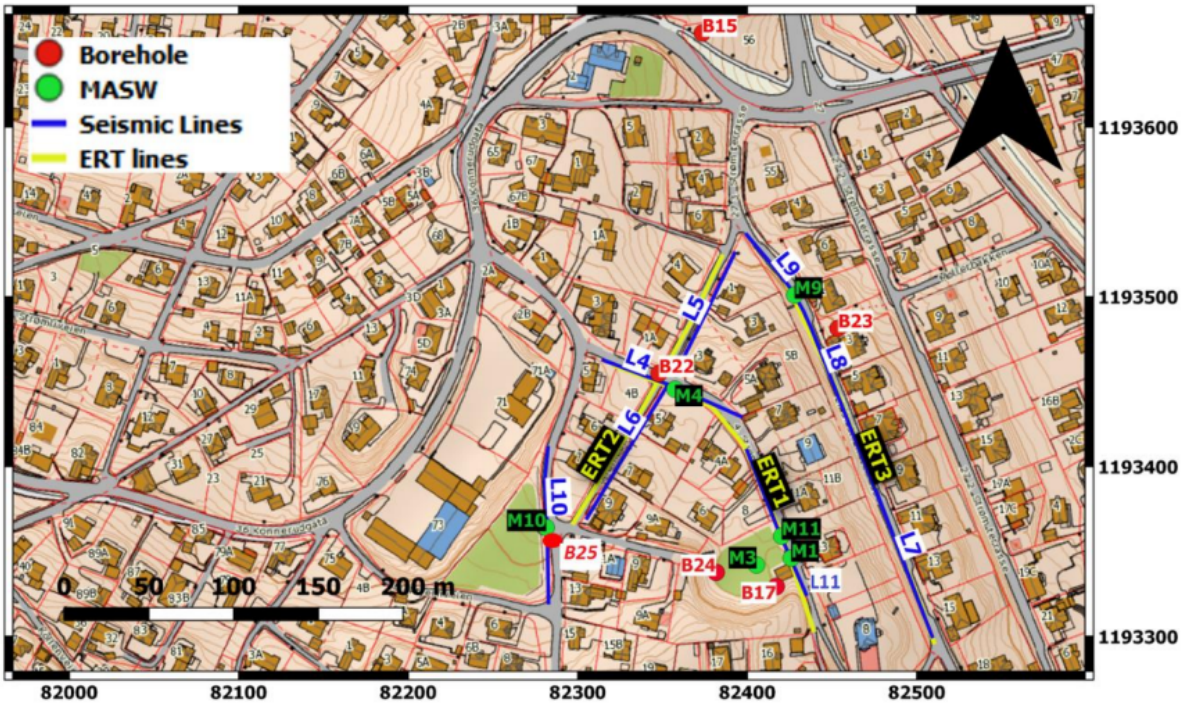

Figure B.2: Overview of the profiles and wells of the preliminary investigations (Norconsult 2017).

Roundness chart

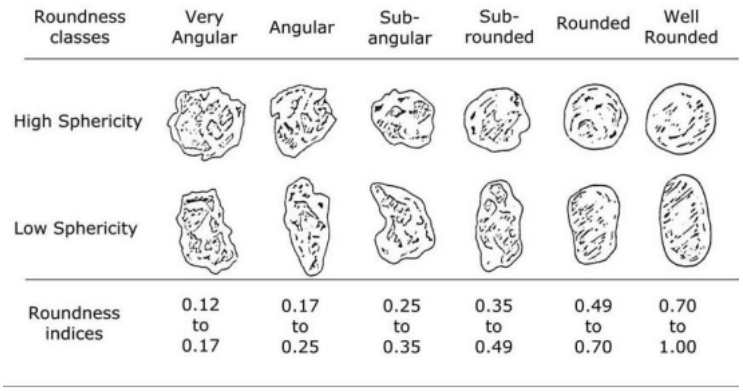

Figure B.3: Roundness chart (Norconsult 2017).

Grain size distribution of B15

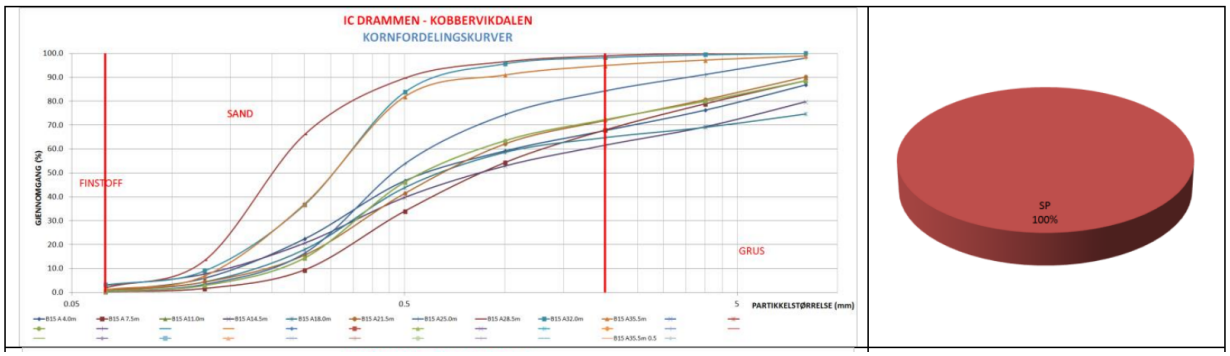

Figure B.4: Grain size distribution of B15.

Grain size distribution of B17

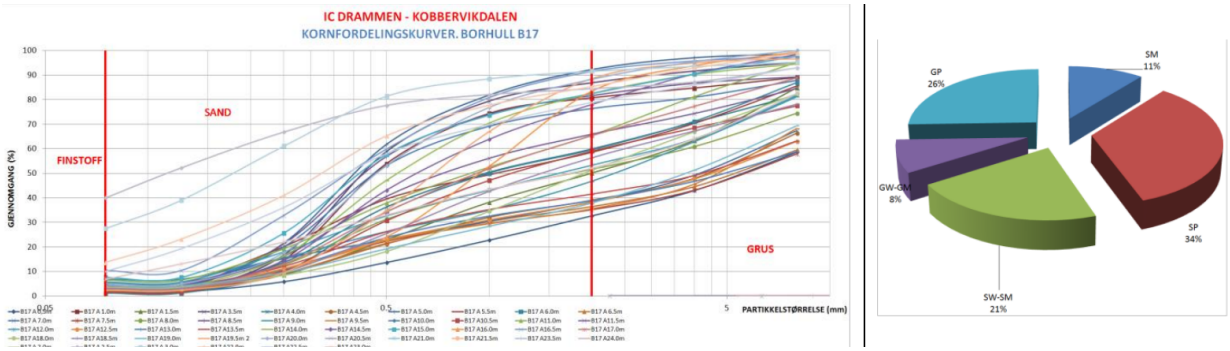

Figure B.5: Grain size distribution of B17.

Grain size distribution of B22 and B23

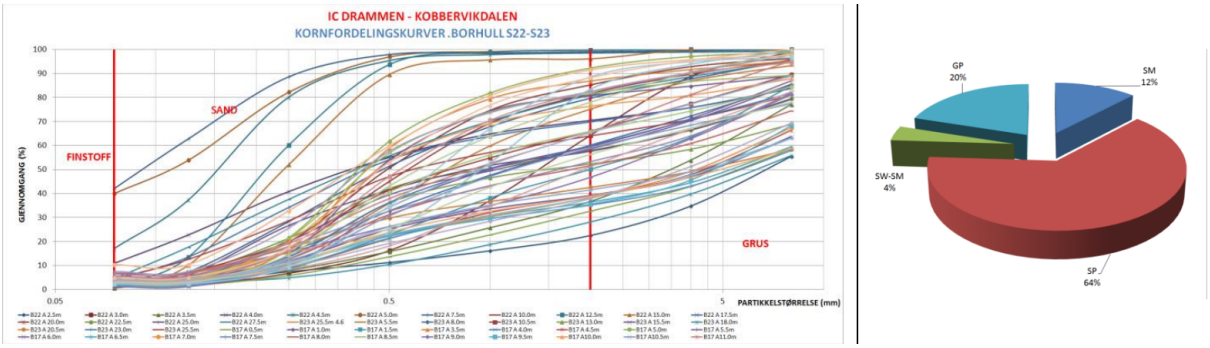

Figure B.6: Grain size distribution of B22 and B23.

Grain size distribution of B24

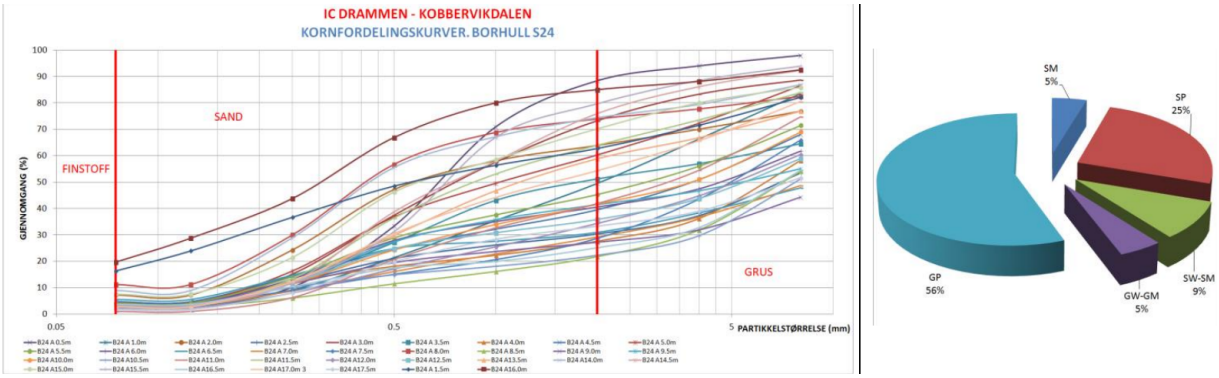

Figure B.7: Grain size distribution of B24.

Young's modulus and unit weight calculation of B17.

Well 17 & L11

Depth	Vp (m/s)	ν	M(Pa)	K(Pa)	Unit weight(kg/m^3)	E-dyn (MPa)	E-sta (MPa)
0.5	408	0.45	361226880	361226880	2170	108	27
1	408	0.45	318445632	318445632	1913	96	24
1.5	453	0.45	432785781	432785781	2109	130	32
2	453	0.45					
2.5	453	0.45					
3	453	0.45					
3.5	453	0.45	426013884	426013884	2076	128	32
4	762	0.45	1261158768	1261158768	2172	378	95
4.5	762	0.45	1122965496	1122965496	1934	337	84
5	762	0.45	1236191076	1236191076	2129	371	93
5.5	762	0.45	1196126640	1196126640	2060	359	90
6	762	0.45	1273352292	1273352292	2193	382	96
6.5	762	0.45	1277997444	1277997444	2201	383	96
7	762	0.45	1296578052	1296578052	2233	389	97
7.5	762	0.45	1243739448	1243739448	2142	373	93
8	762	0.45	1146191256	1146191256	1974	344	86
8.5	762	0.45	1269287784	1269287784	2186	381	95
9	762	0.45	1275094224	1275094224	2196	383	96
9.5	762	0.45	1147933188	1147933188	1977	344	86
10	762	0.45	1212384672	1212384672	2088	364	91
10.5	762	0.45	1218191112	1218191112	2098	365	91
11	762	0.45	1190320200	1190320200	2050	357	89
11.5	762	0.45	1253610396	1253610396	2159	376	94
12	762	0.45	1242403967	1242403967	2139.7	373	93
12.5	762	0.45	1284384528	1284384528	2212	385	96
13	762	0.45	1286707104	1286707104	2216	386	97
13.5	762	0.45	1284965172	1284965172	2213	385	96
14	762	0.45	1145029968	1145029968	1972	344	86
14.5	762	0.45	1151997696	1151997696	1984	346	86
15	762	0.45	1137481596	1137481596	1959	341	85
15.5	762	0.45	1166513796	1166513796	2009	350	87
16	762	0.45	1171158948	1171158948	2017	351	88
16.5	762	0.45	1156062204	1156062204	1991	347	87
17	762	0.45	1204255656	1204255656	2074	361	90
17.5	762	0.45	1177546032	1177546032	2028	353	88
18	762	0.45	1211223384	1211223384	2086	363	91
18.5	762	0.45	1262320056	1262320056	2174	379	95
19	762	0.45	1124707428	1124707428	1937	337	84
19.5	762	0.45	1136900952	1136900952	1958	341	85
20	762	0.45	1110771972	1110771972	1913	333	83
20.5	762	0.45	1210642740	1210642740	2085	363	91
21	762	0.45	1172320236	1172320236	2019	352	88
21.5	762	0.45	1208320164	1208320164	2081	362	91
22	762	0.45	1284965172	1284965172	2213	385	96
22.5	762	0.45	1226900772	1226900772	2113	368	92

23	762	0.45	1238513652	1238513652	2133	372	93
23.5	1866	0.45	7176311316	7176311316	2061	2153	538
24	1866	0.45	7148455668	7148455668	2053	2145	536
24.5	1866	0.45	7110154152	7110154152	2042	2133	533
25	1866	0.45	7110154152	7110154152	2042	2133	533
				Average:	1955.7	318.0	79.5

Figure B.8: Young's modulus and unit weight calculation of B17.

Young's modulus and unit weight calculation of B24

Well 24 & L11

Depth	Vp (m/s)	ν	M (Pa)	K (Pa)	Unit weight (kg/m^3)	E-dyn (Mpa)	E-sta (Mpa)
0.5	408	0.45	322174425.6	322174426	1935.4	97	24
1	408	0.45	346145241.6	346145242	2079.4	104	26
1.5		0.45					
2	452.8	0.45	425145729	425145729	2073.6	128	32
2.5	457.8	0.45	451940123.4	451940123	2156.4	136	34
3	452.8	0.45	417928749.1	417928749	2038.4	125	31
3.5	452.8	0.45	449769572.6	449769573	2193.7	135	34
4	761.9	0.45	1295541175	1295541175	2231.8	389	97
4.5	761.9	0.45	1280448393	1280448393	2205.8	384	96
5	761.9	0.45	1224372904	1224372904	2109.2	367	92
5.5	761.9	0.45	1279809853	1279809853	2204.7	384	96
6	761.9	0.45	1298559732	1298559732	2237	390	97
6.5	761.9	0.45	1311852989	1311852989	2259.9	394	98
7	761.9	0.45	1315335939	1315335939	2265.9	395	99
7.5	761.9	0.45	1288749423	1288749423	2220.1	387	97
8	761.9	0.45	1154075370	1154075370	1988.1	346	87
8.5	761.9	0.45	1182113115	1182113115	2036.4	355	89
9	761.9	0.45	1263323891	1263323891	2176.3	379	95
9.5	761.9	0.45	1262975596	1262975596	2175.7	379	95
10	761.9	0.45	1251365764	1251365764	2155.7	375	94
10.5	761.9	0.45	1245793044	1245793044	2146.1	374	93
11	761.9	0.45	1237375916	1237375916	2131.6	371	93
11.5	761.9	0.45	1195116127	1195116127	2058.8	359	90
12	761.9	0.45	1264136579	1264136579	2177.7	379	95
12.5	761.9	0.45	1282886458	1282886458	2210	385	96
13	761.9	0.45	1242135947	1242135947	2139.8	373	93
13.5	761.9	0.45	1190878538	1190878538	2051.5	357	89
14	761.9	0.45	1160518827	1160518827	1999.2	348	87
14.5	761.9	0.45	1169458398	1169458398	2014.6	351	88
15	761.9	0.45	1200398600	1200398600	2067.9	360	90
15.5	761.9	0.45	1146819225	1146819225	1975.6	344	86
16	761.9	0.45					
16.5	761.9	0.45	1276965444	1276965444	2199.8	383	96
17	761.9	0.45	1197089798	1197089798	2062.2	359	90
17.5	161.9	0.45	55408722.38	55408722.4	2113.9	17	4
18	761.9	0.45	1225824133	1225824133	2111.7	368	92
18.5	761.9	0.45	1198018585	1198018585	2063.8	359	90
19	761.9	0.45	1209105974	1209105974	2082.9	363	91
19.5	761.9	0.45	1264484874	1264484874	2178.3	379	95
20	761.9	0.45	1234009065	1234009065	2125.8	370	93
20.5	761.9	0.45	1282828409	1282828409	2209.9	385	96
21	761.9	0.45	1290723095	1290723095	2223.5	387	97
21.5	761.9	0.45					
22	761.9	0.45	1219961168	1219961168	2101.6	366	91
				Average:	1982	304	76

Figure B.9: Young's modulus and unit weight calculation of B24.

Locations of tensiometers and wells

Figure B.10: Locations of tensiometers and wells used for UDK02 (Norconsult 2018b).

C Labratory work

C.1 Grain size distrubution

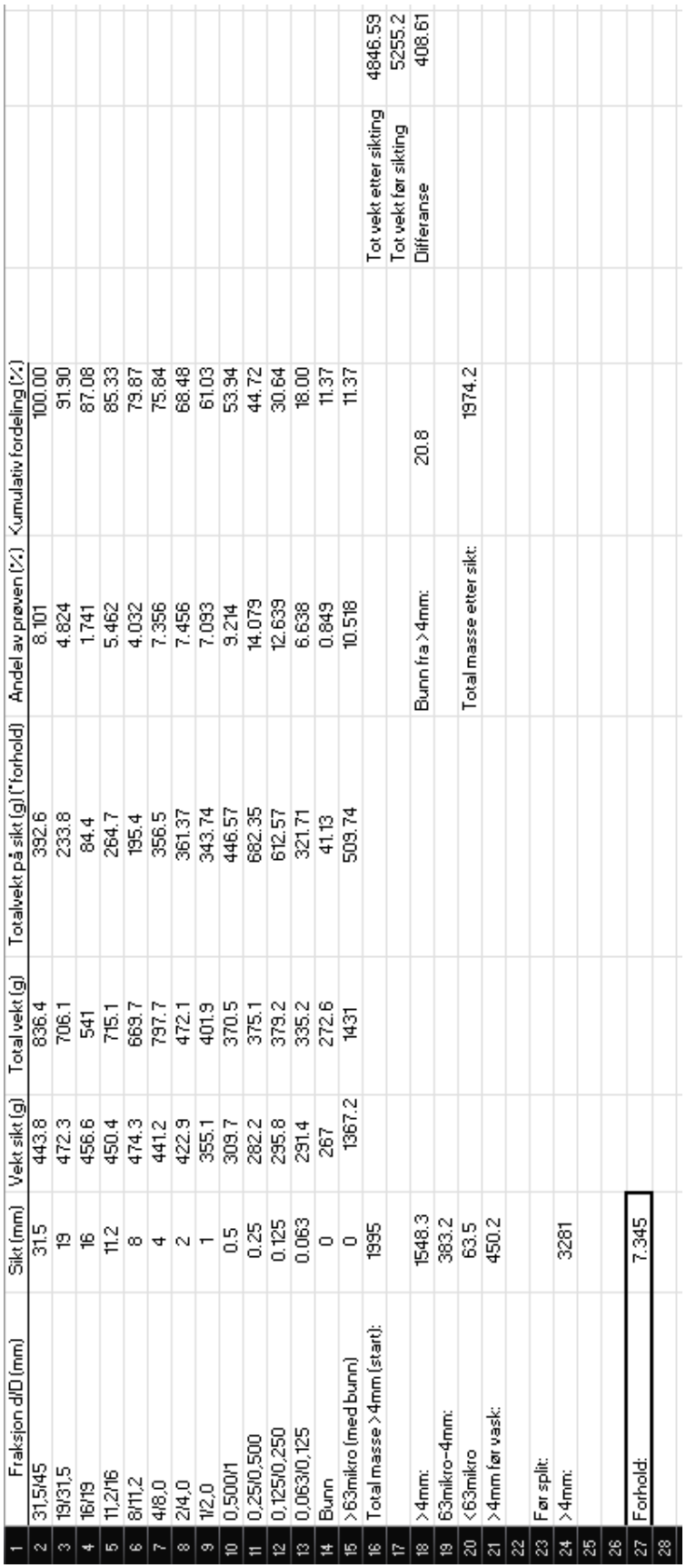

	Fraksjon d/D (mm)	Sikt (mm)	Vekt sikt (g)	Total vekt (g)	Totalvekt på sikt (g) (*forhold)	Andel av prøven (%)	Kumulativ fordeling (%)		
2	31,5/45	31.5	443.8	836.4	392.6	8.101	100.00		
3	19/31,5	19	472.3	706.1	233.8	4.824	91.90		
4	16/19	16	456.6	541	84.4	1.741	87.08		
5	11,2/16	11.2	450.4	715.1	264.7	5.462	85.33		
6	8/11,2	8	474.3	669.7	195.4	4.032	79.87		
7	4/8,0	4	441.2	797.7	356.5	7.356	75.84		
8	2/4,0	2	422.9	472.1	361.37	7.456	68.48		
9	1/2,0	1	355.1	401.9	343.74	7.093	61.03		
10	0,500/1	0.5	309.7	370.5	446.57	9.214	53.94		
11	0,25/0,500	0.25	282.2	375.1	682.35	14.079	44.72		
12	0,125/0,250	0.125	295.8	379.2	612.57	12.639	30.64		
13	0,063/0,125	0.063	291.4	335.2	321.71	6.638	18.00		
14	Bunn	0	267	272.6	41.13	0.849	11.37		
15	>63mikro (med bunn)	0	1367.2	1431	509.74	10.518	11.37		
16	Total masse >4mm (start):	1995						Tot vekt etter sikting	4846.59
17								Tot vekt før sikting	5255.2
18	>4mm:	1548.3			Bunn fra >4mm:	20.8		Differanse	408.61
19	63mikro-4mm:	383.2							
20	<63mikro	63.5			Total masse etter sikt:	1974.2			
21	>4mm før vask:	450.2							
22									
23	Før split:								
24	>4mm:	3281							
25									
26									
27	Forhold:	7.345							
28									

Figure C.1: Spreadsheet used to calculate the grain size distribution.

Figure C.2: Fraction of the sample with grain size above >31mm.

Figure C.3: Fraction of the sample with grain size above >19mm.

Figure C.4: Fraction of the sample with grain size above >16mm.

Figure C.5: Fraction of the sample with grain size above >11.2mm.

Figure C.6: Fraction of the sample with grain size above >8mm.

Figure C.7: Fraction of the sample with grain size above >4mm.

Figure C.8: Fraction of the sample with grain size above >2mm.

Figure C.9: Fraction of the sample with grain size above >1mm.

Figure C.10: Fraction of the sample with grain size above >0.5mm.

Figure C.11: Fraction of the sample with grain size above >0.25mm.

Figure C.12: Fraction of the sample with grain size above >0.125mm.

Figure C.13: Fraction of the sample with grain size above >0.063mm.

D Visit at the construction site

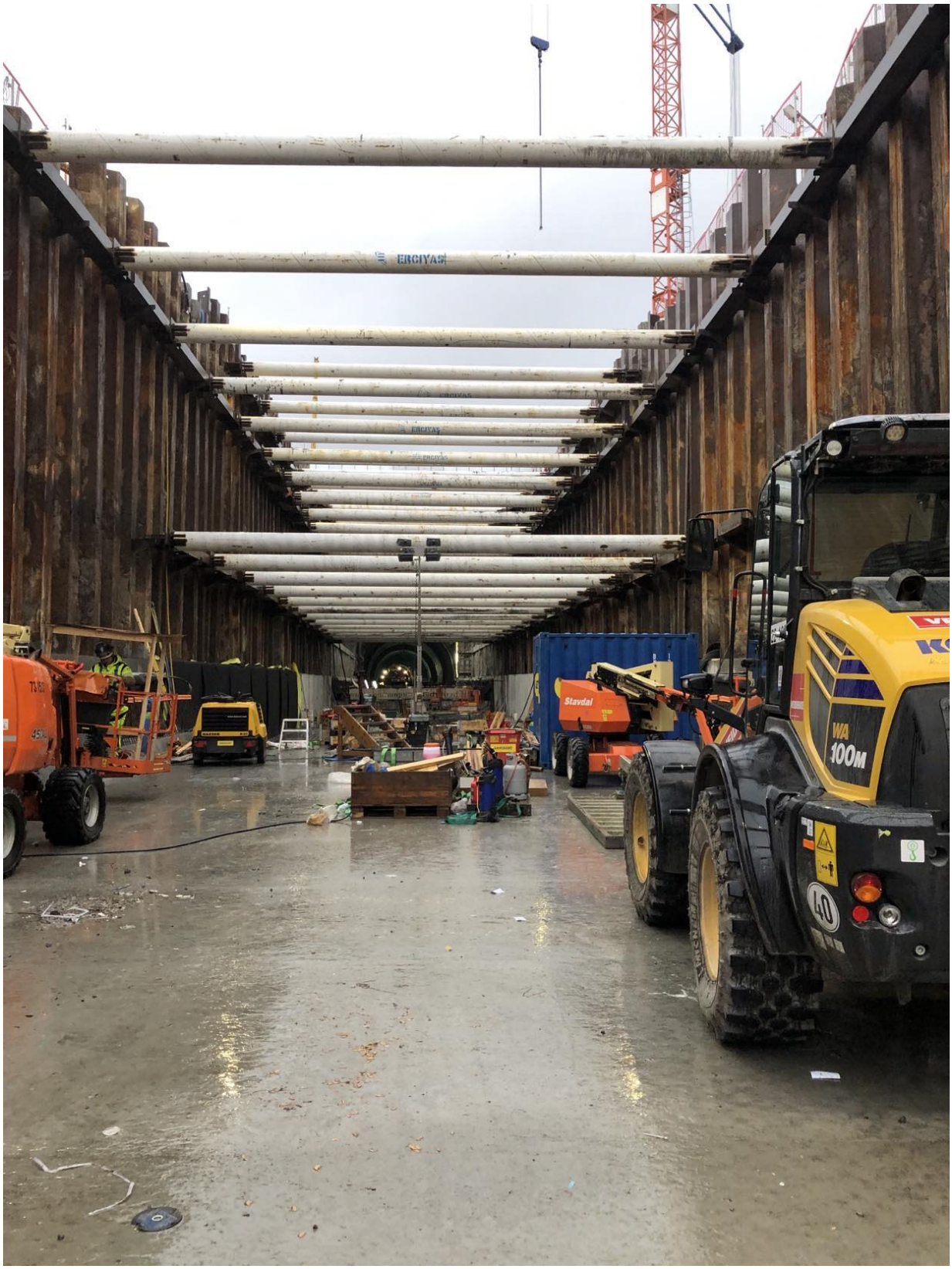

Figure D.1: Picture was taken from within the excavation pit at the site, 28.11.2022.

Figure D.2: Picture of the permanent lining being cast, 28.11.2022.

Figure D.3: Picture of the water sealing membrane, the permanent lining is being established in the distance, 28.11.2022.

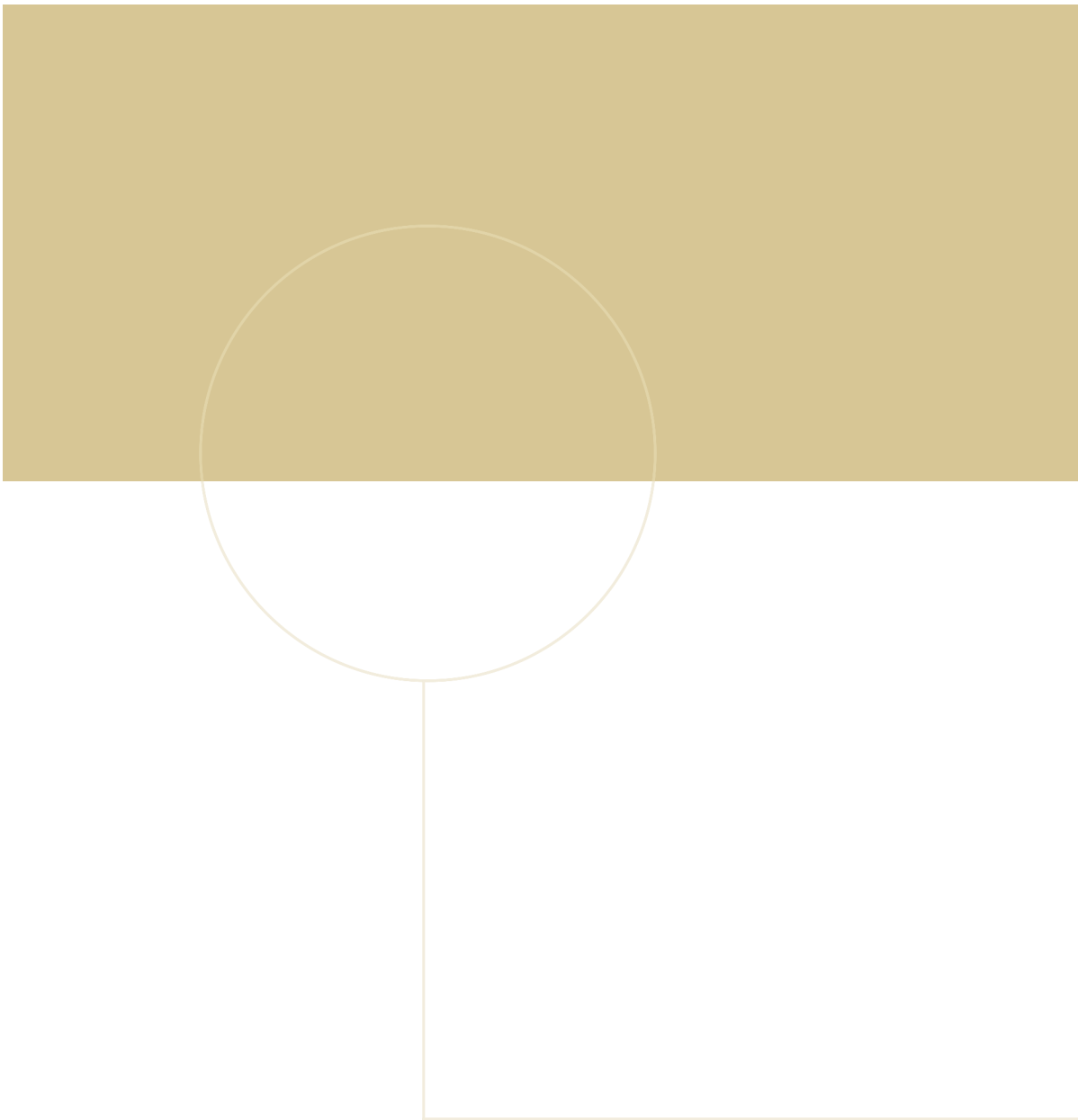

NTNU

Norwegian University of
Science and Technology